

Non-Confidential Report



Final Project Report:

Cryogenic Carbon Capture™ with Energy Storage (CCC ES™)

Agreement Number: D110167  
CCEMC Project Advisor: Vicki Lightbown  
Principal Investigator: Larry L. Baxter  
1489 W. 105 N.  
Orem, UT 84604  
[l.baxter@SESinnovation.com](mailto:l.baxter@SESinnovation.com)  
Work: 801-422-8616  
Cell: 801-850-7091

Project Completion Date: September 1, 2015  
CCEMC Funds Received: \$492,238.34 (CAD Milestone 24 pending)  
CCEMC Funds Held Back: \$50,627.19 (CAD Milestone 24 pending)  
Final Report Submission Date: September 30, 2015  
Lead Institution: Sustainable Energy Solutions  
Project Partners: Brigham Young University

CCEMC makes no warranty, express or implied, nor assume any legal liability or responsibility for the accuracy, completeness, or usefulness of any information contained in this publication, nor that use thereof does not infringe on privately owned rights. The views and opinions of the author expressed herein do not necessarily reflect those of CCEMC. The directors, officers, employees, agents and consultants of CCEMC are exempted, excluded and absolved from all liability for damage or injury, howsoever caused, to any person in connection with or arising out of the use by that person for any purpose of this publication or its contents.

## Table of Contents

|  |    |
|--|----|
| Table of Figures .....   | 5  |
| Table of Tables .....  | 6  |
| 1. Executive Summary .....                                       | 8  |
| 2. Project Description.....                                      | 11 |
| 2.1 Introduction and Background.....                             | 11 |
| 2.2 Technology Description .....                                 | 11 |
| 2.2.1 CCC with Energy Storage .....                              | 12 |
| 2.2.2 Process Energy Storage Features.....                       | 15 |
| Capacity .....   | 15 |
| Efficiency.....  | 16 |
| Response Time.....   | 16 |
| 2.3 Project Goals .....  | 17 |
| 2.4 Work Scope Overview .....                                    | 17 |
| 2.4.1 Task 1 – Process Simulation and Transient Response .....   | 17 |
| Task 1 Deliverables.....   | 17 |
| Task 1 Milestones .....  | 17 |
| 2.4.2 Task 2 – Energy Analysis of the CCC ES™ process .....      | 17 |
| Task 2 Deliverables.....   | 17 |
| Task 2 Milestones .....  | 18 |
| 2.4.3 Task 3 – Economic Evaluation of the CCC ES™ process .....  | 18 |
| Task 3 Deliverables.....   | 18 |
| Task 3 Milestones .....  | 18 |
| 2.4.4 Task 4 – Bench and Skid-scale Demonstrations .....         | 19 |
| Task 4 Deliverables.....   | 19 |
| Task 4 Milestones .....  | 19 |
| 3. Outcomes and Learnings.....                                   | 20 |
| 3.1 Literature review .....                                      | 20 |
| 3.2 Technology Development, Installation and Commissioning ..... | 20 |
| 3.2.1 Process Drawings Development.....                          | 20 |
| Milestone 1 – Finalized Conceptual PFD .....                     | 20 |
| Milestone 6 – Finalized Skid PFD .....                           | 20 |

## Non-Confidential Report

|  |    |
|--|----|
| Milestone 11 – Finalized Skid P&ID.....  | 21 |
| 3.2.2 Capital Costs.....   | 21 |
| Milestone 18 – Capital Equipment Purchasing Complete .....                     | 21 |
| Milestone 19 – Piping Changes to Skid Implemented.....                         | 21 |
| 3.3 Experimental Procedures/Methodology .....                                  | 22 |
| 3.4 Modeling Details .....   | 23 |
| 3.4.1 Process Drawing Development .....  | 23 |
| Milestone 1 – Finalized Conceptual PFD .....                                   | 23 |
| 3.4.2 Fully-Integrated Steady-State Model.....                                 | 23 |
| Milestone 2 – Fully Integrated Steady-State Model .....                        | 23 |
| 3.4.3 Optimized Fully-Integrated Steady-State Model.....                       | 26 |
| Milestone 3 – Optimized Steady-State (SS) Energy Model .....                   | 26 |
| Milestone 4 – Develop Energy Penalty Metrics .....                             | 26 |
| 3.4.4 Transient Modeling.....  | 28 |
| Milestone 5 – Transient Model Demonstration .....                              | 28 |
| Milestone 7 – Energy Penalty Calculated According to Established Metrics ..... | 30 |
| 3.4.5 Energy and Cost Calculations.....  | 31 |
| Milestone 13 – Energy Penalty Sensitivity Analysis .....                       | 31 |
| Milestone 14 – Full Mass and Energy Balance Based on P&ID .....                | 31 |
| Milestone 15 – Updated CCC LCOE.....   | 33 |
| 3.4.6 Sensitivity Analysis .....   | 34 |
| Milestone 13 – Energy Penalty Sensitivity Analysis .....                       | 34 |
| Milestone 16 – Calculated CCC ES™ LCOE .....                                   | 34 |
| 3.4.7 Heat Exchanger Efficiency .....  | 37 |
| Milestone 21 – Heat Exchanger Performance Test.....                            | 37 |
| 3.5 Results of Experiments, Model Simulations.....                             | 38 |
| 3.5.1 Refrigeration System Design.....   | 38 |
| Milestone 1 – Finalized Conceptual PFD .....                                   | 38 |
| Milestone 4 – Develop Energy Penalty Metrics .....                             | 38 |
| 3.5.2 Energy and Cost Requirements .....                                       | 38 |
| Milestone 7 – Energy Penalty Calculated According to Established Metrics ..... | 38 |
| Milestone 10 – Capital Cost Estimates for Full-Scale Major Equipment.....      | 39 |

## Non-Confidential Report

|   |    |
|---|----|
| Milestone 15 – Updated CCC LCOE.....  | 40 |
| Milestone 16 – Calculated CCC ES™ LCOE .....  | 43 |
| 3.5.3 Energy Storage Simulation Results .....   | 46 |
| Milestone 9 – Fully Integrated Transient Model .....                                  | 46 |
| 3.5.4 Mass and Energy Balances .....  | 49 |
| Milestone 14 – Full Mass and Energy Balance Based on P&ID .....                       | 49 |
| 3.5.5 Dynamic Heat Exchanger.....   | 51 |
| Milestone 21 – Heat Exchanger Performance Test.....                                   | 51 |
| 3.5.6 Process Response Time .....   | 52 |
| Milestone 21 – Heat Exchanger Performance Test.....                                   | 52 |
| 3.5.7 Carbon Capture Demonstrations .....   | 54 |
| Milestone 20 – Demonstrate 90% Capture Utilizing LNG as Refrigerant Stream.....       | 54 |
| Milestone 22 – Demonstrate 99% Capture Utilizing LNG as Refrigerant Stream.....       | 55 |
| Milestone 23 – Creating a Sustained LNG Flow Rate Sufficient to Sustain Operation ... | 57 |
| Milestone 24 – Demonstrate 90% Capture for a Full Simulated Load Cycle .....          | 57 |
| 3.6 Project Outcomes .....  | 59 |
| 3.6.1 Task 1 – Process Simulation and Transient Response .....                        | 59 |
| 3.6.2 Task 2 – Energy Analysis of the CCC ES™ Process .....                           | 60 |
| 3.6.3 Task 3 – Economic Evaluation of the CCC ES™ Process.....                        | 60 |
| 3.6.4 Task 4 – Bench and Skid Scale Demonstrations .....                              | 60 |
| 3.7 Analysis of Results.....  | 60 |
| 3.8 Discussion .....  | 62 |
| 3.9 Important Lessons Learned .....   | 64 |
| 4. Greenhouse Gas and Non-GHG Impacts .....   | 66 |
| 4.1 Qualitative Impacts .....   | 66 |
| 4.2 Qualitative Discussion.....   | 67 |
| 4.3 Expected Annual GHG Benefits .....  | 67 |
| 4.4 Non-GHG Benefits.....   | 68 |
| 4.4.1 Multipollutant capture .....  | 68 |
| Mercury Capture Offset .....  | 68 |
| SOx Capture Offset and FGD Replacement .....  | 69 |
| NOx Capture Offset .....  | 69 |

|                                    |    |
|------------------------------------|----|
| 5. Overall Conclusions.....        | 71 |
| 6. Scientific Achievements .....   | 73 |
| 6.1 Journal Articles .....         | 73 |
| 6.2 Conference Presentations ..... | 73 |
| 6.3 Student Theses.....            | 74 |
| 7. Next Steps.....                 | 75 |
| 8. Communications Plan.....        | 76 |
| 9. Abstract and Keywords.....      | 77 |
| 9.1 Abstract .....                 | 77 |
| 9.2 Keywords .....                 | 78 |
| 10. References.....                | 79 |

## Table of Figures

|  |           |
|--|-----------|
| <b>Figure 1. CCC CFG™ version of the CCC process. ....</b>   | <b>8</b>  |
| <b>Figure 2. CCC CFG™ version of the CCC process. The distinction between the inner (I) and outer (II) coolant loops is important to the energy storage discussion.....</b>  | <b>12</b> |
| <b>Figure 3. Conceptual energy storing system diagram during normal operation. Idle operations are indicated by blue, solid-colored fills while active operations are shown by yellow/red gradient fills. Compare with Figure 4 and Figure 5.....</b>  | <b>13</b> |
| <b>Figure 4. Conceptual energy storing system diagram during energy storage operation. Compare with Figure 3 and Figure 5. Natural gas (NG) enters the system at some stage of the compressor (depending on its line pressure). More power is consumed by the compressor. The excess NG is stored as a liquid at low temperature and modest pressure. ....</b>   | <b>14</b> |
| <b>Figure 5. Conceptual energy storing system diagram during energy recovery operation. Compare with Figure 3 and Figure 4. The main compressor is idled, reducing process energy consumption, and the system runs on stored liquid natural gas (NG). In this embodiment, NG enters a turbine generation set after warming to room temperature by driving the CCC system. The NG turbine exhaust enters the boiler at a temperature-matched point and a portion of the cold flue gas from the boiler is used in the NG turbine for turbine inlet temperature control, with only enough air to provide sufficient O<sub>2</sub> for combustion. Most of these latter features are optional, but this system should provide combined-cycle efficiencies at simple cycle costs (use of boiler as a Rankine cycle avoids significant cost), minimal impact on the boiler, and high CO<sub>2</sub> concentrations for efficient NG CO<sub>2</sub> control. ....</b> | <b>15</b> |
| <b>Figure 6. LNG dewar and level sensor. ....</b>  | <b>21</b> |
| <b>Figure 7. LNG cold box CAD design (all hose runs removed). ....</b>   | <b>22</b> |
| <b>Figure 8. Installed energy storage system (i.e., LNG cold box). ....</b>  | <b>22</b> |
| <b>Figure 9. Aspen flow sheet for the CCC ES™ process. ....</b>  | <b>24</b> |

**Figure 10. Optimized Aspen flow sheet of the CCC EST<sup>TM</sup> process ..... 27**

**Figure 11. Aspen flow sheet showing refrigeration portion of the CCC EST<sup>TM</sup> process..... 29**

**Figure 12. Temperature distribution in a heat exchanger prior to reaching steady state. . 31**

**Figure 13. Changes in energy penalty. .... 36**

**Figure 14. COE changes with variation of process variables..... 37**

**Figure 15. COE of several case studies broken into component parts. .... 44**

**Figure 16. Cost of electricity for Cases 11 and 12 from the NETL report [3], a greenfield CCC EST<sup>TM</sup> installation, a single CCC EST<sup>TM</sup> retrofit installation, and CCC EST<sup>TM</sup> retrofit scenario..... 46**

**Figure 17. Results of the energy storage simulation. (A–C) Scenario 1 and (D–F) Scenario 2 (A and D). NG compressor power (orange), refrigerant compressor power (blue), and total power (gray). (B and E) Mass of LNG in the storage tank. (C and F) Temperature of CL output to the CCC process..... 48**

**Figure 18. Dynamic heat exchanger test stand. .... 52**

**Figure 19. Efficiency variation during dynamic heat exchanger testing using a two-stream, counter-current heat exchanger. The idle and active tests were separate experiments; the beginning and end of the time perturbation correspond quite closely, but not exactly, in the two cases. .... 53**

**Figure 20. Efficiency variation in time during operations with the dynamic heat exchanger technology active and idle for a three-stream, counter-current heat exchanger. These are separate experiments and the beginning and ending of the time perturbation correspond quite closely but not exactly in the two cases. .. 53**

**Figure 21. CO<sub>2</sub> inlet and outlet percentages during CCC EST<sup>TM</sup> testing. For the first portion of the test (left of the red line), we stored energy. The second part of the test (right of the red line), we captured CO<sub>2</sub> only using the stored LNG. .... 54**

**Figure 22. 3-hour run with 80 minutes of 90+% capture using stored LNG as a refrigerant (right of the red line). .... 55**

**Figure 23. 99% CO<sub>2</sub> capture demonstrated for 15 minutes. CO<sub>2</sub> inlet and outlet percentages are also shown (right axis). .... 56**

**Figure 24. LNG accumulation as a function of time with the ECL skid system running at full capacity with no additional load. .... 57**

**Figure 25. Adjusting the fuel/air mixture while flaring natural gas after it was used in its condensed phase (LNG) to drive the CCC process..... 58**

**Figure 26. Simulated LNG load cycle. Once the process began to run at steady state (14 min.), we started venting the natural gas. The Cryogenerators were ramped up and shut off periodically (black line) to test the ability of the system to respond to rapid fluctuations in available power. There was some transience in the capture, but the capture level stayed above 90% the entire time. .... 59**

**Figure 27. CCC CFG<sup>TM</sup> version of the CCC process. .... 62**

**Figure 28. CCC EST<sup>TM</sup> integration into the grid resulting in a negative carbon footprint for electrical power production. .... 66**

Table of Tables

**Table 1. Summary of carbon capture energy penalties by technology type (from Ref. 4). . 20**

|   |           |
|---|-----------|
| <i>Table 2. Energy table from Aspen model of the refrigeration portion of the CCC ES™ process.....</i>  | <i>28</i> |
| <i>Table 3. Process parameters for sensitivity analysis.....</i>  | <i>35</i> |
| <i>Table 4. Summary of energy penalty.....</i>  | <i>35</i> |
| <i>Table 5. COE sensitivity summary. ....</i>   | <i>36</i> |
| <i>Table 6. Summary of major equipment costs.....</i>   | <i>40</i> |
| <i>Table 7. List of parasitic loads for CCC.....</i>  | <i>41</i> |
| <i>Table 8. Summary of energy penalty of CCS technologies .....</i>   | <i>42</i> |
| <i>Table 9. Energy requirements for amine-based CCS technologies based on reports from the US, Europe, China, and Australia [26,27]. ....</i>   | <i>42</i> |
| <i>Table 10. Cost comparison between NETL Cases 11 and 12 as well as estimates for the CCC process, both as a greenfield installation and as a retrofit installation.....</i>                                 | <i>45</i> |
| <i>Table 11. Stream conditions during different phases of the CCC ES™ process. ....</i>   | <i>46</i> |
| <i>Table 12. Two scenarios for CCC ES™ implementation; baseline values are included for reference.....</i>  | <i>47</i> |
| <i>Table 13. Results from modeling two CCC ES™ scenarios: Scenario 1 where energy is stored for 12 hr and released for 12 hr, and Scenario 2 where energy is stored for 6 hr and released for 18 hr. ....</i> | <i>49</i> |
| <i>Table 14. CCC mass balance. ....</i>   | <i>50</i> |
| <i>Table 15. Energy balance (25 °C reference).....</i>  | <i>50</i> |
| <i>Table 16. Boiling temperature of natural gas constituents at 1 atm. Species considered “natural gas liquids” are shaded. ....</i>  | <i>56</i> |
| <i>Table 17. Worldwide CCC ES™ CO<sub>2</sub> capture potential by year.....</i>  | <i>68</i> |
| <i>Table 18. NO concentration into and out of the skid-scale CCC system (FTIR measurements).....</i>  | <i>69</i> |

## 1. Executive Summary

The CCC process is a retrofit, post-combustion technology that desublimates CO<sub>2</sub> in the flue gas and produces a separate liquid CO<sub>2</sub> product. Figure 2 illustrates the major steps in the CCC external cooling loop process (CCC CFG<sup>TM</sup>). The process (1) dries and cools flue gas, (2) further cools it in a heat recovery heat exchanger to nominally -107 °C, (3) condenses contaminants (e.g., mercury, SO<sub>2</sub>, NO<sub>2</sub>, Hg, and HCl) at various stages during cooling, (4) separates the solid CO<sub>2</sub> that forms during cooling from the remaining gas, (5) pressurizes the solid CO<sub>2</sub> to 70–80 bar, (6) reheats the CO<sub>2</sub> and the remaining flue gas to near ambient conditions (15–20 °C) by cooling the incoming gases, and (7) compresses the pressurized and now melted CO<sub>2</sub> stream to final delivery pressure (nominally 150 bar). There is a small external refrigeration loop in the process that transfers the enthalpy of pure CO<sub>2</sub> melting to cooler temperatures to avoid heat exchanger temperature crossover.

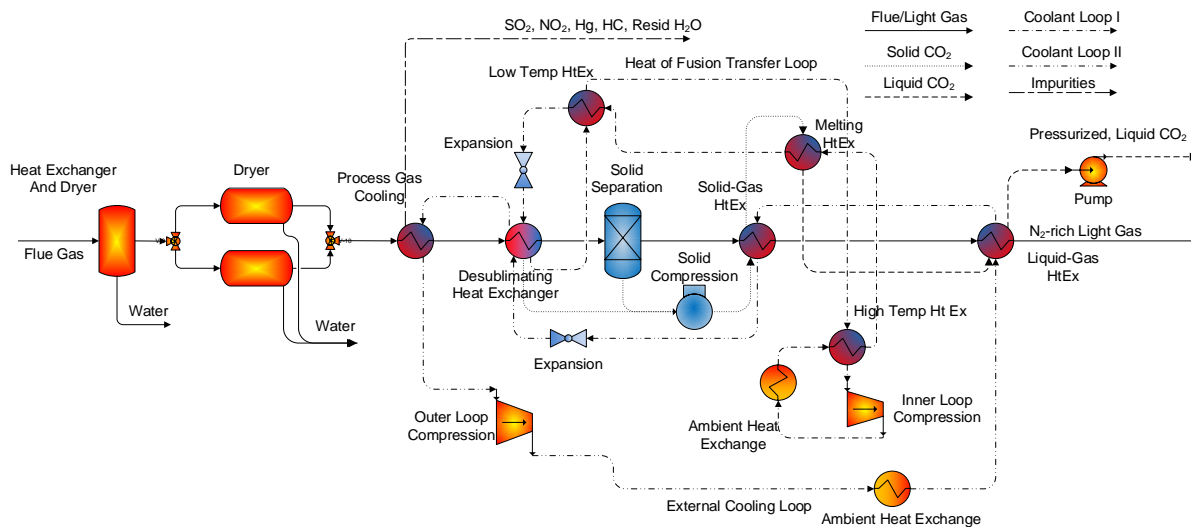


Figure 1. CCC CFG<sup>TM</sup> version of the CCC process.

The CCC process in the configuration shown in Figure 2 only requires low-temperature refrigerant(s) to operate. This project focuses on the energy-storing version of this process, which is designated CCC ES<sup>TM</sup>. During off-peak hours, CCC ES<sup>TM</sup> generates more refrigerant than is needed for the process and stores the excess in an insulated vessel as a liquid at the low-temperature, low-pressure point in the cycle. Such vessels and processes are common commercially. During peak demand, the stored refrigerant could be used in place of continuously generating refrigerant in a steady-state system. This would eliminate nearly all of the energy demand required by CCC for as long as the stored refrigerant lasts.

The objective of this project was to explore the energy storage capability of CCC. This project

1. shows that NG can be used as effectively as other refrigerants in the CCC process;
2. determines that stored LNG refrigerant represents a significant portion of the CCC energy demand;
3. calculates that the LNG energy density suffices to be able to store energy at grid scale;

## Non-Confidential Report

4. develops heat exchanger technologies that allow LNG flow transients to follow energy storage and recovery transients without damage;
5. simulates grid-level incorporation of energy storage into a realistic system;
6. demonstrates as many of these processes as possible at small scale.

This project demonstrates experimentally and theoretically that natural gas provides essentially identical (very slightly better) refrigeration performance as alternative refrigerants and refrigerant blends. Because the critical point of LNG (as low as  $-83\text{ }^{\circ}\text{C}$ ) is well below ambient temperature, it is not possible to compress and then condense LNG near room temperature as is commonly done with traditional refrigerants. However, LNG can still be generated efficiently, albeit in a slightly more complex circuit compared to traditional refrigerants. The project also demonstrated that some NG supplies may require process set point modification or removal of natural gas liquids since there are variations in the amounts of heavy hydrocarbons among NG supplies.

Refrigeration in general represents about 80% of the total energy demand for CCC, depending on the amount of  $\text{CO}_2$  in the flue gas, over half of which can be incorporated into the LNG loop. Therefore, CCC ES<sup>TM</sup> can store and release most of its energy consumption in the form of stored refrigerant, or LNG.

The energy density of LNG suffices to store several hours' worth of refrigeration in tanks that are smaller than commercially available storage tanks. Therefore, CCC ES<sup>TM</sup> has the capacity to store enough energy to supply refrigerant for the entire peak demand time of a typical power plant.

CCC ES<sup>TM</sup> operates with the carbon capture portion of the process matching boiler load, which is typically essentially constant, while the LNG generation portion follows power demand. Power demand on grids with intermittent supplies can change significantly within minutes. Transient analyses and experiments showed that heat exchangers may be able to keep up with such rapidly changing demands, but that they experience rapid internal temperature changes that may exceed thermal stress limits. SES-developed (patent-pending) dynamic heat exchangers remove or greatly reduce these thermal stresses. This project demonstrated that such heat exchangers can follow even step changes in flowrates without compromising heat exchanger efficiency or inducing thermal stresses.

Detailed analyses of energy-storing carbon capture demonstrate that, for example, an 800 MW power plant with this technology can manage  $\pm 400$  MW swings in energy demand on a grid that includes coal, natural gas, wind, and varying daily demands. The data included actual demand variations and corresponding costs of power production. The revenue generated by storing energy during low-demand, low-cost periods and releasing during high-demand, high-cost periods represented a net revenue to the CCC ES<sup>TM</sup> system of slightly over \$20/MWh, which cover 80–90% of the total cost of carbon capture. This large economic benefit can only be realized for a load-following power station, so it is not included in the economic analyses of this report. However, the CCC ES<sup>TM</sup> process allows the power plant to follow load while the boiler

## Non-Confidential Report

remains at a constant firing rate, so nearly every power plant should be able to benefit from this technology.

## 2. Project Description

### 2.1 Introduction and Background

Sustainable Energy Solutions (SES) was founded in 2008 in response to a growing need for solutions to sustainability problems within the energy industry. SES is primarily focused on the development and commercialization of Cryogenic Carbon Capture™ (CCC), a patented carbon capture technology. Since its founding, SES has filed several additional patents on multiple technologies to help realize SES' mission: Create practical solutions to help solve energy problems on regional and global scales.

Sustainable Energy Solution's Cryogenic Carbon Capture™ Energy Storage (CCC ES™) process stores energy efficiently and changes load rapidly over a significant fraction of a power plant's capacity. The energy storage option can reduce peak load parasitic losses by shifting loads to non-peak or cheaper generation times. The rapid load change capability provides major grid management capabilities that are essential to accommodate intermittent supplies, such as wind and solar energy.

### 2.2 Technology Description

The CCC process is a retrofit, post-combustion technology that desublimates CO<sub>2</sub> in the flue gas and produces a separate liquid CO<sub>2</sub> product. Figure 2 illustrates the major process steps. The process (1) dries and cools flue gas, (2) further cools it in a heat recovery heat exchanger to nominally -107 °C, (3) condenses contaminants (e.g., mercury, SO<sub>2</sub>, NO<sub>2</sub>, Hg, and HCl) at various stages during cooling, (4) separates the solid CO<sub>2</sub> that forms during cooling from the remaining gas, (5) pressurizes the solid CO<sub>2</sub> to 70–80 bar, (6) reheats the CO<sub>2</sub> and the remaining flue gas to near ambient conditions (15–20 °C) by cooling the incoming gases, and (7) compresses the pressurized and now melted CO<sub>2</sub> stream to final delivery pressure (nominally 150 bar). There is a small external refrigeration loop in the process that transfers the enthalpy of pure CO<sub>2</sub> melting to cooler temperatures to avoid heat exchanger temperature crossover.

Two cooling loops are illustrated in Figure 2, which are important in understanding the proposed energy storage concept. Coolant loop I is used to transfer the heat of CO<sub>2</sub> fusion from the melting point (near -56 °C) to lower temperatures. Coolant loop II provides cooling for the remainder of the process.

The potential of using natural gas as a refrigerant in coolant loop II is discussed below. Natural gas (mostly methane) can effectively provide the cooling needed in the external loop, but it is not well suited for internal loop cooling because the critical temperature of natural gas (methane) is at about -83 °C, which is well below the triple-point temperature of CO<sub>2</sub> (-56.6 °C). Therefore, there is no combination of temperature and pressure that will simultaneously condense methane and melt CO<sub>2</sub>, rendering natural gas incapable of going through a phase change in the CO<sub>2</sub> melting heat exchanger. Therefore, using liquefied natural gas (LNG) in a heat exchanger with melting CO<sub>2</sub> would result in very inefficient heat exchange. This inefficiency may represent a tolerable loss compared to the gains of the energy storage, but large amounts of energy storage are available without using natural gas in the inner loop and these will be pursued before revisiting these inner loop issues.

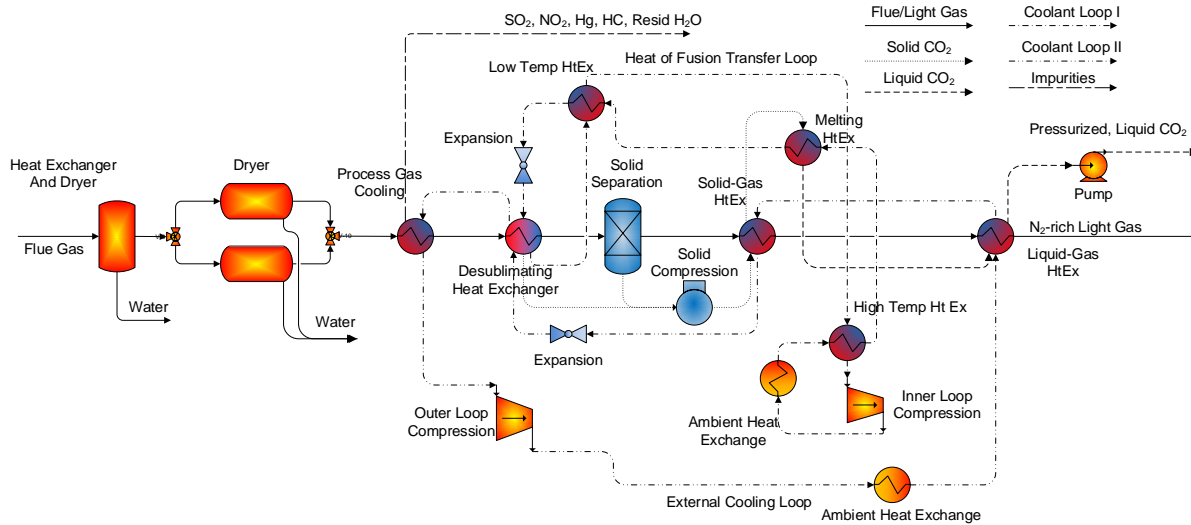


Figure 2. CCC CFG™ version of the CCC process. The distinction between the inner (I) and outer (II) coolant loops is important to the energy storage discussion.

CO<sub>2</sub> purities have been verified as high as 99.95% from the CCC process. Assuming a typical coal flue gas of about 16% CO<sub>2</sub> on a dry basis, most of the potential impurities such as SO<sub>2</sub>, SO<sub>3</sub>, NO<sub>2</sub>, Hg and As will be removed prior to the desublimation of CO<sub>2</sub> and will leave in a separate stream. The remainder would include trace amounts of SO<sub>2</sub>, SO<sub>3</sub>, and NO<sub>2</sub>. Some hydrocarbon contact liquid (CL) would also be present. None of these species would be present in amounts that would pose any issues with enhanced oil recovery. To our knowledge, no comprehensive standard exists for the purity of separation for carbon sequestration in saline aquifers; the specifications for most CO<sub>2</sub> pipelines require CO<sub>2</sub> purity to be 95-99% [1].

### 2.2.1 CCC with Energy Storage

The flow diagram (Figure 2, above) helps illustrate the energy storage concept. After discussing a few of the details, a series of conceptual diagrams shown later illustrate this process and may greatly facilitate the understanding of it. The CCC process in the configuration shown in Figure 2 only requires low-temperature refrigerant(s) to operate. During off-peak hours, the energy storing version of the process would generate more refrigerant than is needed for the process, which would be stored in an insulated vessel as a liquid at the low-temperature, low-pressure point in the cycle. Such vessels and processes are common commercially. During peak demand, the stored refrigerant could be used in place of continuously generating refrigerant in a steady-state system. This would eliminate nearly all of the energy demand required by CCC for as long as the stored refrigerant lasts. The spent refrigerant would then have to be stored at high temperature and low pressure, which would require large storage vessels in comparison to storing the refrigerant at low temperature and pressure.

Storing the gaseous refrigerant at low pressure may become prohibitively expensive because of the size of the vessel required. One way to resolve the high-temperature storage issue is to use natural gas (methane) as the refrigerant. The technology for cryogenic refrigeration of methane closely parallels that for LNG, which is typically stored as a liquid at about -164 °C and 2 bar.

These conditions are well suited for the stored refrigerant for the CCC process. At the high-temperature end of the cycle, a gas turbine combusts the methane, which provides additional power and eliminates the storage problem. The effluent from the gas turbine could enter the boiler and contribute to steam generation, providing combined-cycle efficiencies at simple cycle cost. This energy storage option functionally operates as an LNG plant next to a coal-fired power plant, with the stored LNG driving the CCC process during peak demands and being replenished at off-peak times.

Some conceptual diagrams illustrate this process, highlighting only the energy storage aspects. Under normal operation, the CCC process does not involve NG power generation or flow of NG into the system (Figure 3). The coal combustor generates flue gas that is treated by the CCC process and results in a nitrogen-rich effluent stream and a pressurized CO<sub>2</sub> stream. A compressor provides most of the energy demand of the CCC process, with energy represented by a lightning bolt into the compressor.

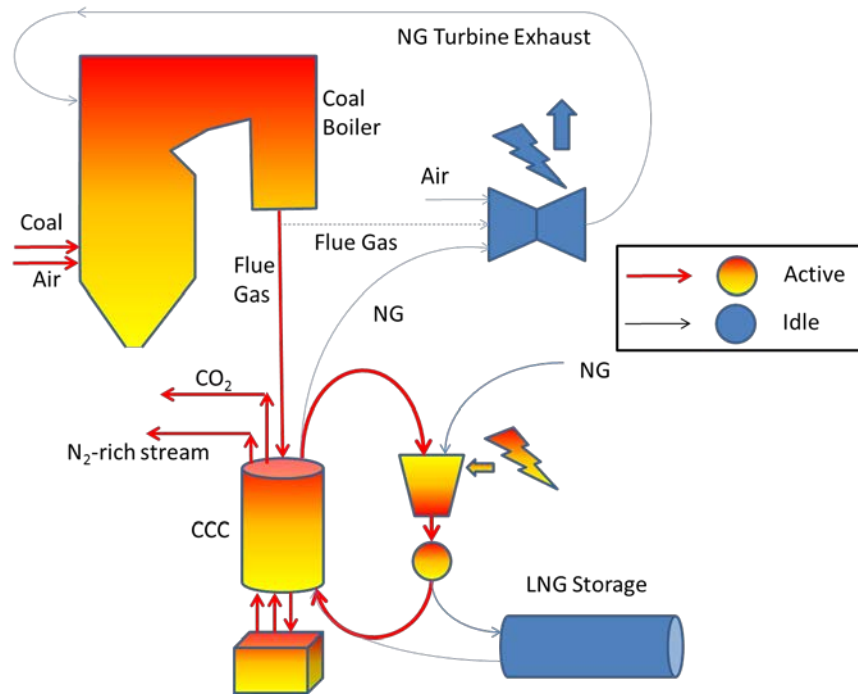


Figure 3. Conceptual energy storing system diagram during normal operation. Idle operations are indicated by blue, solid-colored fills while active operations are shown by yellow/red gradient fills. Compare with Figure 4 and Figure 5.

During energy storage (Figure 4), the process differs only in that the compressor load increases (two lightning bolts) so that additional NG can be prepared as a liquid and stored in the LNG storage vessel. Nothing flows out of the LNG storage vessel, and the NG turbine set does not operate.

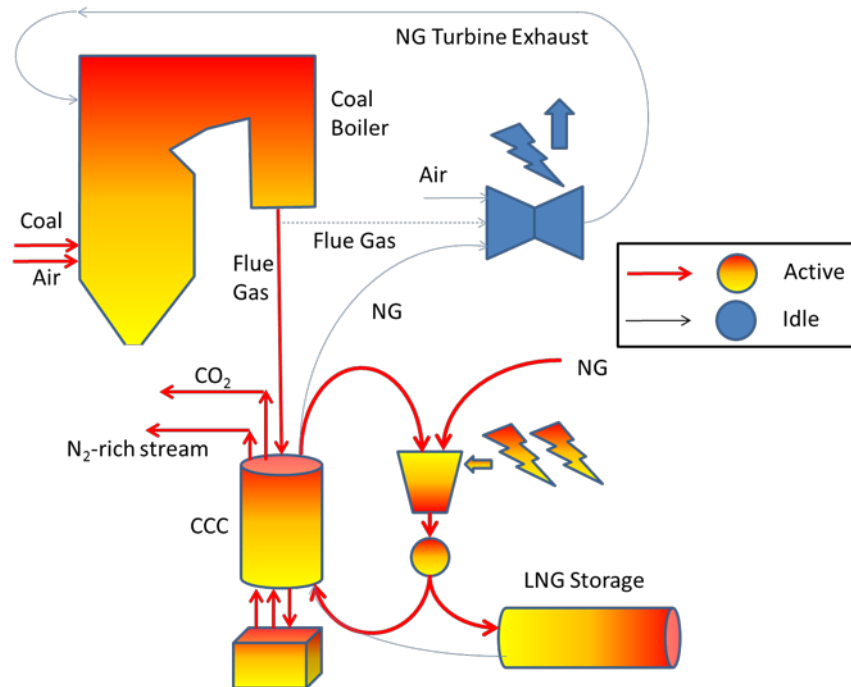


Figure 4. Conceptual energy storing system diagram during energy storage operation. Compare with Figure 3 and Figure 5. Natural gas (NG) enters the system at some stage of the compressor (depending on its line pressure). More power is consumed by the compressor. The excess NG is stored as a liquid at low temperature and modest pressure.

During energy recovery (Figure 5), the process eliminates the parasitic compressor demand and operates only from the stored LNG. The LNG first provides cooling for the CCC process and then—to avoid storage at low-pressure, room-temperature conditions—passes through a NG turbine generation set. The air and NG would not be in the same compressor, as suggested by this simple diagram. However, the compressed NG and air burn in a turbine. This energy storage process minimizes the parasitic load on the coal-fired plant due to carbon capture via CCC. The process also generates additional energy in the form of power from the NG turbine, which is important in daily operation. However, the power from the NG turbine should not be included in an energy storage or efficiency calculation since it is a non-regenerative use of NG. The only true energy storage is the loss of the parasitic load from the CCC process.

Two other recommended system modifications appear in this diagram. First, the effluent from the NG turbine flows to the convection pass of the coal boiler. This provides combined-cycle efficiencies at simple-cycle cost and operation. The NG effluent is small compared to the flow in the coal boiler and it enters the boiler at a temperature-matched location so that it represents a minor perturbation on the temperature distribution in the boiler. This enables the CCC process to capture both the CO<sub>2</sub> and remaining heat in the NG exhaust.

The second modification uses recycled coal flue gas as a portion (most) of the gas entering the turbine, with only enough air to provide oxygen for combustion. This increases CO<sub>2</sub> content in

the NG turbine exhaust, increasing the CO<sub>2</sub> capture efficiency. However, the process works equally well with a simple cycle, atmospheric-exhausted NG generation set.

SES has developed more sophisticated PFD diagrams, similar to Figure 2, that include energy storage.

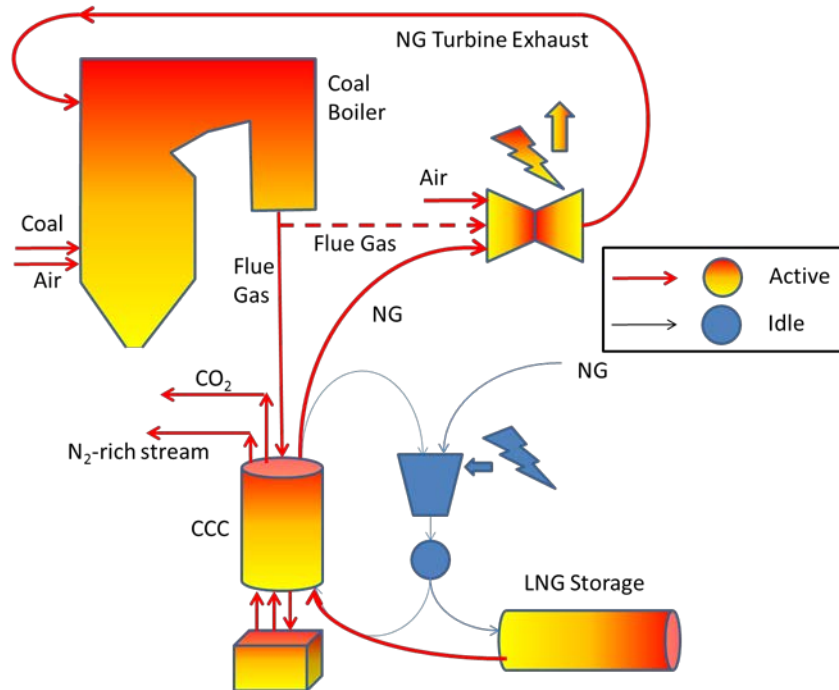


Figure 5. Conceptual energy storing system diagram during energy recovery operation. Compare with Figure 3 and Figure 4. The main compressor is idled, reducing process energy consumption, and the system runs on stored liquid natural gas (NG). In this embodiment, NG enters a turbine generation set after warming to room temperature by driving the CCC system. The NG turbine exhaust enters the boiler at a temperature-matched point and a portion of the cold flue gas from the boiler is used in the NG turbine for turbine inlet temperature control, with only enough air to provide sufficient O<sub>2</sub> for combustion. Most of these latter features are optional, but this system should provide combined-cycle efficiencies at simple cycle costs (use of boiler as a Rankine cycle avoids significant cost), minimal impact on the boiler, and high CO<sub>2</sub> concentrations for efficient NG CO<sub>2</sub> control.

### 2.2.2 Process Energy Storage Features

The process performance is very good, generally best of class, in the three most important aspects of energy storage: capacity, efficiency, and response time. Each of these is discussed separately.

#### *Capacity*

The CCC ES<sup>TM</sup> process provides energy storage capacity of about 2/3 of the parasitic loss associated with carbon capture if applied only to the outer loop. That represents about 10% of the boiler capacity. In addition, it provides about another 10% of capacity in the form of power

## Non-Confidential Report

generation from the gas turbine during energy recovery. The net effect is that the plant capacity actually increases during energy recovery, relative to the baseline coal boiler rated capacity. These preliminary numbers require more detailed vetting and are conservative estimates.

The inner loop could provide similar energy storage capabilities, albeit at a lower overall efficiency or with a refrigerant other than NG. In the latter case, a storage vessel for the room-temperature, low-pressure refrigerant will probably be required. In this scenario, the energy storage capacity increases by about 50% relative to the outer loop only, as illustrated and discussed above.

### *Efficiency*

The effective energy storage efficiency of this process exceeds that of pumped storage or any other large-scale storage system if the plant is committed to carbon capture in any case. A plant committed to carbon capture is most efficient with the CCC option. If the external cooling loop is used, then some refrigerant must necessarily be cooled. The marginal efficiency losses associated with using NG as the coolant only amount to (a) the loss of coolant during storage, and (b) any change in CCC efficiency with NG as a coolant, relative to using a different coolant. The coolant losses during storage are well documented in the LNG industry and amount to about 0.5%/day in a land-based storage tank at  $-163\text{ }^{\circ}\text{C}$ , and about twice this amount for ship-based storage.

The change in process efficiency when using NG as a coolant required both detailed process analysis and experimental confirmation, which occurred as part of this project. However, unlike the CCC process generally, which is a highly innovative process involving several cryogenic processing steps never previously commercialized, LNG processing is a mature technology. Most of the lessons learned and optimization from LNG processing apply directly to this process.

Taking both factors into account, the overall efficiency of CCC ES<sup>TM</sup> implemented with a 24-hour storage cycle ranges from 99.5% (LNG loss only) to 90% (9.5% cycle efficiency loss and 0.5% LNG loss). This exceeds the efficiency of pumped storage systems (i.e., nominally 76-85%) [2] and can be implemented with CCC on any power plant.

### *Response Time*

The major components of this process involved in energy storage and delivery are compressors, room- or low-temperature heat exchangers at modest pressures (compared to superheater headers), and a NG turbine. All of these components have response times on the order of seconds to minutes. This energy storage response time is well matched to intermittent sources, such as wind turbines and solar photovoltaic cells, and is far more rapid than normal daily power demand cycles. Therefore, this energy storage system enables a coal-based boiler to follow even rapidly changing loads without compromising pressure, part integrity, or efficiency. Indeed, the CCC ES<sup>TM</sup> process could become the most strategically important component of the much discussed but slowly developing smart grid, providing the most critical part of such a grid: a rapid energy storage/recovery system.

Similar to the efficiency and capacity arguments, this potential rapid response requires detailed analysis and experimental verification, which we accomplished in this project. While the process

## Non-Confidential Report

is similar to LNG processes, most LNG processes operate near steady state and there is less experience available from processes with rapid load changes. As discussed in Milestone 21, we demonstrated heat exchanger configurations that can respond to transients in well under a minute.

### 2.3 Project Goals

The objective of the proposed project is to accelerate the energy storage options to the same level of maturation as the baseline CCC process, which includes detailed energy and financial analysis, lab- and bench-scale demonstrations of critical process components, integrated bench-scale demonstration, and incorporation into a skid-scale unit.

### 2.4 Work Scope Overview

#### 2.4.1 Task 1 – Process Simulation and Transient Response

The objective of this task is to develop one or more detailed process simulation packages for the CCC ES™ process and incorporate these into the existing baseline CCC process flow diagrams.

The objective of the transient modeling portion of this task is to analyze the transient response of the energy storage system and compare it to transients associated with load leveling and intermittent loads, such as wind and solar.

#### *Task 1 Deliverables*

The deliverables from this task include quantitative process simulation models describing the state (temperature, pressure, composition, and phases) of all significant process streams before and after each unit operation. Ancillary streams such as cooling water, fugitive gases from storage tanks, and makeup refrigerant may be abbreviated or eliminated if they add more clutter than information. Sample model outputs will be discussed in topical reports and technical progress reports.

#### *Task 1 Milestones*

Milestone 1 – Finalized conceptual PFD

Milestone 2 – Fully integrated steady-state model

Milestone 7 – Energy penalty calculated according to established metrics

Milestone 8 – All unit ops functional in transient mode

#### 2.4.2 Task 2 – Energy Analysis of the CCC ES™ process

The objective of this task is to develop detailed process models of the CCC ES™ process and assess the energy demands and storage efficiency relative to the baseline CCC process and alternative energy storage processes. We take pumped storage with nominal overall efficiencies of 76–85% as the best alternative process, where we will assume a round-trip efficiency of 85%. Initial comparisons of CCC ES™ indicate it could exceed this efficiency.

#### *Task 2 Deliverables*

The deliverables from this task include quantitative energy demand estimates for carbon capture in both the energy-storing and traditional modes, with calculations of the effective energy storage

## Non-Confidential Report

efficiency and overall energy demand for carbon capture associated with CCC ES™. Sample estimates will be discussed in topical reports and quarterly progress reports. These reports will include the potential impact on grid management.

### *Task 2 Milestones*

Milestone 3 – Optimized steady-state (SS) energy model

Milestone 4 – Develop energy penalty metrics

Milestone 6 – Finalized skid PFD

Milestone 12 – Obtain quotes and begin purchasing major pieces of equipment

### 2.4.3 Task 3 – Economic Evaluation of the CCC ES™ process

The objective of this task is to complete economic evaluations for the CCC ES™ process, estimating levelized cost of electricity (LCOE) and price structure in a manner similar to our previous analyses and those of the United States Department of Energy (DOE).

One minor change was made to the project plan. The original objective to this milestone was to update the LCOE. The National Energy Technology Laboratory (NETL) of the DOE has published a report entitled “Cost and Performance Baseline for Fossil Energy Plants Volume 1: Bituminous Coal and Natural Gas to Electricity” [3]. SES uses this report as a basis to compare the cost of electricity (COE) for CCC ES™ to competing processes. In past reports, the COE was levelized by accounting for the time value of money in addition to adjusting costs into 2007 dollars. The most current revisions of this report no longer levelize costs, presenting a current COE instead. SES has adopted this convention for this project. The primary objective of this effort is to compare carbon capture technologies and to assess the implementation of carbon capture and storage using the CCC ES™ process. All of this can be done just as effectively without leveling costs.

### *Task 3 Deliverables*

The deliverables from this task include estimated costs of electricity for the CCC ES™ process, including its structure (i.e., capital, fuel, fixed operating, variable operating, transportation, storage, and monitoring components). This analysis will include the potential financial benefits of energy storage in terms of (a) local demand management (load shifting), (b) regional intermittent source management (storing and releasing wind or solar energy), and (c) grid stabilization. These costs become increasingly more difficult to quantify and more subjective in the order listed.

### *Task 3 Milestones*

Milestone 9 – Fully integrated transient model

Milestone 14 – Full mass and energy balance based on P&ID

Milestone 15 – Updated CCC LCOE

Milestone 16 – Calculated CCC ES™ LCOE

## Non-Confidential Report

### 2.4.4 Task 4 – Bench and Skid-scale Demonstrations

The objective of this task is to provide laboratory- and bench-scale demonstrations of the most essential technical steps in the CCC ES™ process. Lab- and bench-scale demonstrations of essential individual process steps are already completed for the CCC process.

#### *Task 4 Deliverables*

The deliverables from this task include laboratory demonstration of CCC ES™. The experimental outcomes will be documented in topical and technical reports, and the experiments themselves will be available for demonstration to any CCEMC personnel willing to travel to them.

#### *Task 4 Milestones*

- Milestone 5 – Transient model demonstration
- Milestone 10 – Capital cost estimates for full-scale major equipment
- Milestone 11 – Finalized skid P&ID
- Milestone 13 – Energy penalty sensitivity analysis
- Milestone 17 – CCC ES™ LCOE sensitivity analysis
- Milestone 18 – Capital equipment purchasing complete
- Milestone 19 – Piping changes to skid implemented
- Milestone 20 – Demonstrate 90% capture utilizing LNG as refrigerant stream
- Milestone 21 – Heat exchanger performance test
- Milestone 22 – Demonstrate 99% capture utilizing LNG as refrigerant stream
- Milestone 23 – Creating a sustained LNG flow rate sufficient to sustain operation
- Milestone 24 – Demonstrate 90% capture for a full simulated load cycle

### 3. Outcomes and Learnings

#### 3.1 Literature review

To date, several technologies have been investigated to remove CO<sub>2</sub> from power plant exhaust. These technologies can be separated into two categories: pre- and post-combustion capture. The energy penalties for these types of carbon capture are included here in Table 1. Pre-combustion technologies include oxy-fuel combustion and chemical looping. Both of these technologies require significant, if not total, modifications of a plant to allow implementation. Post-combustion carbon capture technologies include absorbents (e.g., amine, chilled ammonia), adsorbents (e.g., zeolites, molecular sieve, activated carbon), membranes (e.g., polymeric membranes), and cryogenic processes (e.g., CCC, thermal swing, inertial carbon extraction).

Table 1. Summary of carbon capture energy penalties by technology type (from Ref. 4).

| <b>Process</b>   | <b>Mean<br/>(MJ<sub>e</sub>/kg CO<sub>2</sub>)</b> | <b>Low<br/>(MJ<sub>e</sub>/kg CO<sub>2</sub>)</b> | <b>High<br/>(MJ<sub>e</sub>/kg CO<sub>2</sub>)</b> | <b>References</b> |
|------------------|--|---|--|-------------------|
| Oxy-combustion   | 1.69   | 1.51  | 2.02   | [5,6]             |
| Chemical Looping | -  | -   | -  |                   |
| Absorbents       | 1.72   | 0.97  | 4.20   | [7–16]            |
| Adsorbents       | 3.39   | 2.02  | 5.60   | [7,17]            |
| Membranes        | 1.30   | 0.95  | 1.90   | [18,19]           |
| Cryogenics       | 0.98   | 0.74  | 1.18   | [4,20,21]         |

#### 3.2 Technology Development, Installation and Commissioning

##### 3.2.1 Process Drawings Development

###### *Milestone 1 – Finalized Conceptual PFD*

We created a fundamental process flow diagram (PFD) to facilitate both modeling and construction of the CCC ES™ process.

###### *Milestone 6 – Finalized Skid PFD*

A few details of the PFD underwent several revisions as first attempts at sizing/costing indicated certain systems could not be implemented efficiently at small scale.

###### **R-14 Loop Eliminated**

The R-14 loop was eliminated due to the cost and size of the units required, and was replaced with a chilled water loop and additional sterling cooling instead. This reduces the efficiency of the operating system, but retains the ability to demonstrate the CO<sub>2</sub>-handling aspects. Additional simple heat exchangers were necessary, but are simple to design and manufacture.

###### **Natural Gas Liquefaction with Sterling Cycle Cooler**

A sterling cycle cooler was chosen to liquefy the natural gas. It has a relatively simple operation and greatly reduced the equipment required for a typical LNG liquefaction process. Even though it is less efficient than typical LNG liquefaction processes, considering that LNG is a commercially mature technology at large scales but does not exist at this small scale, substituting

## Non-Confidential Report

the small sterling cooler simplifies construction and operation and reduces cost without compromising the robustness of the process relative to commercial processes.

### *Milestone 11 – Finalized Skid P&ID*

We created a piping and instrumentation diagram (P&ID) to facilitate construction of the CCC ES™ process.

### 3.2.2 Capital Costs

#### *Milestone 18 – Capital Equipment Purchasing Complete*

The equipment was purchased under the cost-sharing contract to prevent cash flow issues associated with items having a longer lead time (some longer than 9 months). The custom LNG dewar and the level sensor shown in Figure 6 were the last pieces of equipment that arrived at SES.



Figure 6. LNG dewar and level sensor.

#### *Milestone 19 – Piping Changes to Skid Implemented*

Installation of the new system required a detailed design to solidify the placement of all major pieces of equipment. Figure 7 shows a CAD drawing of the LNG cold box. All of the braided stainless hose runs are removed for better equipment viewing. The cold box is designed such that it can be removed from the system with relatively little effort.

The installed LNG cold box is shown in Figure 8. The system is designed to operate at 300 psi. Operational pressure will be about half that. All of the instrumentation and controls are designed to operate in a Class 1 Division 2 area (i.e., will not ignite flammable vapors if present). Once

## Non-Confidential Report

every connection was tested at  $-200\text{ }^{\circ}\text{C}$ , the hoses and fittings were insulated. The cold box (red frame in Figure 8) is made to be filled with perlite. Perlite is a white expanded mineral that is often used in the cryogenic industry to insulate processes with complex geometries.

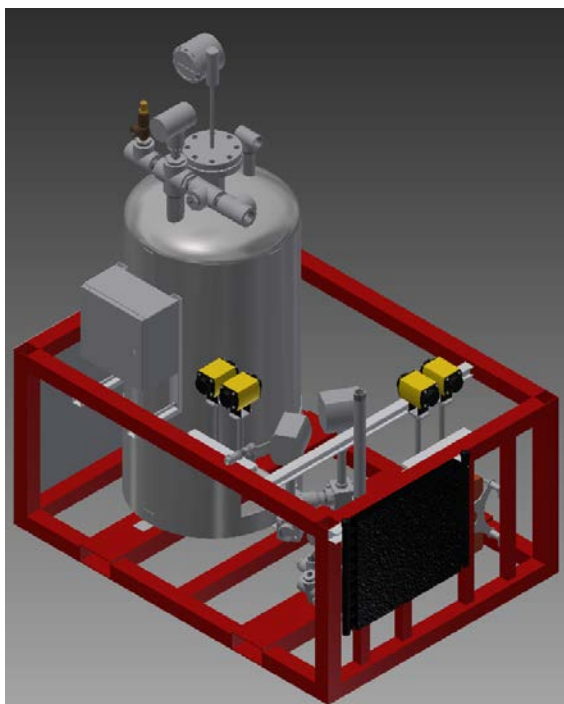


Figure 7. LNG cold box CAD design (all hose runs removed).

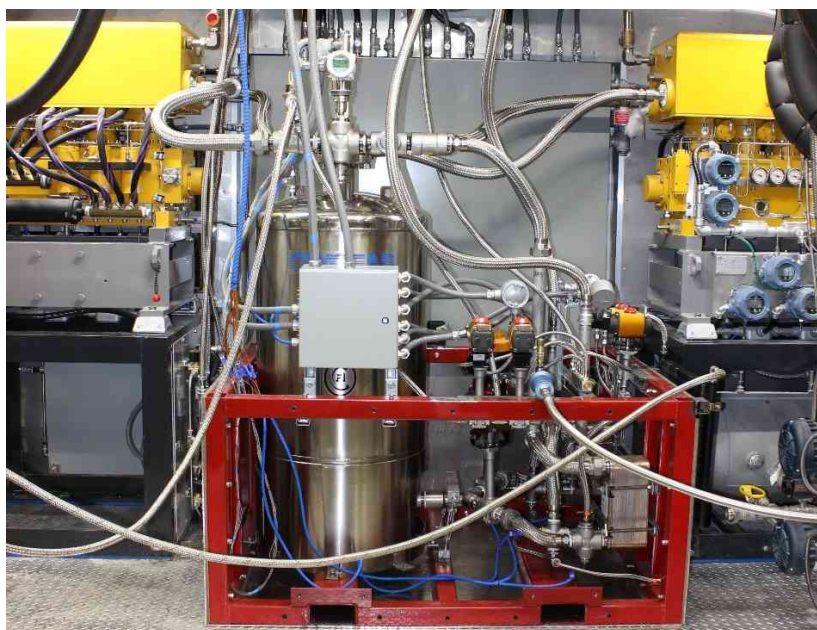


Figure 8. Installed energy storage system (i.e., LNG cold box).

### 3.3 Experimental Procedures/Methodology

CO<sub>2</sub> capture data was gathered using two redundant instruments: an ABB EL 3040 non-dispersive infrared (NDIR) CO<sub>2</sub> detector that is commonly used in industry and a MKS 2030 Fourier transform infrared spectrometer (FTIR) that can provide a redundant CO<sub>2</sub> measurement and can measure NO, CO, NO<sub>2</sub>, SO<sub>x</sub>, and various other combustion- and process-related compounds. The ABB NDIR instrument can measure CO<sub>2</sub> concentrations simultaneously from two CO<sub>2</sub> measurement cells. One cell is dedicated to measuring CO<sub>2</sub> prior to capture and one is used to measure CO<sub>2</sub> after capture (both on a dry basis). The FTIR can only gather data from one source at a time, so the operator manually changes a 3-way valve to change the sample from the inlet to the outlet of the CCC process.

### 3.4 Modeling Details

#### 3.4.1 Process Drawing Development

##### *Milestone 1 – Finalized Conceptual PFD*

We created a series of process drawings to facilitate modeling and construction of the process. A fundamental PFD was created as part of Milestone 1 to set up the process model in Aspen Plus<sup>®</sup> (Aspen). We used this PFD to identify key unit parameters, as well as determine preliminary optimization algorithms. These preliminary models used AA basis.

#### 3.4.2 Fully-Integrated Steady-State Model

##### *Milestone 2 – Fully Integrated Steady-State Model*

The model was developed in accordance with the energy-storage PFD. The approach was to take an existing process concept for liquefying natural gas and model it in Aspen. Adaptations were needed to meet the production needs of the CCC ES<sup>™</sup> process.

##### *Aspen Flow Sheet and Stream Table*

The flow sheet of the model is shown in Figure 9. The Wilson method was used for calculation of the thermodynamic properties.

##### *Natural Gas conditions*

The inlet and outlet of the model are matched with streams L502 and L500, respectively, from the PFD. The flow rate of natural gas into the model, L502, varies throughout the day. The most typical flow rate of natural gas is that of a closed-loop system, and can be estimated by determining the cooling load required to operate the CCC process for a 500 MW power plant. The inlet natural gas temperature is limited by heat integration, and—as determined in the PFD—is limited to the temperature of stream L111. The composition is estimated to be the same as pipeline gas, including the highest allowable CO<sub>2</sub> concentration for a worst-case scenario of the cycle.

##### *Process Unit Conditions*

Each of the units identified in the PFD from the model (Figure 9) are listed below with their modeling conditions. Several units were not modeled because of their low capacity factor (V-502, T-523, G-500, E-513, and C-523) or transient use (TK-503).

Non-Confidential Report

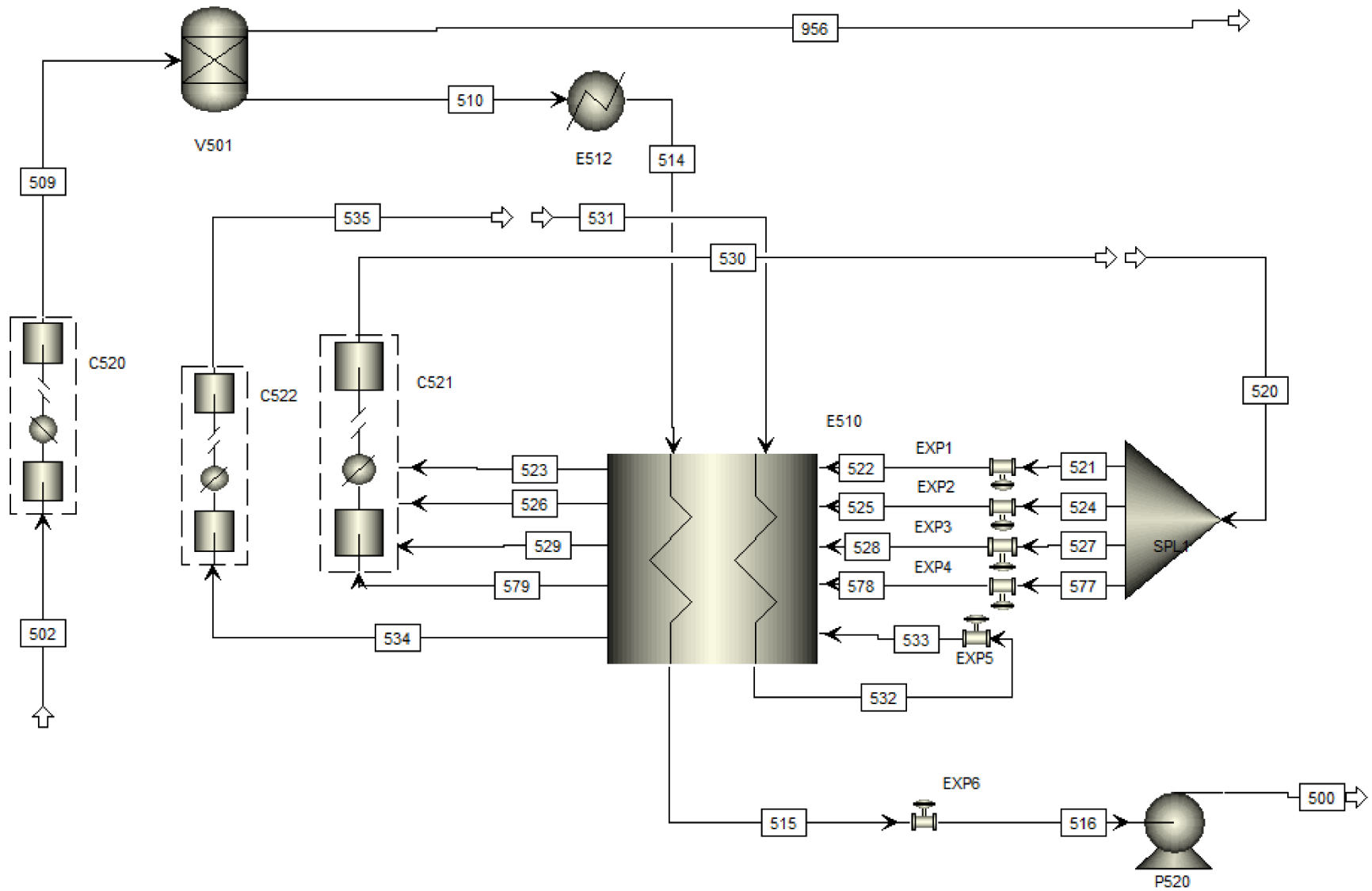


Figure 9. Aspen flow sheet for the CCC EST™ process.

## Non-Confidential Report

### C-520 Natural Gas Booster

The preliminary LNG process design necessitated a high natural gas inlet pressure for comparison with existing LNG processes and to facilitate model convergence.

### V-501 CO<sub>2</sub> Removal

The vessel was modeled as a molecular sieve packed-bed dryer. The pressure drop was determined by preliminary sizing of the vessel to provide a 4-hour operation time at worst-case conditions. Viscosity was estimated to be 0.0152 cp using the Lee, Gonzalez, and Eakin correlation for viscosity [22] and CNGA correlation [23] for the compressibility factor. This provides a worst-case scenario for CO<sub>2</sub> concentration. It is anticipated that natural gas with a lower CO<sub>2</sub> concentration will be available in actual application.

### E-512 Natural Gas Pre-Cooler

A simple heat exchanger with cooling water was chosen to achieve cooling back down to 18 °C.

### E-510 Natural Gas Liquefying Heat Exchanger

The natural gas is liquefied in an aluminum brazed-plate heat exchanger. To visualize the efficiency of the heat exchanger, temperature is plotted on the y-axis and cumulative heating duty on the x-axis. Cooling of the hot stream and warming of the cool stream stay in close proximity throughout the heat exchanger. The minimum temperature difference is 1.55 °C. Although the curves provide adequate efficiency, during optimization, we will be allowing the composition of the mixed refrigerant system to change in order to enhance the thermodynamic efficiency of the heat exchanger.

### P-520 LNG Pump

Within typical operational regimes, the LNG pump will be bypassed because the natural gas loop will act as a closed-loop refrigeration system. However, to provide worst-case energy consumption, the LNG pump is included in the model.

### C-521 Propane Compressor

The propane refrigeration loop is staged with four streams at four pressures to improve the cooling duty match in E-510. Each of the streams enters the compressor at subsequent stages. The propane stream splitter (SPL1) divides the four propane streams into non-equal flow rates. During optimization, we will allow the model to adjust pressures, but maintain constant compression ratios across each stage.

### C-522 Mixed Refrigerant Compressor

The entire stream was introduced into the compressor at the first stage and no special staging was required. This compressor consumes the most significant portion of energy for LNG production and has the most opportunity for contribution to efficiency gains in the LNG production through manipulation of the mixed refrigerant composition and pressure outlet/inlet.

### E-511 Refrigerant Regenerating Heat Exchanger

To best model the practical application, intercoolers and aftercoolers were integrated with each of the refrigerant compressors. Thus, E-511 is eliminated in the model as a stand-alone component, but is integrated into C-521 and C-522.

## Non-Confidential Report

### 3.4.3 Optimized Fully-Integrated Steady-State Model

#### *Milestone 3 – Optimized Steady-State (SS) Energy Model*

In conjunction with Milestone 4, we determined that LNG could be used at higher pressures (i.e., 11.7 bar) while still providing 90% CO<sub>2</sub> capture. The flow sheet is shown in Figure 10 for further details of the operational process and modeling.

#### *Moving CO<sub>2</sub> Removal System and Pipeline Natural Gas Inlet*

To improve the efficiency and accuracy of the model, the CO<sub>2</sub> removal system was moved from processing all of the natural gas to processing only the pipeline natural gas. This allows for a smaller system to be built and operated. Additionally, the pipeline natural gas is mixed in with the natural gas returning from the CCC process after it has been compressed to 21 bar. This modification decreases the energy consumption of the natural gas compressor compared with the previous layout.

A similar change was made at the LNG outlet with a portion being expanded and sent to the tank for storage, while the bulk of the LNG is fed into the CCC process.

#### *Objective Function*

The objective function is defined as the sum of power consumption by the natural gas, propane, and mixed refrigerant compressors normalized against the amount of LNG produced. Initial user improvements were able to achieve an objective of 8.5 kWh/kmol. With application of the SQP and Hessian update optimization algorithms, the model was optimized with 10 variables to achieve an objective of 7.2 kWh/kmol while satisfying all constraints. The energy consumption of the LNG pump, P-520, was not included in the objective function because it will likely only be used in the event of dynamic changes (i.e., start up).

#### *Constraints*

Constraints were added to the model to ensure the practicality of the heat exchanger: For the first constraint, we defined minimum approach temperatures for the hot and cold streams in the liquefaction heat exchanger. The second constraint was added to ensure that at least 98% of the natural gas was liquefied. Since liquefaction is built into the objective function, the optimization yielded 100% liquefaction, as expected.

#### *Milestone 4 – Develop Energy Penalty Metrics*

The model was initially developed to optimize the refrigeration system for traditional CCC. The system was modeled in Aspen. Adaptations for the CCC ES™ cooling system were needed to adjust for different phase-change temperatures of the refrigerant, and thus the cooling scheme is somewhat different, but just as effective in cooling the CL for CO<sub>2</sub> capture.

#### *Refrigerant Selection*

Ethane was chosen as the refrigerant of choice because 1) it is a single-component refrigerant for a single-temperature phase change, 2) the vapor–liquid phase change occurs at near-ambient temperatures and reasonable pressure, and 3) the liquid–vapor phase change occurs at a reasonable pressure at cryogenic temperatures. Other options were analyzed, including CF<sub>4</sub>, NF<sub>3</sub>, and longer chain hydrocarbons.

Non-Confidential Report

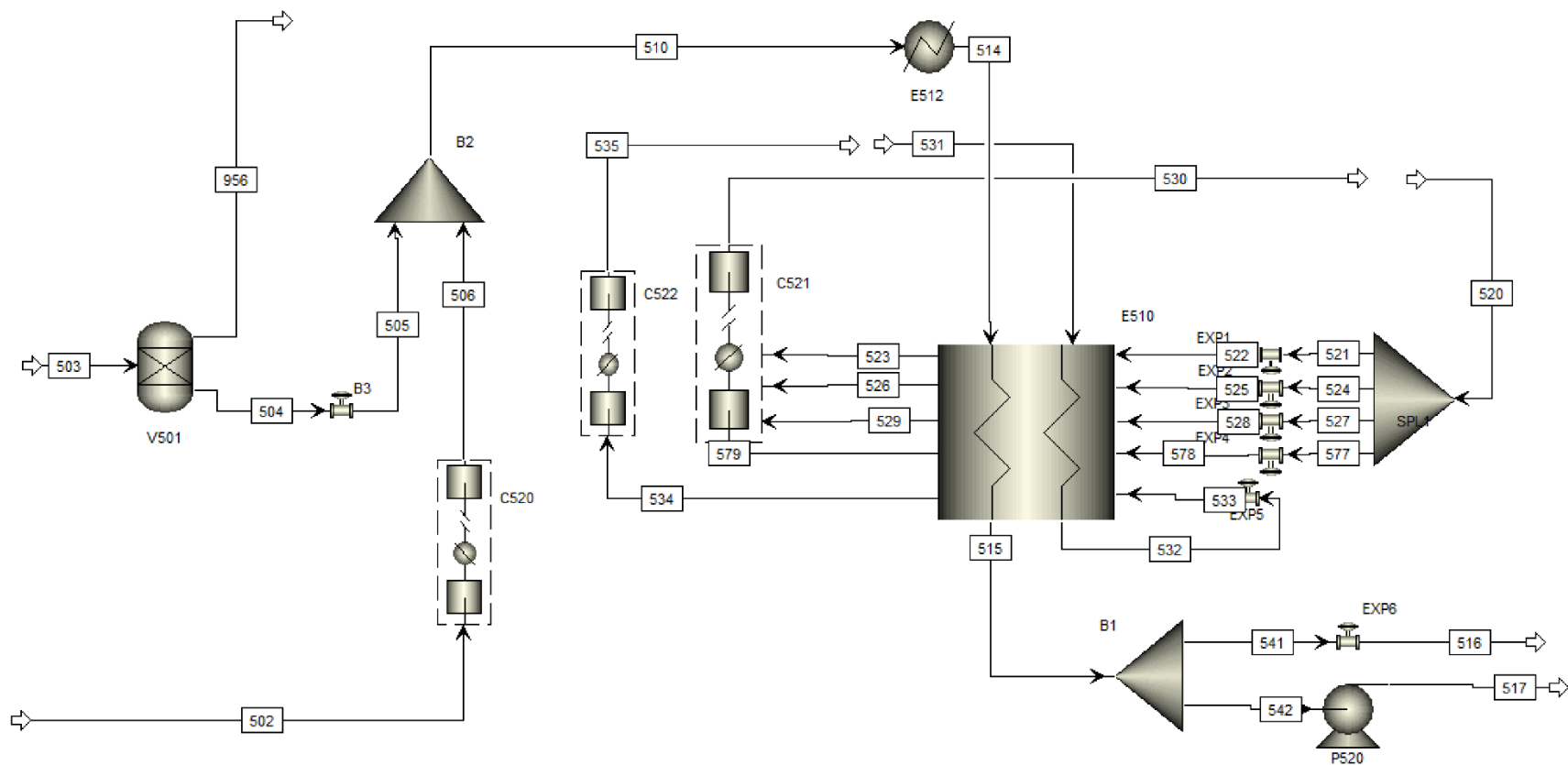


Figure 10. Optimized Aspen flow sheet of the CCC ES™ process

## Non-Confidential Report

While we selected ethane with a CF<sub>4</sub> supporting system for refrigeration, CF<sub>4</sub> is limited to 95% CO<sub>2</sub> capture. If 99% capture is desired, it requires reducing the CF<sub>4</sub> pressure during cryogenic expansion to less than atmospheric pressure.

### Model Description

The flow sheet of the Aspen model (Figure 11) details the refrigeration system of the CCC process. An energy table (Table 2) is included that summarizes the compressor power requirements.

The default Aspen chemical database APV80 PURE27 was found to be unreliable for estimating CF<sub>4</sub> heat capacities at near-ambient pressures and cryogenic temperatures. The APV80 HYSYS database was used instead.

Table 2. Energy table from Aspen model of the refrigeration portion of the CCC ES™ process.

|                            | <b>Units</b> | <b>Net Work Required</b> | <b>Net Cooling Duty</b> |
|----------------------------|--------------|--------------------------|-------------------------|
| Ethane Compressor          | MW           | 25.36                    | -42.31                  |
| CF <sub>4</sub> Compressor | MW           | 47.09                    | -52.11                  |
| <b>Total</b>               | <b>MW</b>    | <b>72.45</b>             | <b>-94.42</b>           |

### Energy Penalty Quantified

The energy penalty metric is defined as the difference in energy consumption of the CCC process in comparison with the CCC ES™ process. Both the CCC and CCC ES™ systems are required to achieve the same cooling duty for the CL. Secondly, each system has a different level of lower-grade cooling and heating and the difference was quantified as a secondary energy penalty metric. If CCC ES™ has more low-grade cooling duty than the CCC process, it could have a net water reduction at the power plant.

### 3.4.4 Transient Modeling

#### *Milestone 5 – Transient Model Demonstration*

The process simulator built in-house at SES—known as the “SES Process Designer”—is now enhanced to allow transient modeling. Prior to this change, only steady-state conditions could be simulated. This enhancement will enable SES to predict the transient behavior of the CCC ES™ process.

For a given process modeled using the SES Process Designer, a transient response is introduced by varying the temperature, pressure, flowrate, and/or composition of one or more streams entering the process with time. Presently, these variations are defined in an external data file read by the program. The added functionality of the process simulator is described below.

### Existing Unit Ops

Existing steady-state unit ops continue to function in the transient mode as if the streams entering each unit are at steady-state conditions. Thus, these unit ops do not introduce any additional transient responses into the process themselves. Strictly speaking, these unit ops may introduce transient phenomena into the process, but on time scales too short to be of interest. Some examples of these unit ops are pumps and valves.

Non-Confidential Report

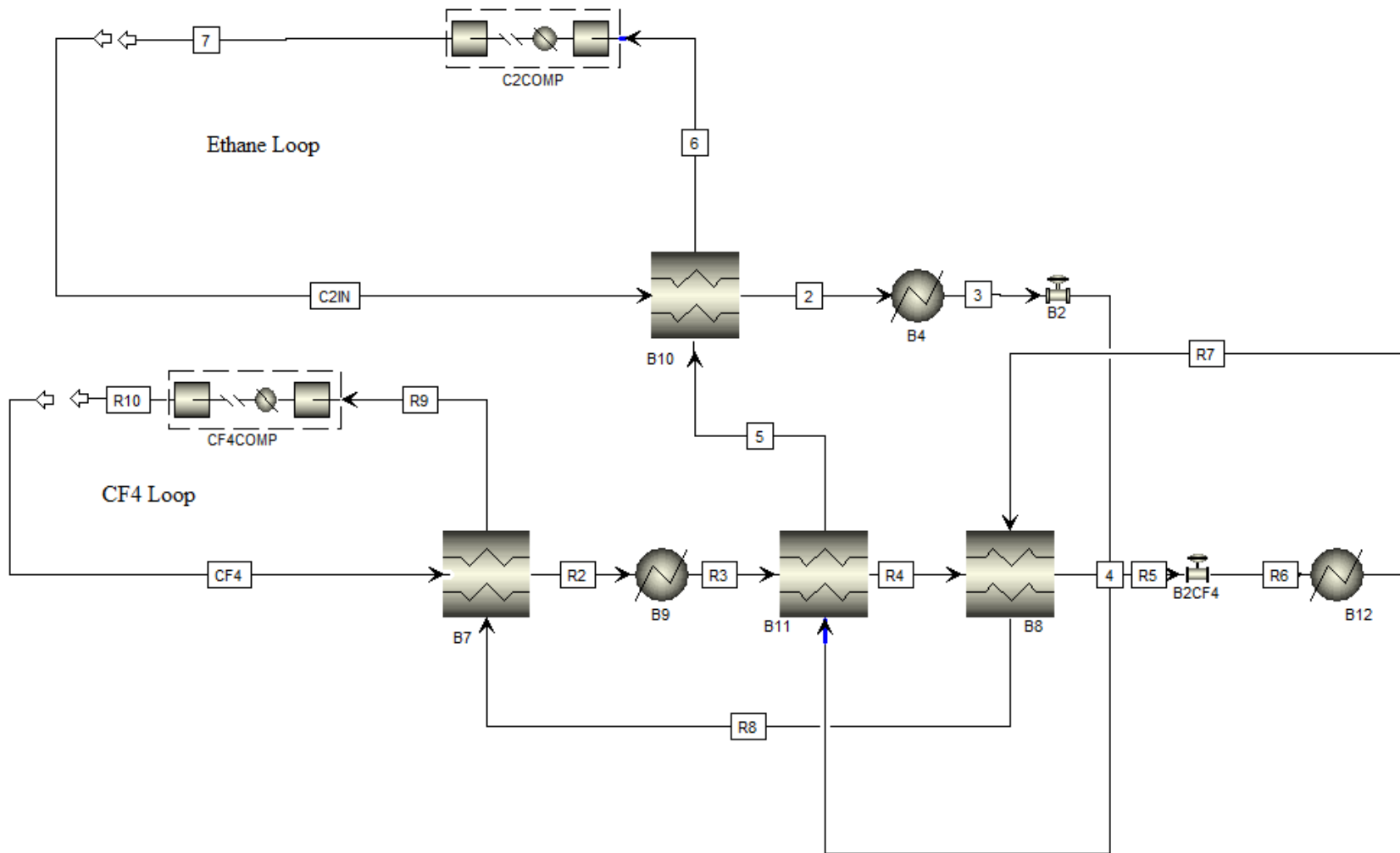


Figure 11. Aspen flow sheet showing refrigeration portion of the CCC ES™ process.

## Non-Confidential Report

### New Transient Unit Ops

Some new unit ops that function in the full transient mode have been added to the simulator. These transient unit ops are capable of introducing or transferring transient responses with long time scales. The new transient unit ops that have been added are the continuous stirred tank, thermal mass, and buffer.

### Continuous Stirred Tank

The continuous stirred tank is a variable-volume, fully-mixed tank. When the temperature, volumetric flowrate, or composition of an input stream changes, the tank can be used like a “capacitor” to dampen process changes. The tank can also be used to store excess product when production is high or demand is low, or release stored product when production is low or demand is high. In the CCC ES™ process, the tank stores excess LNG during off-peak times, and releases LNG during peak times.

### Thermal Mass

The thermal mass dampens temperature changes in the process. Conceptually, it is similar to an “energy tank” whose design equations are similar to those of the continuous stirred tank. It can be used in conjunction with nearly any unit to introduce a “thermal swing” response into the process. The only information required is an estimate of the mass and heat capacity of the unit.

### Buffer

The buffer introduces a time-delay into the process. Material entering the buffer is held for a specific period of time, and then released. In process flow terms, this is equivalent to perfect plug-flow. This unit can be used to model long piping runs.

### *Milestone 7 – Energy Penalty Calculated According to Established Metrics*

### Heat Exchanger

The transient heat exchanger is modeled as a two-stream (co- or counter-current) heat exchanger. The heat exchange surface is a rectangular plate; fluid flows parallel to and on each side of the plate. The thickness, length, and width of the plate and the thickness of the flow channels are all adjustable. Convection coefficients are calculated using accepted empirical correlations for internal flow, using the hydraulic diameter of the flow channel to calculate the Reynolds number. The transient solution is obtained through a system of PDEs. Figure 12 shows the temperature distribution within a heat exchanger at a particular time step.

Most existing unit ops have parameters that can be varied with time to introduce transient phenomena, or to respond to transient effects occurring elsewhere in the process. This is done with a C-style scripting language and can simulate, conceivably, any kind of transient effect or control scheme.

## Non-Confidential Report

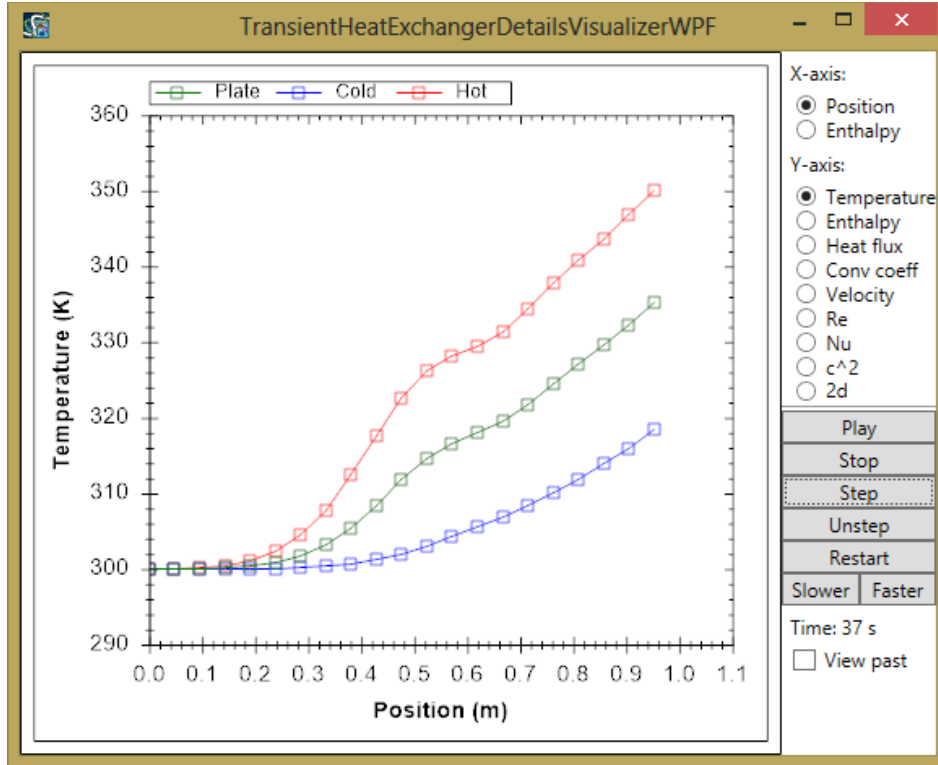


Figure 12. Temperature distribution in a heat exchanger prior to reaching steady state.

### 3.4.5 Energy and Cost Calculations

#### *Milestone 13 – Energy Penalty Sensitivity Analysis*

The energy penalties were determined using Aspen simulations of the CCC and CCC ES<sup>TM</sup> processes. The energy penalty is based on 90% CO<sub>2</sub> capture at a 550 MW coal-fired power plant. The previously reported energy penalties were 99.5 and 98.1 MW for traditional and energy-storing versions of CCC, respectively. With updates, energy penalties are now 96.2 and 96.6 MW, respectively.

The process variables (refrigerant composition, system pressure, and primary heat exchanger exit temperature) were adjusted by 5%, provided the model did not become over-constrained. For example, if the support refrigeration for the traditional CCC process decreased by 5%, there would be insufficient cooling in the heat exchanger and the process model would crash; therefore its sensitivity was tightened to +/- 1% rather than +/- 5%.

The primary refrigerants for the CCC and CCC ES<sup>TM</sup> processes are CF<sub>4</sub> and LNG, respectively. A secondary refrigerant loop was necessary for both primary refrigeration systems to liquefy the primary refrigerant at cold temperatures and is termed the mixed refrigerant. The mixed refrigerant includes methane, ethane, and propane.

#### *Milestone 14 – Full Mass and Energy Balance Based on P&ID*

The basis of the CCC ES<sup>TM</sup> simulation's flue gas is taken from Case 12 of the 2013 NETL report [3]. Here, we present the case for a 550 MW net output coal-fired power plant with carbon

## Non-Confidential Report

capture provided by CCC ES™. For the sake of comparison with competing technologies, the simulation achieves 90% CO<sub>2</sub> capture.

For this simulation, cooling water is available at 16 °C, to maintain consistency with the NETL report. However, particular installations may have different availability and cooling water temperature is an active process constraint.

Results from various thermodynamic packages were compared with existing binary data at the closest operating conditions. The Predictive Soave Redlich Kwong thermodynamic package was selected because it is the closest match to experimental data and it has the most conservative CO<sub>2</sub> capture predictions.

Heat exchange in the simulation occurs in several unit operations. Three of the heat exchangers have 3+ streams and conform to guidelines received from a leading brazed aluminum heat exchanger manufacturer, including a maximum of 3% solids in process streams. A 1 °C minimum internal approach temperature is maintained throughout the heat exchangers. In the case of shell and tube heat exchangers, a 5 °C minimum internal approach temperature is maintained.

The melting CO<sub>2</sub> heat exchanger is similar in design to a jacketed stirred tank with the CF<sub>4</sub> condensing in the jacketing tubes while the solid melts and is stirred on the inside of the tank. A conservative approach is taken by simulating this as a co-current heat exchanger with the limitation of a 1 °C minimum internal temperature approach. It is conceivable that this heat exchange could take place in a countercurrent fashion, which would improve the efficiency, but initial work undertaken at SES shows that too much energy was expended forming solid CO<sub>2</sub> to a traditional heat exchanger shape.

Pressure drops of 5 kPa are imposed on every process stream in every heat exchanger and process vessel. In the case of the dryer, a 7 kPa pressure drop is imposed, based on its design as a packed bed dryer. The desublimating heat exchanger is simulated using 0.37 kPa pressure drop per stage.

The blower and CO<sub>2</sub> compressor are simulated as single-stage compressors, operating at 90% polytropic efficiency with no cooling. The CF<sub>4</sub>, natural gas, and mixed refrigerant compressors are simulated as 8-stage compressors, operating at 90% polytropic efficiency with interstage cooling using 16 °C cooling water. The efficiency and number of stages have a significant effect on the primary energy consumption of the CCC ES™ process and are in accordance with established performance specifications. The aggressive and demonstrated performance simulation specifications are conservative relative to full-scale implementation. Intercoolers conformed to the 5 °C minimum internal temperature approach and 5 kPa pressure drop. Pumps operate with 95% efficiency.

The modeled CL is isopentane (2-methylbutane). However, available vapor pressure data for isopentane is only available down to -85.78 °C. Because of the uncertainty in extrapolating vapor pressure down to the temperature required for 90% CO<sub>2</sub> capture, measurements must be made to ensure compliance with hydrocarbon emission standards. In the event that CL levels are

## Non-Confidential Report

deemed too high in the nitrogen-rich exhaust gas, an alternative CL mixture will achieve reduced hydrocarbon emissions.

### *Milestone 15 – Updated CCC LCOE*

#### Energy Performance Comparisons

One of the key aspects of any carbon capture and storage (CCS) technology is the parasitic load that must be absorbed by the power plant for the separation and pressurization of CO<sub>2</sub>. The efficiency of the separation and pressurization steps are manifest in the cost of generated electricity. A power plant with a higher parasitic load requires more fuel to achieve the same output. The plant itself, and all of its components, must be larger to handle these larger fuel flow rates. Additionally, the amount of gas that then needs to be processed increases, thus requiring an increase in size of both the equipment and total loading for the CCS technology.

The NETL report [3] contains detailed mass and energy balances for twelve power plant configurations, each labelled with a case number. In addition to mass and energy balances, each case contains detailed estimates for capital expenditures, operating costs, consumables and fuel costs, etc. These numbers are then amortized to create a reported cost of electricity, allowing for a financial comparison between the different power plant options on the same terms. Cases 12 and 11 of this report discuss a supercritical (SC) pulverized coal (PC) power plant with and without carbon capture, respectively, and are used as the baselines for comparison in this report. Case 11 is the detailed study of a greenfield SC PC power plant installation without carbon capture, providing a baseline for energy and cost comparisons. Case 12 is the detailed study of a greenfield SC PC power plant installation with carbon capture. The CCS technology chosen for the Case 12 study is an amine CO<sub>2</sub> capture system utilizing monoethanolamine (MEA) that captures 90% of the CO<sub>2</sub>. In both cases, the net power generation capacity of the power plant is 550 MW. All mass and energy balance numbers as well as all financial figures are quoted from or based on the Revision 2a, September 2013 version of the report [3]. To stay as close as possible to the report, all CCC simulations were carried out at 90% capture, although the CCC process can easily cope with capture efficiencies at and above 99%.

Detailed thermodynamic process simulations quantify the energy penalty associated with utilizing the CCC technology. These simulations have been independently verified by several technology leaders in industry and academia. For the process simulations detailed in this report, turbomachinery isentropic efficiencies, including the refrigerant compressors, were assumed to be 90%. All pump efficiencies were assumed to be 85%. All of these assumption lie within the ranges of commercially available equipment.

There are several ways to measure the energy penalty associated with a CCS technology. This analysis uses the energy penalty of CCC and compares it to the published MEA system in terms of the processed output CO<sub>2</sub> stream and in terms of the effect on the power plant. The first of these is presented in the form of electric gigajoules required per metric ton of CO<sub>2</sub> produced (GJ<sub>e</sub>/tonne). This number is instructive in that it provides a scalable value that can then be applied to other similar flue gas streams. The effect on the power plant is presented in terms of the percent increase in the net plant high heating value (HHV) heat rate. This was chosen because it is a key parameter stated in the NETL report and used in costing simulations. The net

## Non-Confidential Report

plant HHV heat rate is the amount of thermal energy (based on the HHV of the fuel) input per unit of electricity output, and is presented in the NETL report in units of BTU/kWh. This number is instructive because it takes into account the effect of decreasing the total amount of fuel required to achieve the same net power plant output.

### 3.4.6 Sensitivity Analysis

#### *Milestone 13 – Energy Penalty Sensitivity Analysis*

##### *Preliminary Analysis*

We performed a preliminary sensitivity analysis based on the Aspen models described above. Important features of the results are:

- 1) No case has both a lower net work required and higher Heat exchanger minimum internal temperature approach (HX MITA) baseline case. This confirms that the optimization was able to find the optimum where no single variable change is able to improve the optimum.
- 2) The maximum net work required (i.e., energy penalty) is only 2% higher than the baseline scenario. This indicates that the process is relatively robust to process variations within the range tested here (generally +/- 5%).
- 3) While CCC has a lower maximum net work required (97.6 MW) than CCC ES™ (98.8 MW), this occurs when the process variable primary Component A flow was varied by 2% rather than the full 5% of its baseline value. Otherwise, CCC and CCC ES™ have similar sensitivities.
- 4) No case has a HX MITA that significantly drops below the lower threshold of 0.5 °C (minimums of 0.46 and 0.47 °C).

#### *Milestone 16 – Calculated CCC ES™ LCOE*

SES performed a detailed sensitivity analysis of the CCC ES™ process. Key process parameters were identified that affect both the process parasitic load and the calculated COE. The parameters identified to be changed were the CO<sub>2</sub> inlet percentage, CO<sub>2</sub> capture efficiency, cooling water temperature, natural gas and mixed refrigerant turbine efficiencies, minimum internal approach temperatures for the multi-stream heat exchangers, and pressure drop through the heat exchangers, as well as efficiencies of the blower and the CF<sub>4</sub>, natural gas, and mixed refrigerant compressors. Table 3 shows the levels that were set for each process parameter at the base level and for two variation levels. The basic philosophy of a sensitivity analysis is to determine the effect of a design change or process perturbation. Therefore, a typical perturbation would include both an increase and a decrease from the baseline. The base levels are associated with those of a 550 MW coal-fired power plant. The CO<sub>2</sub> inlet percent was only decreased because we assumed that coal flue gas would be the highest concentration of CO<sub>2</sub> where CCC ES™ would be used. In the case of the heat exchanger approach temperature, they were already designed with the minimum approach temperature (1 °C) that is common to brazed aluminum heat exchangers. The effect of increasing the pressure drop through the system was studied previously under other funding associated with the CCC compressed flue gas (CCC CFG™) process. It is reported here because the effect is large and it was felt that it should be reported even though the CCC ECL™ and CCC CFG™ processes are not direct analogues. Only one

## Non-Confidential Report

level was studied because the base level and variation 1 brackets most of the reasonable values for pressure drop through the system.

Table 3. Process parameters for sensitivity analysis

| Variable                              | Units | Base Level | Variation 1 | Variation 2 |
|---------------------------------------|-------|------------|-------------|-------------|
| CO <sub>2</sub> inlet Percent         | (%)   | 16         | 12          | 14          |
| CO <sub>2</sub> Capture Percentage    | (%)   | 90         | 89          | 91          |
| Cooling Water Temp                    | (°C)  | 16         | 8           | 30          |
| NG Turbine Efficiency                 | (%)   | 92         | 89          | 94          |
| MR Turbine Efficiency                 | (%)   | 92         | 89          | 94          |
| Approach Temperatures                 | (°C)  | 1          | 2           | 4           |
| Pressure Drop                         | (kPa) | 5          | Hi          | n/a         |
| CF <sub>4</sub> Compressor Efficiency | (%)   | 90         | 85          | 92          |
| NG Compressor Efficiency              | (%)   | 90         | 85          | 92          |
| MR Compressor Efficiency              | (%)   | 90         | 85          | 92          |
| Blower                                | (%)   | 90         | 85          | 92          |

### Energy Sensitivity

Using the base-level values, the energy used for capturing 90% CO<sub>2</sub> from the flue gas is 82,593 kWe. This corresponds to an energy penalty of 0.738 GJ<sub>e</sub>/tonne CO<sub>2</sub>. Table 4 gives a summary of the effect on energy penalty resulting from each scenario, which are also visually represented in Figure 13.

The increase in energy penalty is most drastic when changing the inlet CO<sub>2</sub> percentage, minimum internal approach temperatures, and adding significantly more pressure drop to the system. The largest energy penalty decreases are seen by adjustments in the cooling water temperature and CO<sub>2</sub> capture percentage.

Table 4. Summary of energy penalty

| Variable                              | Energy (kWe) |             |             | Energy Penalty (GJ <sub>e</sub> /tonne) |             |             |
|---------------------------------------|--------------|-------------|-------------|---|-------------|-------------|
|                                       | Base Level   | Variation 1 | Variation 2 | Base Level                              | Variation 1 | Variation 2 |
| CO <sub>2</sub> Inlet Percent         | 82,594       | 76,905      | 80,213      | 0.738                                   | 0.920       | 0.819       |
| CO <sub>2</sub> Capture Percentage    | 82,594       | 78,718      | 83,833      | 0.738                                   | 0.711       | 0.740       |
| Cooling Water Temp                    | 82,594       | 80,256      | 86,420      | 0.738                                   | 0.717       | 0.772       |
| NG Turbine Efficiency                 | 82,594       | 82,752      | 82,551      | 0.738                                   | 0.738       | 0.737       |
| MR Turbine Efficiency                 | 82,594       | 82,564      | 82,529      | 0.738                                   | 0.737       | 0.737       |
| Approach Temperatures                 | 82,594       | 86,461      | 96,667      | 0.738                                   | 0.772       | 0.863       |
| Pressure Drop                         | 82,594       | 93,199      | n/a         | 0.738                                   | 0.832       | n/a         |
| CF <sub>4</sub> Compressor Efficiency | 82,594       | 84,229      | 81,921      | 0.738                                   | 0.752       | 0.732       |

Non-Confidential Report

| Variable                 | Energy (kWe) |        |        | Energy Penalty (GJe/tonne) |       |       |
|--------------------------|--------------|--------|--------|----------------------------|-------|-------|
|                          | 82,594       | 83,657 | 82,132 | 0.738                      | 0.747 | 0.734 |
| NG Compressor Efficiency | 82,594       | 83,795 | 82,082 | 0.738                      | 0.748 | 0.733 |
| Blower                   | 82,594       | 83,390 | 82,231 | 0.738                      | 0.745 | 0.734 |

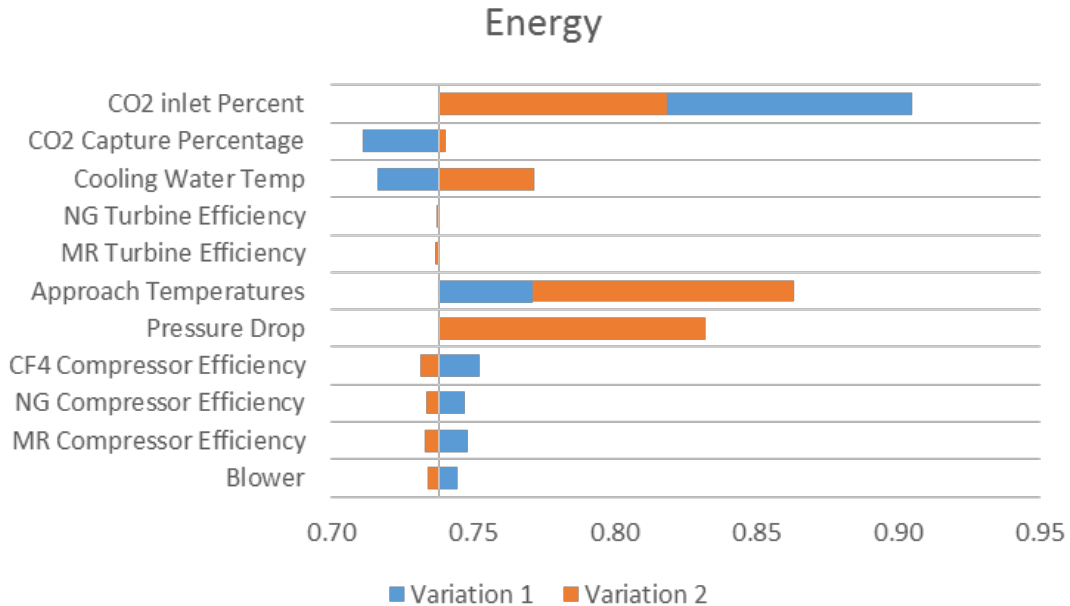


Figure 13. Changes in energy penalty.

Cost of Electricity

Using Aspen, capital cost estimates were collected for each scenario. These capital costs were amortized along with operating costs, fuel costs, and the costs of transportation, storage, and monitoring for the sequestered CO<sub>2</sub> to calculate the COE. The results are presented in Table 5 and Figure 14.

Table 5. COE sensitivity summary.

| Variable                              | COE (¢/kWh) |            |             |
|---------------------------------------|-------------|------------|-------------|
|                                       | Variation 1 | Base Level | Variation 2 |
| CO <sub>2</sub> Inlet Percent         | 9.18        | 9.00       | 9.08        |
| CO <sub>2</sub> Capture Percentage    | 8.93        | 9.00       | 9.03        |
| Cooling Water Temp                    | 8.97        | 9.00       | 9.06        |
| NG Turbine Efficiency                 | 9.00        | 9.00       | 8.99        |
| MR Turbine Efficiency                 | 9.00        | 9.00       | 9.00        |
| Approach Temperatures                 | 8.88        | 9.00       | 8.95        |
| Pressure Drop                         | 9.16        | 9.00       |             |
| CF <sub>4</sub> Compressor Efficiency | 9.02        | 9.00       | 8.99        |

## Non-Confidential Report

| Variable                 | COE (¢/kWh) |      |      |
|--------------------------|-------------|------|------|
| NG Compressor Efficiency | 9.01        | 9.00 | 8.99 |
| MR Compressor Efficiency | 9.01        | 9.00 | 8.99 |
| Blower                   | 9.01        | 9.00 | 8.99 |

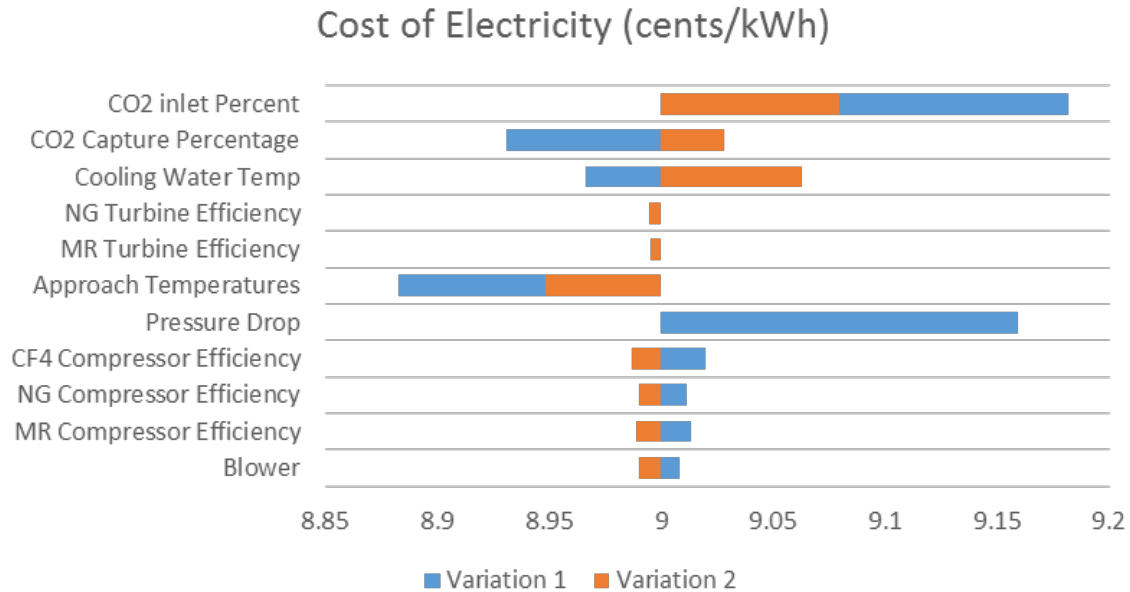


Figure 14. COE changes with variation of process variables.

The biggest changes in cost are similar to the biggest changes in energy. For a lower CO<sub>2</sub> inlet concentration, the cost increases because a larger total flow rate of gas needs to be treated. Interestingly, even though the minimum internal approach temperatures have a higher energy penalty, the total COE decreases. This is because the capital cost of the heat exchangers decreases with a larger approach temperature. Less surface area is required to achieve the same total heat transfer because the larger temperature differential compensates for the decrease in surface area. Because the heat exchangers represent such a large fraction of the capital cost, the cost savings overcomes the extra cost due to the increase in energy penalty.

### 3.4.7 Heat Exchanger Efficiency

#### *Milestone 21 – Heat Exchanger Performance Test*

Heat exchanger efficiency is used here conceptually to describe a change in availability or thermodynamic ability to do work. Specifically, heat exchanger efficiency is the difference in Gibbs energy between the streams entering and leaving a heat exchanger normalized by the largest possible difference in the Gibbs energy. The largest possible difference occurs if all the streams come to the same temperature. These analyses assume there are no heat losses or gains between the exchanger and the environment. This assumption means the steady-state enthalpy of the incoming stream equals that of the outgoing stream. Therefore, the Gibbs energy difference becomes a difference in the product of the temperature and entropy. The steady-state mass flow

of the incoming streams also equals that of the exiting streams, so the specific efficiency can be written in terms of the specific entropies and temperatures. The mathematical description becomes

$$\begin{aligned}\eta &= 1 - \frac{\sum_{outlet} m_i \hat{g}_i - \sum_{inlet} m_i \hat{g}_i}{\sum_{eq} m_i \hat{g}_i - \sum_{inlet} m_i \hat{g}_i} = 1 - \frac{(\Delta Ts)_{obs}}{(\Delta Ts)_{eq}} \\ &= 1 - \frac{\sum_{outlet} T_i m_i \hat{s}_i - \sum_{inlet} T_i m_i \hat{s}_i}{\sum_{eq} T_i m_i \hat{s}_i - \sum_{inlet} T_i m_i \hat{s}_i}\end{aligned}\quad (1)$$

where  $(\Delta Ts)_{obs}$  represents the net change in the product of temperature and entropy observed in the streams,  $(\Delta Ts)_{eq}$  represents the entropy change that would occur if the streams came to thermal equilibrium,  $\sum_{outlet} T_i m_i \hat{s}_i$  represents the sum of the product of the temperature, mass flow rate, and specific entropy summed over all outlet streams,  $\sum_{inlet} T_i m_i \hat{s}_i$  represents a similar sum over all inlet streams, and  $\sum_{eq} T_i m_i \hat{s}_i$  represents this product summed over outgoing streams at the equilibrium temperature, that is, the temperature that results from all streams reaching thermal equilibrium. This efficiency is unity if the inlet and outlet streams transfer heat with no temperature difference (ideal heat exchanger) and is zero if all outlet streams come to the same equilibrium temperature, which would be the poorest possible heat exchanger performance from an efficiency or entropy point of view.

### 3.5 Results of Experiments, Model Simulations

#### 3.5.1 Refrigeration System Design

##### *Milestone 1 – Finalized Conceptual PFD*

Identification of C<sub>3</sub>MR process for NG liquefaction in CCC ES™.

##### *Milestone 4 – Develop Energy Penalty Metrics*

Identification of the operating conditions of the CCC process without the constraint of an LNG refrigerant for energy storage purposes. The overall energy consumption of the process is used as a baseline for comparison to help quantify the added energetic cost of adding the energy storage feature to CCC. The ethane-based CCC refrigeration system delivers 51.3 MW of cooling duty to the CL over a temperature range of -125 to -122 °C. The CF<sub>4</sub>, which delivers the cooling duty to the CL, is used not only to transfer the cooling duty of the ethane cycle, but also transfers the cooling duty of the solid CO<sub>2</sub> melting. Thus the CF<sub>4</sub> stream has two essential purposes that would change the CF<sub>4</sub> operating conditions if optimized for only one purpose.

#### 3.5.2 Energy and Cost Requirements

##### *Milestone 7 – Energy Penalty Calculated According to Established Metrics*

The models were developed and optimized in Aspen, Hysys, and Unisym. The energy consumption of the CCC and CCC ES™ processes after optimization were 99.5 and 98.1 MW, respectively. The energy consumption difference between the two processes is near 1%. When accounting for the remainder of the process energy consumption, it results in a -0.04% energy penalty for the energy storage system. That is, the CCC ES™ system consumes slightly less (essentially the same) energy as the non-energy-storing CCC system.

## Non-Confidential Report

While the two systems have similar energy consumption at steady-state operation, the transient operation of CCC ES™ could increase the energy penalty of the energy storage system. Currently, both models are designed to satisfy a minimum approach temperature of 2.0 °C in the heat exchangers. Transitions through transient load conditions may increase this minimum approach temperature for the CCC ES™ process, resulting in increased compressor loads. However, we have developed some supplemental heat exchanger designs that could increase both the efficiency and speed through transients.

### *Milestone 10 – Capital Cost Estimates for Full-Scale Major Equipment*

Capital costs for each major piece of equipment were first estimated with pricing correlations, and then estimated using Aspen Plus Economic Analysis as a secondary estimate. Any unit estimated to be greater than 1% of the total equipment cost was estimated further by obtaining budgetary quotes from vendors.

The models created in Aspen for Milestones 3 and 7 were used to appropriately size the equipment for cost estimation with industry correlations and the equipment analysis package integrated into Aspen.

We used preliminary costing correlations from *Analysis, Synthesis, and Design of Chemical Processes* [24]. Costs were adjusted to 2012 dollars using CEMCI indexes. An industry correlation created by the Brattle Group was used for the natural gas simple-cycle equipment. The correlation stems from the analysis of five recently built and commissioned natural gas simple-cycle power plants.

We obtained manufacturer quotes for the compressors. Due to the large amount of energy storage, the mixed refrigerant compressor is near the cutting edge of power rating for large compressors. Thus, if compressors were needed for a 1+ GW power plant, it may require multiple compressors in parallel, resulting in cost estimation changes for multiple pieces of the same equipment rather than scaling a single piece of equipment in size.

A manufacturer's quote for the primary natural gas liquefying heat exchanger was obtained. Pricing fluctuations are particularly likely, as indicated specifically in communications with the manufacturer, as the number of manufacturers for this realm of heat exchanger are limited and are often tied to long-term projects for LNG plants.

Instead of a manufacturer quote for the natural gas simple-cycle equipment, pricing information was pulled from a 144 MW simple-cycle project as recorded and published by the URS Washington Division Internal Cost Estimation Database [25].

The primary capital costs for CCC ES™ at full scale (installed on a net 550 MW power plant) are available in

Table 6. Costs are dominated by the natural gas compressor, mixed refrigerant compressor, natural gas liquefying heat exchanger, and natural gas simple cycle equipment. These four

## Non-Confidential Report

groups of equipment account for over 99% of the project capital cost. Of most particular importance is the mixed refrigerant compressor, which accounts for over 50% of the total equipment cost.

Table 6. Summary of major equipment costs.

| Unit               | Unit Description                         | Purchased Cost |              |              | Best Estimate       |
|--------------------|--|----------------|--------------|--------------|---------------------|
|                    |  | Aspen          | Correlation  | Mfg Quote    |                     |
| C-570              | Natural Gas Compressor                   | \$12,257,000   | \$4,467,000  | \$8,006,456  | \$8,006,456         |
| C-700              | Mixed Refrigerant Compressor             | \$57,054,239   | \$8,263,000  | \$38,710,950 | \$38,710,950        |
| E-510              | NG Liquefying Heat Exchanger             | \$4,245,200    | \$5,632,000  | \$4,700,000  | \$4,700,000         |
| P-526              | LNG Pump                                 | \$31,900       | \$9,586      | \$0          | \$31,900            |
| TK-503             | LNG Storage Tank                         | \$0            | \$130,700    | \$0          | \$130,700           |
| V-501              | CO <sub>2</sub> Mol Sieve Vessel         | \$42,400       | \$10,980     | \$0          | \$42,400            |
| V-502              | NG Particulate Filter                    | \$313,400      | \$61,870     | \$0          | \$313,400           |
| NGSC-1             | NG Simple Cycle<br>(C-824, E-513, T-523) | \$0            | \$27,399,450 | \$23,400,000 | \$23,400,000        |
| <b>Grand Total</b> |  |                |              |              | <b>\$75,335,806</b> |

The incremental cost of incorporating energy storage into CCC is the LNG storage tank and pump, which account for about 0.2% of the total equipment capital cost. The compressors, heat exchanger, and vessels are direct replacements of equipment that would be necessary for a typical CCC installation and are not included as part of the incremental energy storage cost. Accounting for the incremental increased size of the compressors, heat exchanger, and vessels to handle the large, transient, energy-storing loads is accounted for below and is quantified in the LCOE calculations shown in Figure 16. The natural gas simple-cycle equipment is deemed as additional power production capacity and is not included as incremental equipment necessary for energy storage since they would not be necessary if natural gas were simply stored in the existing pipeline network.

### *Milestone 15 – Updated CCC LCOE*

The CCC process is a fully retrofitable post-combustion technology for removing CO<sub>2</sub> from any stationary source. While the CCC process requires essentially no changes to the upstream plant, there are several integration steps that provide significant ancillary benefits compared with

## Non-Confidential Report

existing systems. Most of these involve either removing existing process steps or very simple low-grade heat and cooling integrations. One of the core ancillary benefits of CCC is that it can replace current state-of-the-art pollutant removal technologies and capture all criteria pollutants, including Hg and air toxics, with the notable exceptions of CO and NO, more efficiently than current best available control technologies. Since CCC is able to capture pollutants so effectively, it has the capacity to replace the FGD unit in a greenfield installation and will bring retrofitted plants well past current US standards for pollutant levels of the stated compounds.

The ability to replace the FGD unit also allows for additional integration that can vastly improve power plant efficiency. Current greenfield coal-fired power plants utilize steam to heat the boiler feed water back to the temperature at which point it enters the coal boiler. If there is no FGD unit, the flue gas exiting the bag house in a power plant that utilizes CCC must nevertheless be cooled to ambient temperatures. Rather than using additional cooling water, this cooling can be performed in a counter-current heat exchanger with the boiler feed water, a stream that benefits from the low-grade heat that can be extracted from the flue gas. This increases the flow rate of steam through the low-pressure turbine by decreasing the load of the heat recuperators, and improves the cycle efficiency of the power plant. The energy penalty and cost of CCC can also decrease via the removal of the FGD and implementation of boiler feed water heating. The specific effect of these integrations will be addressed in detail later.

### Energy Performance of CCC

The energy penalty associated with CCC is due exclusively to the work needed to power the compressors and pumps in the process. As such, summing the total work of all compressors and pumps yields the total energy required for the CCC process. Table 7 itemizes the parasitic loads in the CCC process with an initial inlet gas matching that reported in the NETL report for a net 550 MWe plant [3]. As expected, flue gas compression and the work of the refrigerant compressors make up the vast majority of the parasitic load.

The real benefit of the CCC numbers can be seen in the established energy metrics stated above. In terms of the processed outlet stream, the energy penalty of CCC is 0.714 GJ/tonne. The calculated net HHV heat rate for CCC is 10,144 BTU/kWh, corresponding to a parasitic load of 14.4%. The parasitic load of either CCC process as-is, without any additional integration, is approximately half of the corresponding parasitic load of the amine process.

Table 7. List of parasitic loads for CCC.

| <b>Energy Source</b>    | <b>Work<br/>(MW)</b> |
|-------------------------|----------------------|
| Flue Gas Compression    | 16.3                 |
| Refrigerant Compression | 74.7                 |
| Separations Compression | 2.0                  |
| Condensed Phase Pumping | 2.0                  |
| <b>Total</b>            | <b>95.0</b>          |

## Non-Confidential Report

### Energy Performance of Integrated CCC

As stated above, the CCC technology can be integrated with the power plant by removal of the FGD and utilization of the low-grade heat available in the flue gas. While there is some parasitic load associated with the operation of the FGD, it is not explicitly stated in the NETL report. The NETL report does give a sum total for the auxiliary power requirement of the power plant, but there is no simple method for identifying how much of this stated value can be contributed to operation of the FGD. As this is the case, the net energy effect from removing the FGD from the power plant does not affect the energy penalty of the CCC process.

Table 8 presents a comparison of CCC and integrated CCC to amine, in which the parasitic load for integrated CCC drops to 11.1% and the energy penalty to 0.555 GJ/tonne.

Table 8. Summary of energy penalty of CCS technologies

|                            |                          | Case 11 | Case 12<br>(amine) | CCC   | Integrated<br>CCC |
|----------------------------|--------------------------|---------|--------------------|-------|-------------------|
| <b>Net Power Required</b>  | GJ/tonne CO <sub>2</sub> | 0.000   | 1.379              | 0.714 | 0.555             |
| <b>Plant HHV Heat Rate</b> | BTU/kWh                  | 8687    | 12002              | 10144 | 9776              |
| <b>Parasitic Load</b>      | %                        | 0.00    | 27.62              | 14.4  | 11.1              |

Additional reviews of amine performance also confirm the findings of Case 12 regarding the energy requirements of amine carbon capture (Table 9) [26,27]. These techno-economic studies come from the US, Europe, China, and Australia, with similar assumptions as those used in the NETL study (e.g., MEA-based processes, flue gas pre-processing to enable amine CCS, compression of the final CO<sub>2</sub> stream).

Table 9. Energy requirements for amine-based CCS technologies based on reports from the US, Europe, China, and Australia [26,27].

|   |                          | CMU   | EPRI  | TNO   | TPRI  | CSIRO |
|---|--------------------------|-------|-------|-------|-------|-------|
| <b>Power Needed</b>                     | GJ/tonne CO <sub>2</sub> | 1.42  | 1.41  | 1.52  | 1.44  | 1.42  |
| <b>Base Plant HHV Heat Rate</b>         | BTU/kWh                  | 8676  | 8979  | 7982  | 8257  | 8868  |
| <b>Plant with Capture HHV Heat Rate</b> | BTU/kWh                  | 11402 | 12342 | 11586 | 11439 | 12053 |
| <b>Parasitic Load</b>                   | %                        | 23.91 | 27.25 | 31.11 | 27.82 | 26.42 |

### Cost Comparisons

Cost comparisons were performed in a similar manner to the energy penalty calculations, using the NETL report [3] as an outline for all financial assumptions. Additionally, the Excel-based costing program, Power Systems Financial Model (PSFM), developed by NETL was used for all COE calculations; this program was also used to develop the reported cost estimates for Case 11 and Case 12 within the report. This has allowed for all COE estimates to be performed without introducing error caused by differing assumptions in the financial models, ancillary costs, and contingencies.

## Non-Confidential Report

### Cost of Electricity for CCC

Staying as true as possible to the costing assumptions available, and utilizing real-world cost estimates and vendor quotes for capital cost totals, we calculated the COE for a greenfield power plant installation utilizing CCC as the capture technology. This includes increases in fuel, operating, maintenance, and capital costs for scaling up the power plant due to the parasitic load in addition to the cost of the CCC process equipment itself. The resulting COE for CCC is 8.53 ¢/kWh, which corresponds to an increase of 44.8%, a little over half the increase in cost of Case 12 (amine).

### Cost of Integrated CCC

If the extra benefits of an integrated CCC process are taken into account, namely the removal of the FGD, and the corresponding benefits, then the COE calculation further improves. The FGD represents a very large avoided capital cost, and the decrease in fuel requirements and corresponding decrease in process equipment size also represent a significant portion of cost savings. For the purposes of this study, the capital cost of the CCC process equipment was assumed to be equal for the CCC and integrated CCC scenarios. In reality, the capital cost would be smaller for the integrated CCC process because it is processing a lower flow rate of gas. Once the additional benefits of integration are taken into account, the COE for integrated CCC is only 7.12 ¢/kWh, which corresponds to an increase of 20.9% over Case 11 (no capture). This represents less than 26% of the increased cost of Case 12 (amine).

### Cost of CCC Retrofit

CCC is a minimally invasive bolt-on technology that can be retrofitted to existing power plants. This is a key aspect of the technology when evaluating it from an economic perspective. Other competing technologies, such as amine absorption, would require significant rebuilding of existing plant equipment in order to accommodate a retrofit, while still others, such as oxyfuel combustion, have almost no retrofit capability.

Utilizing the same assumptions and the same model as the other costing scenarios presented in this work, we calculated estimates of the COE for retrofitting the CCC technology. Retrofitting allows for the energy market to meet enforced carbon restrictions by leveraging existing capital resources rather than having to decommission and replace existing plants. In the United States, the vast majority of capital of existing power plants has been paid off and has no effect on current COE. The ability to leverage this existing capital resource sets CCC apart from the other core CCS technologies. These numbers have been generated without taking into account any of the integration benefits. Cost numbers for the CCC portion of the retrofit costs are assumed to be the same as those at a greenfield installation. A summary of these findings is given in Figure 15.

### *Milestone 16 – Calculated CCC ES™ LCOE*

SES also utilizes the PSFM for the COE calculations for CCC ES™. We utilize this model with the same assumptions as are present in the September 2013 release of the Cost and Performance Baseline for Fossil Energy Plants by DOE/NETL [3].

Additionally, utilizing the same assumptions and the same model, we are able to estimate the COE for retrofit applications. Retrofitting allows for the energy market to meet enforced carbon

## Non-Confidential Report

restrictions by leveraging existing capital resources rather than having to decommission and replace existing plants. The benefits of this advantage have been presented in terms of total plant cost in previous reports, but are updated and expanded here to also include the effect on the COE. A quick explanation of the methodology of calculating the retrofit COE cost follows.

Cost numbers are taken from the COE analysis provided in this report. Current energy penalty calculations indicate that a new (i.e., greenfield) power plant of the same size as that described in the COE calculations without carbon capture would nominally produce 642 MW<sub>e</sub>. Retrofitting this hypothetical existing 642 MW plant with CCC would represent a capital cost investment of the CCC portion of the process and an expanded cooling water system. This would reduce the net power output of the existing plant by 92 MW, resulting in a 550 MW plant. This means that for every 6 plants of this size that are retrofitted, a brand new plant would have to be built to replace the lost capacity.

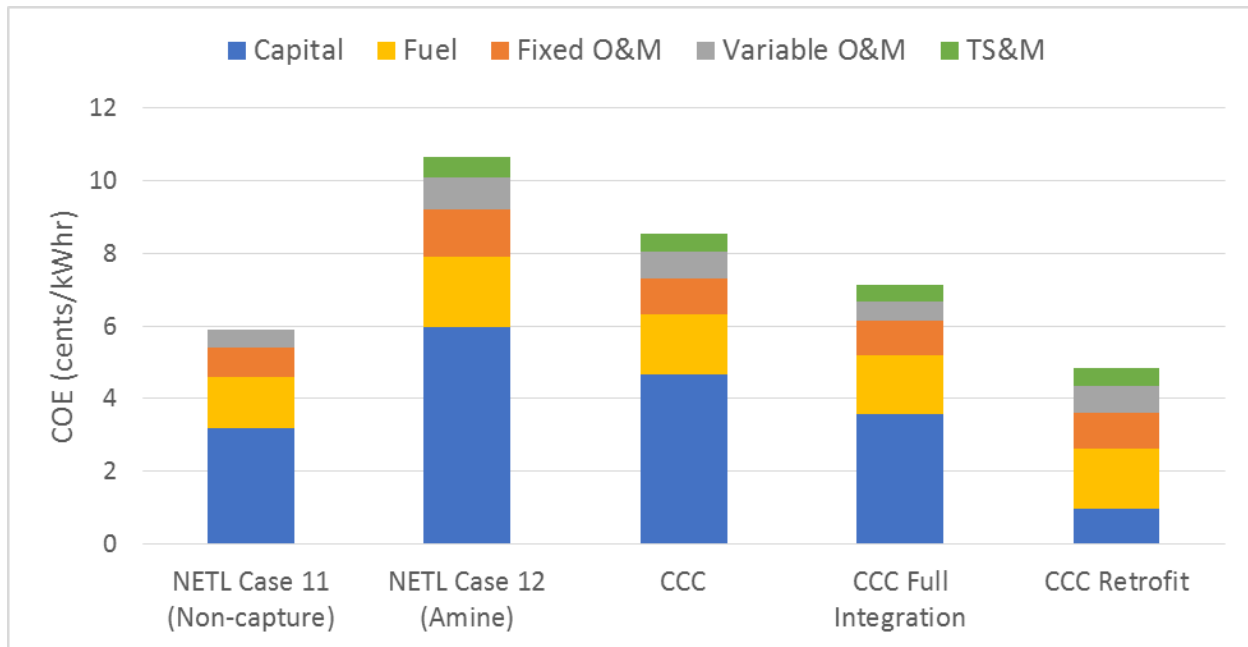


Figure 15. COE of several case studies broken into component parts.

By taking the same operating and maintenance costs that were calculated for a new installation with CCC and utilizing the same assumptions for all ancillary costs and contingencies, we completed a financial simulation of a 642 MW plant where the capital cost of the plant was already paid off. The fuel and operating maintenance costs still persisted along with the energy penalty of the CCC process and the installation costs of an entire retrofitted plant. A combined COE was then created by averaging the COE of 6 of these hypothetical retrofit plants with the COE of 1 brand new installation to make up for the lost power. A summary of the results of these simulations is presented Table 10 and Figure 16, along with the results from the supercritical pulverized coal without CO<sub>2</sub> capture and the supercritical pulverized coal with amine CO<sub>2</sub> capture presented in the NETL report [3].

## Non-Confidential Report

These costs include all impacts on the base plant associated with increased power production, CO<sub>2</sub> transportation, storage, and monitoring costs, and all costs directly associated with CCC. SES estimates the increase in COE at 2.64 ¢/kWh, which corresponds to a 44.79% increase in COE for a greenfield plant. For the retrofitted plant scenario, the decrease in COE is 0.53¢/kWh, which corresponds to a 9.03% decrease in COE compared to Case 11 (greenfield, no capture). Real-world applications for the CCC process would be closer to the retrofit average than for the new CCC installation. All assumptions were made using high-risk parameters, which are the same as those used in Case 12 of the NETL report. Additionally, operation and maintenance costs and other contingencies were estimated on a line-by-line basis.

Table 10. Cost comparison between NETL Cases 11 and 12 as well as estimates for the CCC process, both as a greenfield installation and as a retrofit installation.

|                       |       | <b>NETL<br/>Case 11<br/>(Non-<br/>capture)</b> | <b>NETL<br/>Case 12<br/>(Amine)</b> | <b>CCC ES™</b> | <b>Single<br/>CCC ES™<br/>retrofit</b> | <b>CCC ES™<br/>retrofit<br/>scenario</b> |
|-----------------------|-------|--|-------------------------------------|----------------|--|--|
| Total Plant Cost      | ×1000 | \$905,902                                      | \$1,602,024                         | \$1,249,228    | \$254,057                              | \$397,033                                |
| Fixed O&M             | ×1000 | \$32,635                                       | \$53,198                            | \$41,538       | \$41,538                               | \$41,538                                 |
| Variable O&M          | ×1000 | \$20,633                                       | \$35,730                            | \$30,132       | \$30,132                               | \$30,132                                 |
| Process Contingency   | %     | 0.00   | 2.80                                | 2.80           | 2.80                                   | 2.80                                     |
| Project Contingency   | %     | 8.70   | 10.20                               | 10.20          | 10.20                                  | 10.20                                    |
| Other Contingency     | %     | 24.90  | 25.51                               | 25.80          | 24.45                                  | 24.34                                    |
| COE                   | ¢/kWh | 5.89   | 10.65                               | 8.53           | 4.83                                   | 5.36                                     |
| TS&M Costs            | ¢/kWh | 0.00   | 0.56                                | 0.48           | 0.48                                   | 0.48                                     |
| Fuel Costs            | ¢/kWh | 1.42   | 1.96                                | 1.66           | 1.66                                   | 1.66                                     |
| Variable Costs        | ¢/kWh | 0.50   | 0.87                                | 0.73           | 0.73                                   | 0.73                                     |
| Fixed Costs           | ¢/kWh | 0.80   | 1.30                                | 1.02           | 1.02                                   | 1.02                                     |
| Capital Costs         | ¢/kWh | 3.17   | 5.96                                | 4.65           | 0.95                                   | 1.48                                     |
| Increase over Case 11 | %     | 0.00   | 80.81                               | 44.79          | -18.07                                 | -9.03                                    |
| Base Plant Scale-up   | ×1000 | n/a  | \$468,782                           | \$103,934      | \$0                                    | \$14,932                                 |

## Non-Confidential Report

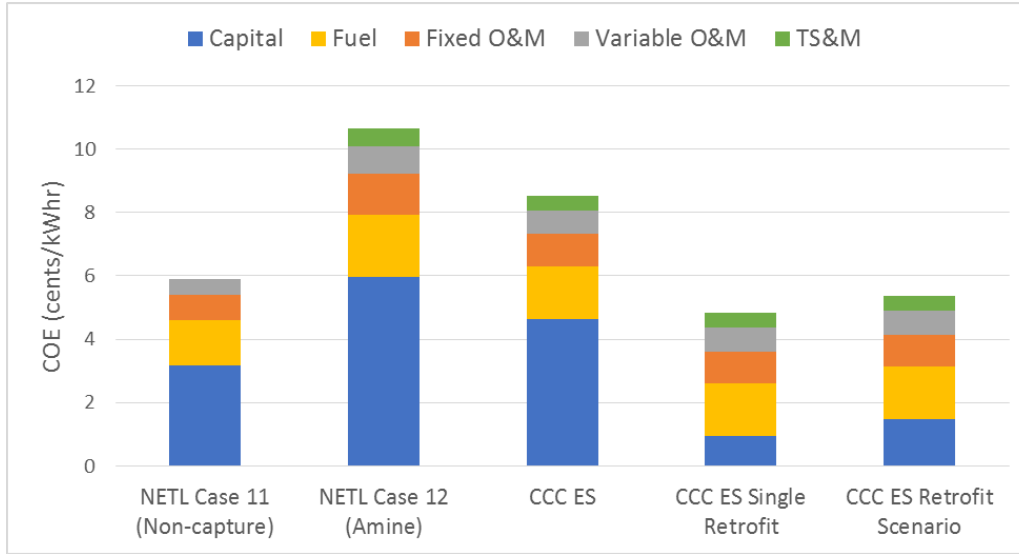


Figure 16. Cost of electricity for Cases 11 and 12 from the NETL report [3], a greenfield CCC ES™ installation, a single CCC ES™ retrofit installation, and CCC ES™ retrofit scenario.

### 3.5.3 Energy Storage Simulation Results

#### *Milestone 9 – Fully Integrated Transient Model*

SES modeled the energy storage process in a transient simulation. Natural gas is liquefied by an external refrigerant cycle. During times of low power demand on the grid (energy storage phase), additional NG from the pipeline is utilized, liquefied, and stored in a tank. During peak demand times (energy release phase), the compressors are turned down. The stored LNG is released from the tank, used to cool the CCC CL, and then released to a natural gas turbine. Table 11 provides qualitative descriptions of stream conditions during the energy release and energy storage phases, relative to the baseline values (neither energy stored nor released).

Table 11. Stream conditions during different phases of the CCC ES™ process.

|                                 | <b>Energy release</b> | <b>Energy storage</b> |
|---------------------------------|-----------------------|-----------------------|
| NG from pipeline flowrate       | No flow               | Flow                  |
| NG to turbine                   | Flow                  | No flow               |
| LNG storage tank                | Flow from tank        | Flow to tank          |
| NG compressor flowrate          | Less than baseline    | Equal to baseline     |
| Refrigerant compressor flowrate | Less than baseline    | Greater than baseline |

We simulated two energy storage scenarios. Each spans a 24-hour period of varying power grid demand. During each phase, process streams ramp to their peak flowrates, then ramp back to the baseline values. In Scenario 1, the energy is stored for 12 hours and then released over 12 hours. In Scenario 2, the energy is stored for 18 hours and then released over 6 hours. Each scenario has the same energy storage capability (LNG tank size). The two scenarios are summarized in Table 12. In the table, the baseline values are given for reference.

## Non-Confidential Report

Table 12. Two scenarios for CCC ES™ implementation; baseline values are included for reference.

|                                 | <b>Scenario 1</b> |                       |                       | <b>Scenario 2</b> |                       |                       |
|---------------------------------|-------------------|-----------------------|-----------------------|-------------------|-----------------------|-----------------------|
|                                 | <b>Baseline</b>   | <b>Energy release</b> | <b>Energy storage</b> | <b>Baseline</b>   | <b>Energy release</b> | <b>Energy storage</b> |
| Peak flowrates (tonne/hr)       |                   |                       |                       |                   |                       |                       |
| + Into process or into tank     |                   |                       |                       |                   |                       |                       |
| - Out of process or out of tank |                   |                       |                       |                   |                       |                       |
| NG from pipeline                | 0                 | 0                     | +90                   | 0                 | 0                     | +60                   |
| NG to turbine                   | 0                 | -90                   | 0                     | 0                 | -180                  | 0                     |
| LNG storage tank                | 0                 | -90                   | +90                   | 0                 | -180                  | +60                   |
| NG compressor                   | 900               | 810                   | 900                   | 900               | 720                   | 900                   |
| Refrigerant compressor          | 866               | 714                   | 1007                  | 866               | 649                   | 963                   |
| Length of phase (hr)            | N/A               | 12                    | 12                    | N/A               | 6                     | 18                    |

Results of the two simulations are shown in Figure 17 and summarized in Table 13. In each scenario, the total compressor power is reduced during the energy-release phase, and is increased during the energy-storage phase.

Non-Confidential Report

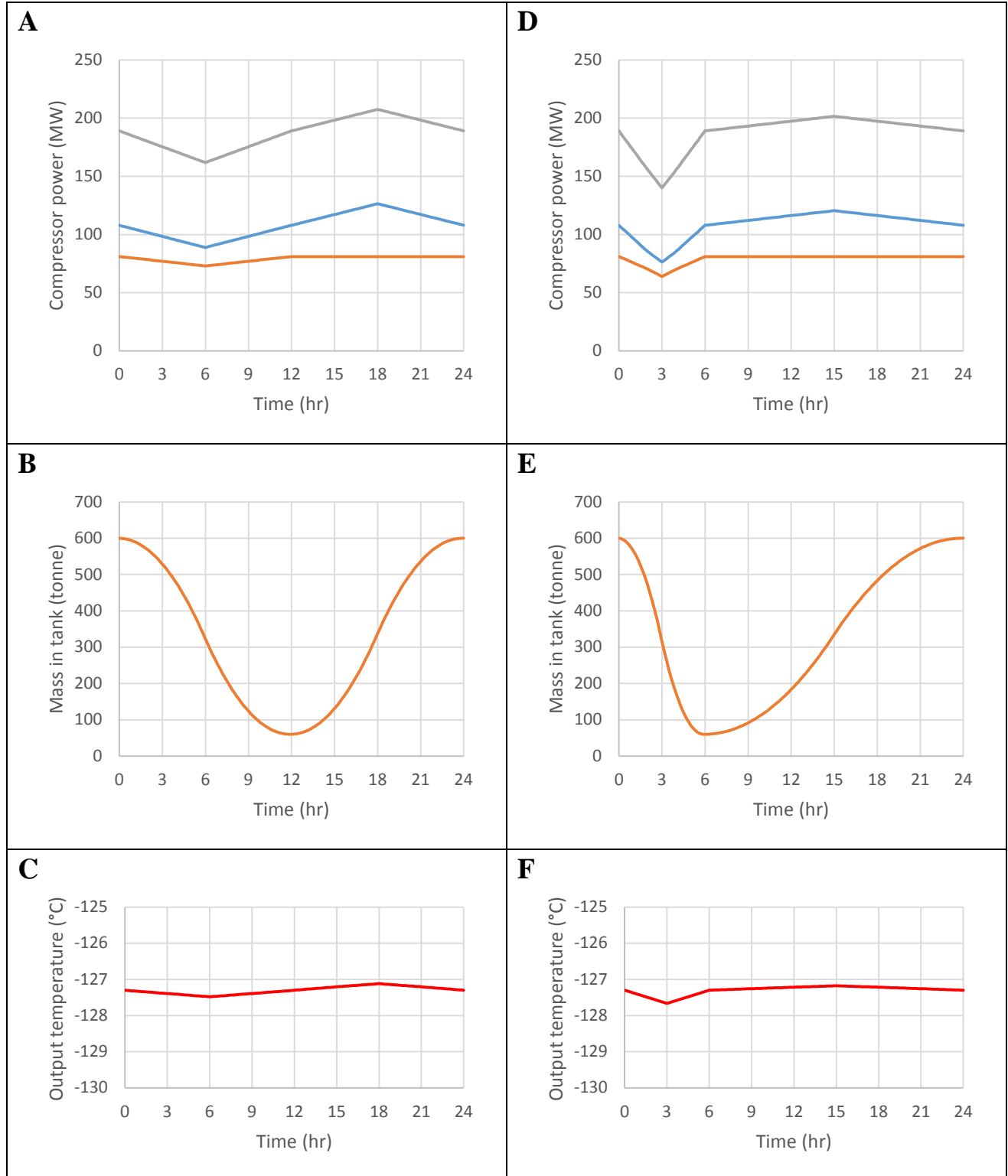


Figure 17. Results of the energy storage simulation. (A–C) Scenario 1 and (D–F) Scenario 2 (A and D). NG compressor power (orange), refrigerant compressor power (blue), and total power (gray). (B and E) Mass of LNG in the storage tank. (C and F) Temperature of CL output to the CCC process.

## Non-Confidential Report

Table 13. Results from modeling two CCC ES<sup>TM</sup> scenarios: Scenario 1 where energy is stored for 12 hr and released for 12 hr, and Scenario 2 where energy is stored for 6 hr and released for 18 hr.

|  | Scenario 1 |                |                | Scenario 2 |                |                |
|--|------------|----------------|----------------|------------|----------------|----------------|
|  | Baseline   | Energy release | Energy storage | Baseline   | Energy release | Energy storage |
| Peak compressor power (MW)             |            |                |                |            |                |                |
| NG compressor                          | 81.1       | 73.0           | 81.1           | 81.1       | 63.9           | 81.1           |
| Refrigerant compressor                 | 107.9      | 88.8           | 126.4          | 107.9      | 76.3           | 120.5          |
| Total                                  | 189        | 161.8          | 207.5          | 189        | 140.1          | 201.6          |
| Change from baseline                   | 0%         | -14.4%         | +9.8%          | 0%         | -25.9%         | +6.7%          |
| Temperature output to CCC process (°C) | -127.3     | -127.5         | -127.1         | -127.3     | -127.7         | -127.2         |

For example, in Scenario 1, the total compressor power is reduced by 14.4% during the energy release phase, and is increased by 9.8% during the energy storage phase. The lengths of the phases in Scenario 1 are equal, so at first it seems like more energy is released than is being stored. This is because the excess NG released to the turbine during the energy release phase occurs at low pressure, while NG from the pipeline is delivered at high pressure during the energy storage phase. The excess energy is due to the difference in stored energy in the NG at high pressure versus NG at low pressure.

### 3.5.4 Mass and Energy Balances

#### *Milestone 14 – Full Mass and Energy Balance Based on P&ID*

The mass balance is presented in Table 14. A 1 kmol/hr imbalance occurs for CO<sub>2</sub> that stems from the mass balance of the 10-stage bubbler model. Due to the much larger flowrates of CL and the precision employed by the Aspen software, the molar flowrate of CO<sub>2</sub> averages a molar imbalance of 0.1 kmol/hr per stage. The CO<sub>2</sub> imbalance is well within the error of the thermodynamic simulations. Taking the CO<sub>2</sub> imbalance into consideration on the total mass balance, it reflects an imbalance of less than the default 0.0001 tolerance.

Some contact liquid in the system is lost during direct contact with the flue gas and during CO<sub>2</sub> separation. Concerns are primarily the environmental and economic impacts of the combined losses. As simulated, the isopentane present in the exhausted nitrogen-rich gas is acceptable by EPA source guidelines for hydrocarbon emissions. Isopentane in the CO<sub>2</sub>-rich stream is of less environmental concern since isopentane exists in the ground where the stream will be sequestered or used for enhanced oil recovery (EOR).

Non-Confidential Report

Table 14. CCC mass balance.

|                              | Molar Flowrate (kmol/hr) |                |                |                 |                  |                                |              | Total Mass Flowrate (tonne/hr) |
|------------------------------|--------------------------|----------------|----------------|-----------------|------------------|--------------------------------|--------------|--------------------------------|
|                              | #                        | O <sub>2</sub> | N <sub>2</sub> | CO <sub>2</sub> | H <sub>2</sub> O | C <sub>5</sub> H <sub>12</sub> | Total        |                                |
| <b>In</b>                    |                          |                |                |                 |                  |                                |              |                                |
| Flue Gas                     | 100                      | 1804           | 51799          | 10172           | 11405            | 0                              | 75180        | 2161.9                         |
| Makeup CL                    | 230                      | 0              | 0              | 0               | 0                | 51                             | 51           | 3.7                            |
| <b>Totals</b>                |                          | <b>1804</b>    | <b>51799</b>   | <b>10172</b>    | <b>11405</b>     | <b>51</b>                      | <b>75231</b> | <b>2165.6</b>                  |
| <b>Out</b>                   |                          |                |                |                 |                  |                                |              |                                |
| N <sub>2</sub> -Rich Gas     | 114                      | 1804           | 51799          | 1014            | 0                | 1                              | 54617        | 1553.5                         |
| CO <sub>2</sub> -Rich Liquid | 416                      | 0              | 0              | 9159            | 0                | 50                             | 9207         | 406.7                          |
| Water                        | 991                      | 0              | 0              | 0               | 10131            | 0                              | 10131        | 182.5                          |
| Water                        | 995                      | 0              | 0              | 0               | 1274             | 0                              | 1274         | 23.0                           |
| <b>Totals</b>                |                          | <b>1804</b>    | <b>51799</b>   | <b>10173</b>    | <b>11405</b>     | <b>51</b>                      | <b>75229</b> | <b>2165.6</b>                  |
| <b>Differences (%)</b>       |                          | <b>0.00</b>    | <b>0.00</b>    | <b>-0.01</b>    | <b>0.00</b>      | <b>0.00</b>                    | <b>0.00</b>  | <b>0.00</b>                    |

The energy balance is presented in

Table 15. The total parasitic loss of power from running the carbon-capture equipment is 97.6 MW. Of that, 54.3 MW is consumed by the energy storage refrigeration compressors, which can be turned off during peak demand. Therefore, only a 43.3 MW gas turbine would be necessary to maintain peak capacity, while capturing 90% CO<sub>2</sub> at all times. Parasitic losses stem from multiple sources, including numerical error, imperfect prediction of phase transition heats, turbomachinery, etc. Losses are 0.25% of the total heat, which is in accordance with benchmark NETL studies of 0.27% of the total heat [3].

Table 15. Energy balance (25 °C reference).

|                              | Sensible + Latent (MW) | Power (MW) | Total (MW) |
|------------------------------|------------------------|------------|------------|
| <b>Heat In</b>               |                        |            |            |
| Flue Gas                     | -1858.3                |            | -1858.3    |
| Makeup CL                    | -2.5                   |            | -2.5       |
| Flue Gas Blower              |                        | 11.7       | 11.7       |
| CO <sub>2</sub> Compressor   |                        | 1.6        | 1.6        |
| Liquid CO <sub>2</sub> Pump  |                        | 1.1        | 1.1        |
| Slurry Pump & Screw Press    |                        | 2.2        | 2.2        |
| CF <sub>4</sub> Compressor   |                        | 26.7       | 26.7       |
| Mixed Refrigerant Compressor |                        | 30.2       | 30.2       |

## Non-Confidential Report

|                              | Sensible<br>+ Latent | Power       | Total          |
|------------------------------|----------------------|-------------|----------------|
| Natural Gas Compressor       |                      | 24.1        | 24.1           |
| <b>Totals</b>                | <b>-1860.8</b>       | <b>97.6</b> | <b>-1763.3</b> |
| <b>Heat Out</b>              |                      |             |                |
| N <sub>2</sub> -Rich Gas     | -111.2               |             | -111.2         |
| CO <sub>2</sub> -Rich Liquid | -1032.8              |             | -1032.8        |
| Water Condensate 991         | -806.3               |             | -806.3         |
| Water Condensate 995         | -101.2               |             | -101.2         |
| BFW Heating                  | 150.9                |             | 150.9          |
| E109 Cooling Water           | 8.8                  |             | 8.8            |
| E510 Cooling Water           | 1.5                  |             | 1.5            |
| C306 Cooling Water           | 29.7                 |             | 29.7           |
| C570 Cooling Water           | 27.5                 |             | 27.5           |
| C700 Cooling Water           | 65.4                 |             | 65.4           |
| Process Losses*              | 4.4                  |             | 4.4            |
| <b>Totals</b>                | <b>-1763.3</b>       | <b>0.0</b>  | <b>-1763.3</b> |
| <b>Difference</b>            |                      |             | <b>0.00%</b>   |

\* Process losses are estimated to match the heat input to the plant.

Important features to note are:

- 1) CL losses are 0.8 kmol/hr (13 ppm) in the nitrogen-rich exhaust gas, which is within the EPA requirements for hazardous air pollutants (which these contact liquids are not, but it is assumed that this requirement is more stringent than for hydrocarbons generally, so we aimed to meet these requirements) [28] and 50 kmol/hr in the CO<sub>2</sub>-rich liquid.
- 2) The total power for CCC ES<sup>TM</sup> capturing 90% CO<sub>2</sub> from a 550 MW coal-fired power plant is 82.6 MW.
- 3) The total energy cost per amount of CO<sub>2</sub> captured is 0.738 GJ/tonne.

### 3.5.5 Dynamic Heat Exchanger

#### *Milestone 21 – Heat Exchanger Performance Test*

When the energy storage process is implemented on the grid, differing amounts of LNG will be produced depending on the electrical demand dispatched to the power plant. When the flowrate of LNG through a heat exchanger changes, the response time of a traditional heat exchanger would be limited by thermal stresses. The dynamic heat exchanger being developed by SES will allow rapid changes in LNG production or usage while minimizing thermal stresses.

Imbalance in a heat exchanger occurs when the thermal flow rate ( $\dot{m}C_p$ ) changes on one side of the heat exchanger. The dynamic heat exchanger seeks to prevent this unbalanced condition by adding additional material from a warm or cold tank to offset changes in flowrate on either side of the heat exchanger. Two dynamic heat exchanger configurations were developed. In the two-

## Non-Confidential Report

stream configuration, the process stream is augmented by additional flow from the cold or warm tank, depending on how the heat exchanger is out of balance.

A second three-stream configuration was also developed. In this configuration, the two process streams do not come mix with the third control stream. This configuration would have an advantage if the two process streams were made up of different materials or if the streams were made of gases, causing the two tanks to become so large that supplementing the process flow would be prohibitive.

### 3.5.6 Process Response Time

#### *Milestone 21 – Heat Exchanger Performance Test*

We tested the dynamic heat exchanger concepts on the test stand shown in Figure 18. The temperature of the incoming and outgoing streams were measured and water was used as the heat exchange medium.

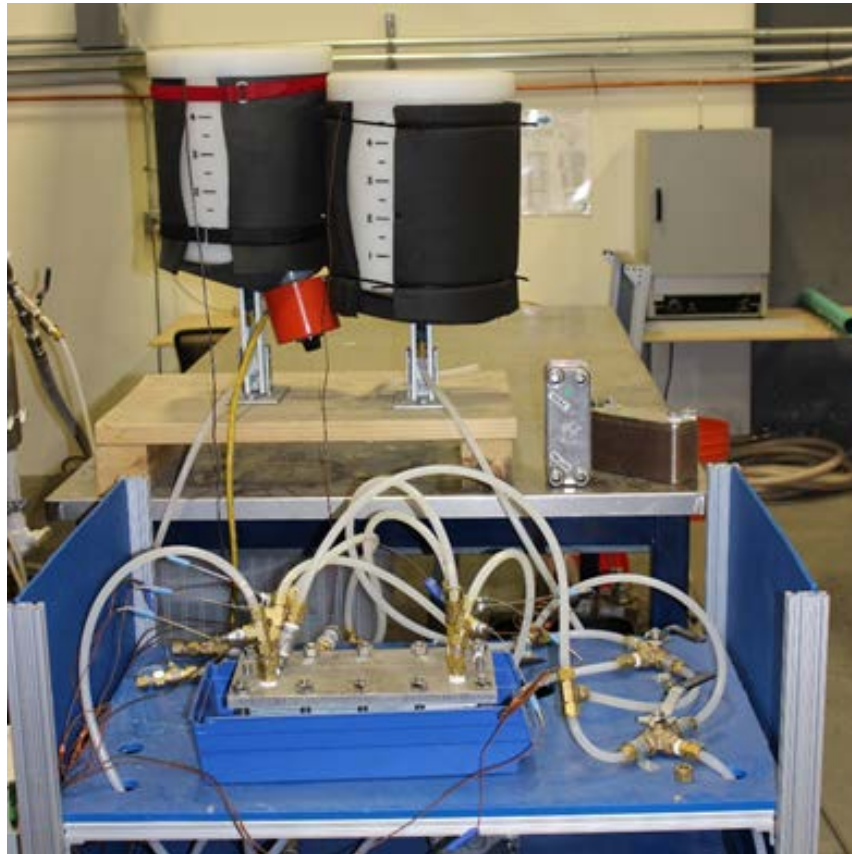


Figure 18. Dynamic heat exchanger test stand.

Figure 19 shows the heat exchanger efficiency for a test where warm and cold water exchanged heat with each other in a two-stream heat exchanger. The flow of the cold side was reduced using a valve to simulate a process upset. In the “Active” case, the cold side was supplemented using cold water from a tank. The “Idle” case is given to show the behavior of a two-stream heat exchanger in a traditional configuration. It is clear that the dynamic heat exchanger configuration is effective at maintaining a near-constant efficiency through a process upset.

## Non-Confidential Report

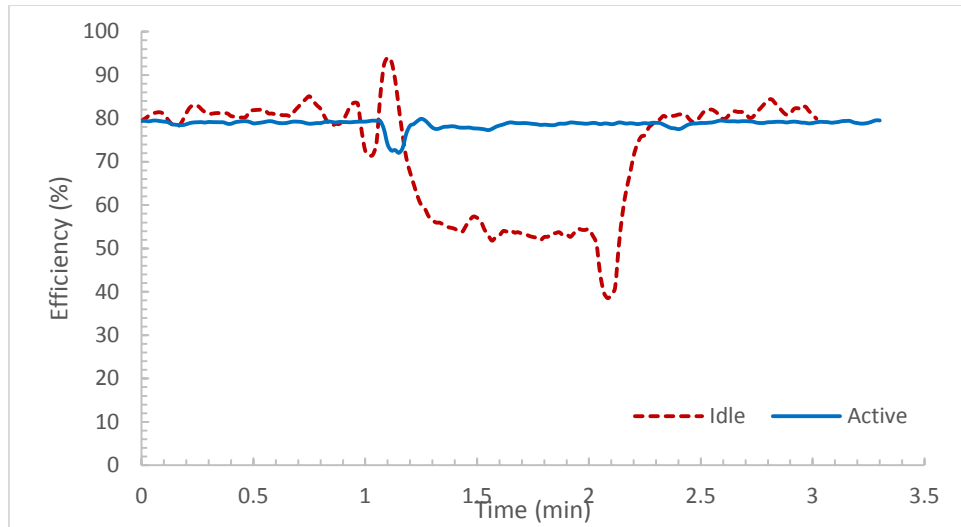


Figure 19. Efficiency variation during dynamic heat exchanger testing using a two-stream, counter-current heat exchanger. The idle and active tests were separate experiments; the beginning and end of the time perturbation correspond quite closely, but not exactly, in the two cases.

Figure 20 shows the same test using a three-stream heat exchanger of our own design. This configuration is also effective at maintaining heat exchanger efficiency.

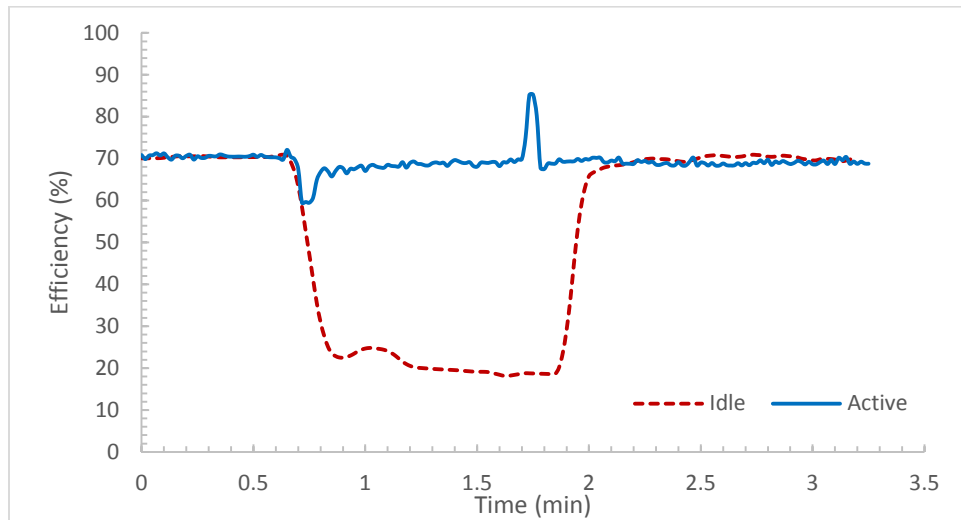


Figure 20. Efficiency variation in time during operations with the dynamic heat exchanger technology active and idle for a three-stream, counter-current heat exchanger. These are separate experiments and the beginning and ending of the time perturbation correspond quite closely but not exactly in the two cases.

These heat exchangers have implications much wider than the CCC ES™ process. Communications with industry partners have indicated that transients cause significant damage to heat exchangers if they are shorter than an hour. These heat exchanger configurations can respond to transients in well under a minute.

### 3.5.7 Carbon Capture Demonstrations

#### *Milestone 20 – Demonstrate 90% Capture Utilizing LNG as Refrigerant Stream*

We demonstrated 90% capture using LNG as a refrigerant. The longest of these demonstrations was 3 hours and some preliminary energy storage results were also gathered.

These tests were conducted using a test gas composed of bottled nitrogen and CO<sub>2</sub>. Figure 21 shows the inlet and outlet concentration of the CO<sub>2</sub> as a function of time. The inlet concentration was changed at 28 minutes to illustrate the ability of the system to capture at higher CO<sub>2</sub> concentrations. The outlet concentration remains relatively steady throughout the duration of the test because the outlet concentration is only dependent on the temperature that the gas reaches, not on the inlet concentration. The end of the test is marked by the sudden increase in CO<sub>2</sub> concentration to the maximum readable level of the sensor (i.e., 3%).

Figure 22 shows CO<sub>2</sub> capture as a function of time as well as the total mass accumulated by the system. The system was maintained using energy storage for over an hour, with the capture rates well above 90% for the majority of the test. The cryogenerators were turned off and all of the cooling was handled by stored LNG.

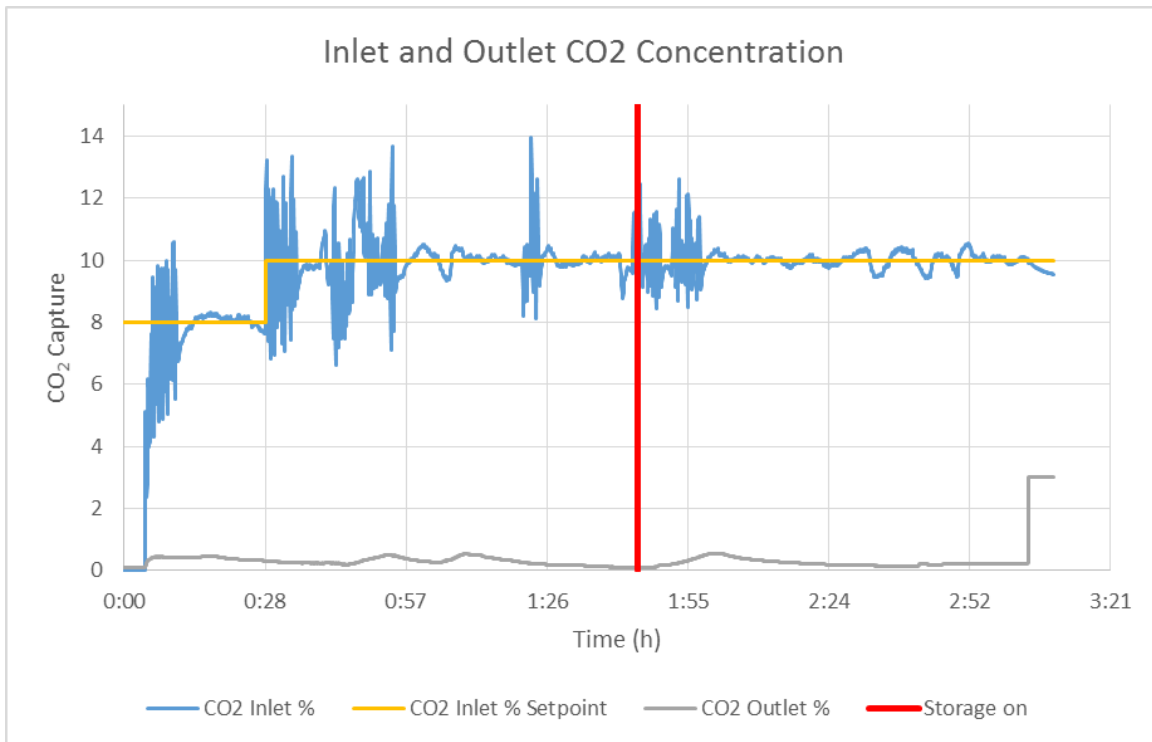


Figure 21. CO<sub>2</sub> inlet and outlet percentages during CCC ES<sup>TM</sup> testing. For the first portion of the test (left of the red line), we stored energy. The second part of the test (right of the red line), we captured CO<sub>2</sub> only using the stored LNG.

## Non-Confidential Report

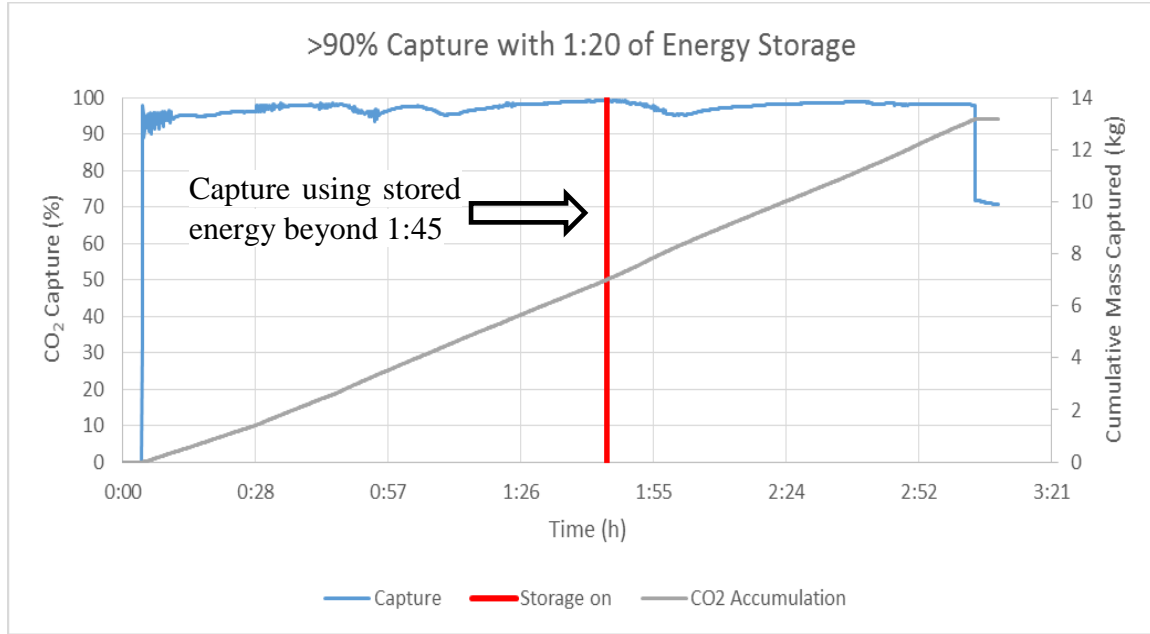


Figure 22. 3-hour run with 80 minutes of 90+% capture using stored LNG as a refrigerant (right of the red line).

### *Milestone 22 – Demonstrate 99% Capture Utilizing LNG as Refrigerant Stream*

Under this milestone, 99% capture using LNG as a refrigerant was demonstrated. However, the longest demonstration was only about 15 minutes in length.

These tests were conducted using a test gas composed of bottled nitrogen and CO<sub>2</sub>. Figure 23 shows the inlet and outlet concentration of the CO<sub>2</sub> as a function of time. The inlet concentration was changed at 12 minutes to illustrate the ability of the system to capture at a higher CO<sub>2</sub> concentration. This should have resulted in a higher capture rate, but caused the capture rate to go down. This was likely caused by the methane concentration in the LNG being too low. Even though the inlet concentration is transient, the outlet concentration remains relatively steady through the duration of the test.

The flue gas was cooled with CL and the CL was cooled by boiling LNG. The boiling temperature of LNG is determined by the pressure in the LNG dewar and is also dependent on the composition of the LNG. The higher the methane content, the lower the boiling temperature at a given pressure.

## Non-Confidential Report

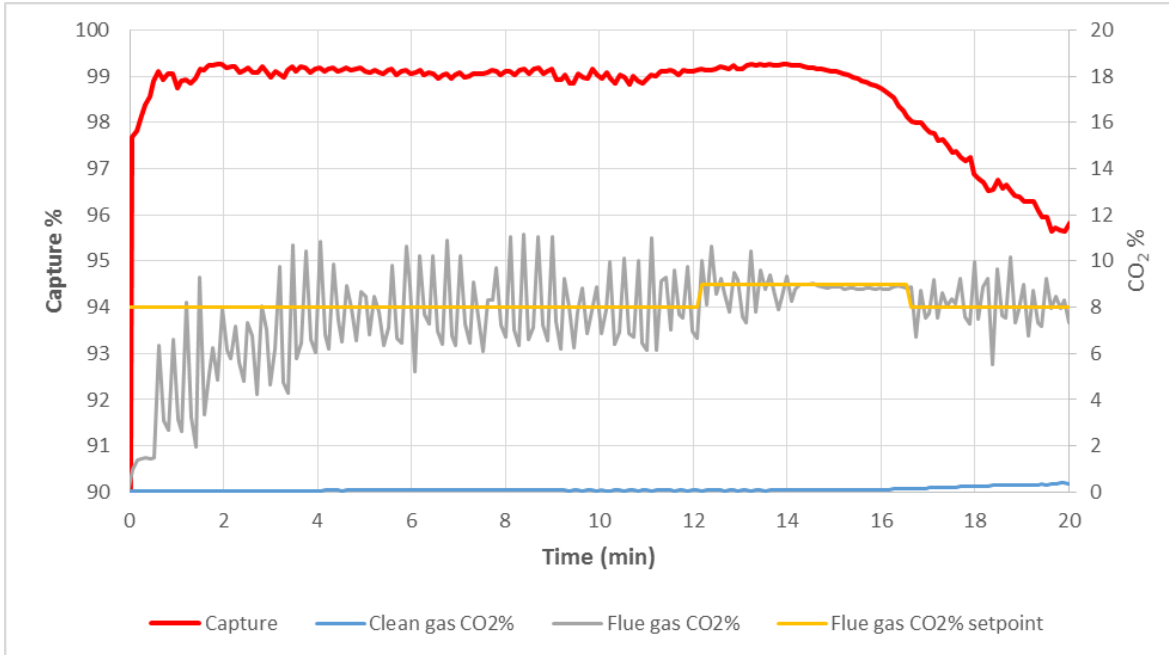


Figure 23. 99% CO<sub>2</sub> capture demonstrated for 15 minutes. CO<sub>2</sub> inlet and outlet percentages are also shown (right axis).

Table 16 shows the boiling temperatures of a few components that are commonly found in LNG, with the most volatile species first (methane) followed by other potential (less-volatile) species. Natural gas composition differs from well to well. The current low price of natural gas requires that producers use wells that are high in natural gas liquids (ethane, propane, butane). It is likely that as a result of this condition, the LNG used as a refrigerant to produce the data in Figure 23 contained more natural gas liquids than typical LNG. When the CO<sub>2</sub> composition increased, the CL warmed up, causing more LNG to boil, which caused the pressure to go up in the NG system. The data suggest that this caused the LNG to stop boiling in the heat exchanger where the CL is cooled. LNG is fed into these heat exchangers by gravity. Thus when the LNG stopped boiling, this dramatically reduced the convective heat transfer coefficient to zero and the CL could not be cooled. This explains the precipitous drop in capture at about 15 minutes in Figure 23. In practice, the pressure of the natural gas could be lowered to produce a lower boiling point. However, there is a possibility of drawing air into the system if the pressure is below atmospheric pressure. This line of action was not pursued because introducing air into the system could cause an explosion hazard.

Table 16. Boiling temperature of natural gas constituents at 1 atm. Species considered “natural gas liquids” are shaded.

| Natural Gas Species | Boiling Temperature (1 atm) |
|---------------------|-----------------------------|
| Methane             | -161.5 °C                   |
| Ethane              | -88.5 °C                    |
| Propane             | -42.3 °C                    |
| Butane              | -1.0 °C                     |

## Non-Confidential Report

When the CCC ES™ process is built at a larger scale and natural gas is liquefied to store energy, the composition of the natural gas will need to be monitored to ensure a consistent rate of capture. Knowing the composition will allow for engineering and/or controls to ensure that there is enough cooling available to condense the CO<sub>2</sub> in the flue gas.

### *Milestone 23 – Creating a Sustained LNG Flow Rate Sufficient to Sustain Operation*

LNG was condensed from a gas stream that entered at near room temperature. LNG was accumulated in a dewar and the level was tracked over time to see how fast the system could condense the LNG. The heat of vaporization was then used to determine how much cooling the system could provide. Figure 24 shows how fast the system can accumulate LNG with no load other than the condensing NG. About 20 liters of LNG were produced in 10 minutes. This corresponds to a cooling potential of 4 MJ of cooling. Using just the linear portion of the plot (i.e., from 2 to 10 minutes), the system can produce about 7.5 kW of cooling.

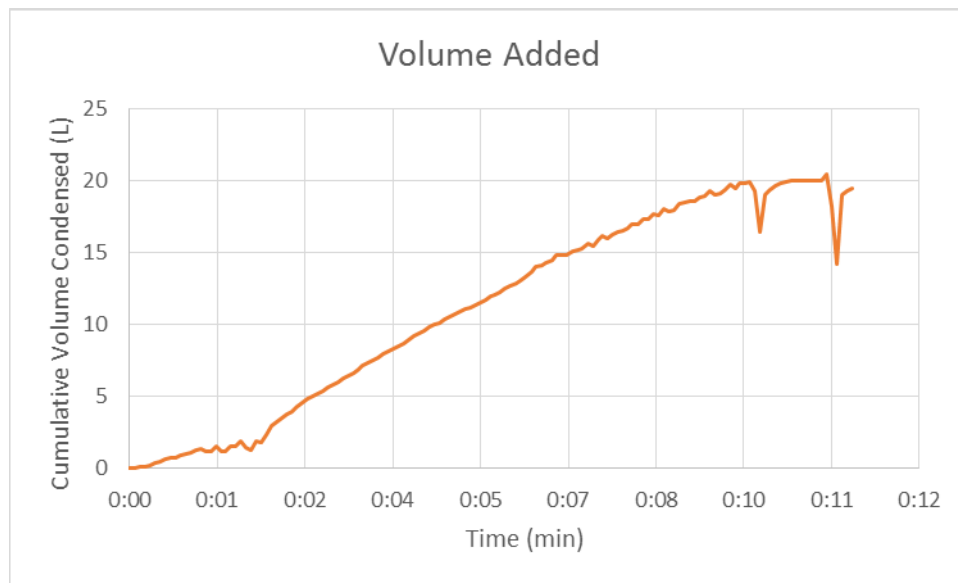


Figure 24. LNG accumulation as a function of time with the ECL skid system running at full capacity with no additional load.

According to the CCC model, capturing 99% of the CO<sub>2</sub> from a flue gas with 16% CO<sub>2</sub> (on a dry basis) requires 3.7 kW of cooling when treating flue gas at 25 scfm. This is the upper limit of the flue gas flowrate that will be used for Milestone 24. This means that the system should have roughly twice the capability required (not including losses). The power consumption of the system will increase with increasing CO<sub>2</sub> content. Nonetheless, the system has proven to be robust with concentrations from 5% to 22% CO<sub>2</sub>. In any case, the LNG flowrate is sufficient to sustain operation even during energy storage mode.

### *Milestone 24 – Demonstrate 90% Capture for a Full Simulated Load Cycle*

We demonstrated that the CCC process could be operated using stored LNG. This was accomplished by shutting the Stirling cryocoolers off and releasing the warmed natural gas from

## Non-Confidential Report

the system. In a full-scale system, this natural gas would either re-enter the pipeline or it would get consumed in a natural gas single-cycle turbine. The single-cycle turbine has the added advantage that it adds power to the grid at peak demand, which is when the energy stored in the LNG would be most needed. At the scale of the current system, it was not feasible to drive a turbine with the natural gas so it was ported outdoors and flared (Figure 25).

The capture data used to meet this milestone are also presented in as part of milestone 20 because it was a longer run at 90% capture. The data is replotted in Figure 26, along with other data, for the purpose of this discussion.

Once the process began to run at steady state (at 14 min in Figure 26), we started venting the natural gas. Thereafter, the cryogenerators were ramped up and shut off periodically to test the ability of the system to respond to rapid fluctuations in available power. The so called cryocooler load is associated with the motor speed setting on the cryocooler and should not be confused with overall system load or efficiency. There was some small transience in the capture, but the capture level stayed above 90% for the entire time. The LNG was vented from the system via a proportional hand valve. This valve was adjusted only periodically, which caused the pressure of the boiling LNG to change, which in turn caused the mild fluctuations seen in the figure.



Figure 25. Adjusting the fuel/air mixture while flaring natural gas after it was used in its condensed phase (LNG) to drive the CCC process.

Throughout this test, the LNG level in the tank dropped until the float on the level sensor reached the stop, indicating the tank was near empty (and the level sensor could no longer detect liquid) at the 2 hour and 14 minute mark. The float stop is required to ensure that the LNG float stays within the tank and does not restrict the flow of LNG to the rest of the system. LNG continued to boil off and the system continued to run in spite of having no level indicator within the tank. It was verified that natural gas continued to flow by watching the lit flare, although this was only a qualitative measure.

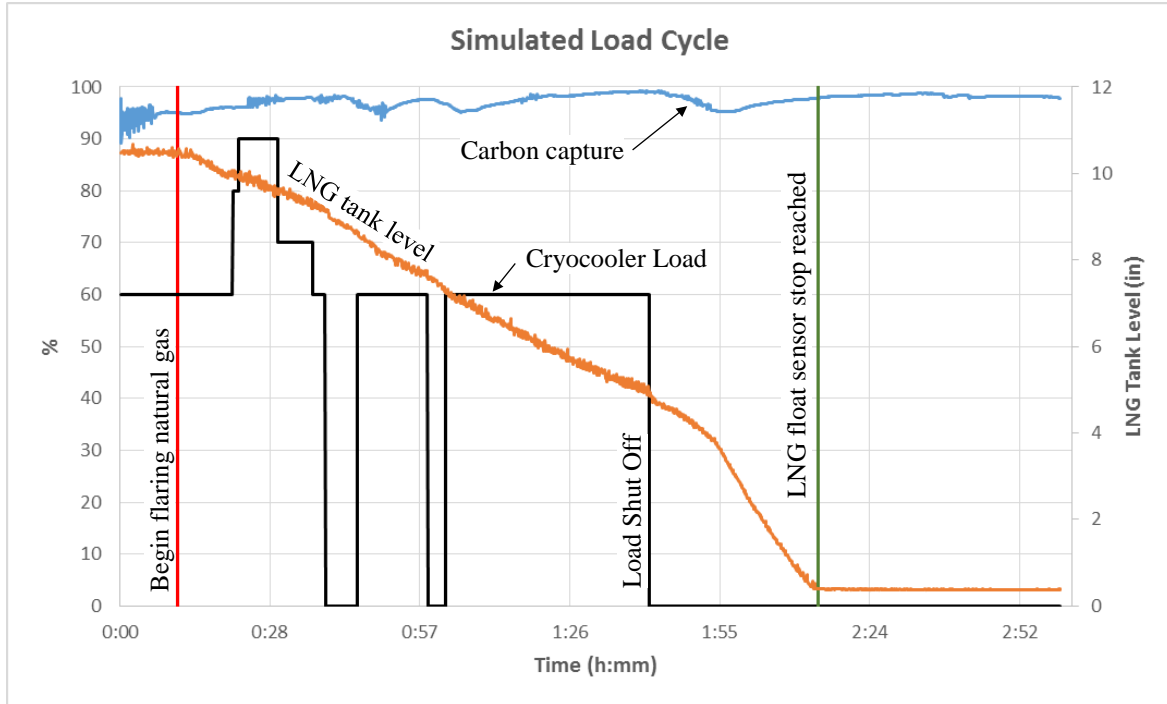


Figure 26. Simulated LNG load cycle. Once the process began to run at steady state (14 min.), we started venting the natural gas. The Cryogenerators were ramped up and shut off periodically (black line) to test the ability of the system to respond to rapid fluctuations in available power. There was some transience in the capture, but the capture level stayed above 90% the entire time.

This milestone verified that switching from condensing LNG or using boiling LNG from a tank makes no difference to the process. This was the final test required to ensure that CCC ES™ was ready for the next scale of testing.

### 3.6 Project Outcomes

CCC has been in development since 2008. The energy storage concept was not conceived of until 2011. This put the development of CCC ES™ well behind the CCC process. Therefore, the primary purpose of this project was to bring CCC ES™ up to the same level of development as CCC. The outcomes of this project were successful. A brief summary of the results of each task will now be discussed.

#### 3.6.1 Task 1 – Process Simulation and Transient Response

The first step in developing a process as complex as CCC ES™ is to develop a sophisticated model. The purpose of the model is to give confidence that the process will behave in an expected manner and to remedy any design flaws, such as temperature crossover within a heat exchanger. All such flaws were discovered during steady-state modeling.

During this effort, SES developed a new in-house software package to model processes. CCC has always been difficult to model because solids formation within any unit is not allowed by commercial software. Further, purchasing a seat for these commercial packages is prohibitive from a cost perspective. Previous to this project, processes were modeled using mid-level

## Non-Confidential Report

languages such as C#. The process designer that was developed under this project has a graphical interface and can be used by chemical engineers without programming experience.

The second, more sophisticated, step was to model the transience of the process. Energy storage is transient by nature. For LNG to be stored during times of excess supply, flow rates in the process have to change. Flow rates through rotating pieces of equipment could be ramped up and down to meet demands, but the heat exchangers require time to reach equilibrium. This is why a transient heat exchanger was designed, modeled, built, and tested as part of this project.

### 3.6.2 Task 2 – Energy Analysis of the CCC ES™ Process

The objective of this task was to compare the CCC ES™ process to the traditional CCC process. SES has developed significant expertise in process modeling. When the CCC ES™ project began, CCC had been modeled and verified by numerous organizations (and has since been verified by others). CCC ES™, however, had not been modeled extensively and it was not known whether it would have all the same energy penalty advantages of CCC. Through this effort, it was shown that CCC ES™ is actually slightly more efficient than the standard CCC process.

### 3.6.3 Task 3 – Economic Evaluation of the CCC ES™ Process

The objective of this task was to show that the cost of building a CCC ES™ plant was attractive when considering the added benefit of energy storage. This was done by evaluating the LCOE of the process. This was done previously by SES for the CCC process and had been compared to the LCOE of other carbon capture technologies evaluated by the US DOE. This analysis included industry quotes for all major pieces of equipment. It was shown that CCC ES™ had essentially the same construction, equipment, and operating costs as CCC, which is about half the cost of alternatives. From this analysis, it was concluded that energy storage could be implemented with CCC for essentially the cost of an LNG tank, which is both commercially available and relatively inexpensive.

### 3.6.4 Task 4 – Bench and Skid Scale Demonstrations

To bring the CCC ES™ process up to the same level of development as the rest of the CCC process, it had to be demonstrated at small scale. A skid-scale demonstration is the largest demonstration that you can fit on one semi-truck. SES was already in the process of building a skid-scale version of the CCC process, which could be modified to store and release energy. At large scale, the CCC process can become a CCC ES™ process by modifying the cooling loop to handle natural gas, rather than ethane, and by adding a tank. The skid-scale version of the process was not much different. Therefore, the small-scale CCC process was modified by adding a vacuum-insulated LNG tank and by changing the operating parameters of the liquefaction process. This was completed and several data sets were gathered where LNG was used as a refrigerant to drive the CCC process. Furthermore, energy storage was verified by turning the liquefaction process off and running the system on stored refrigerant. This verification of energy storage completed the verification of the CCC ES™ process.

## 3.7 Analysis of Results

## Non-Confidential Report

The successful implementation of energy-storing Cryogenic Carbon Capture™ requires addressing several issues:

1. The LNG refrigerant must not compromise the cycle efficiency.
2. Transients must be isolated in the LNG portion of the process.
3. Process transients must be manageable on short time scales.
4. Process transients must not compromise the integrity of heat exchangers or other major equipment.

Each of these issues is discussed the following paragraphs. This analysis includes theoretical descriptions and experimental investigations that suggest that all of these issues have been successfully demonstrated.

This project demonstrates experimentally and theoretically that natural gas provides essentially identical (very slightly better) refrigeration performance as alternative refrigerants and refrigerant blends. Because the critical point of LNG (as low as  $-83\text{ }^{\circ}\text{C}$ ) is well below ambient temperature, it is not possible to compress and then condense LNG near room temperature, as is commonly done with traditional refrigerants. However, LNG can still be generated efficiently, albeit in a slightly more complex circuit compared to traditional refrigerants. The project also demonstrated that some NG supplies may require process set point modification or removal of natural gas liquids since there are variations in the amounts of heavy hydrocarbons among NG supplies.

Refrigeration in general represents about 80% of the total energy demand for CCC, depending on amount of  $\text{CO}_2$  in the flue gas, over half of which can be incorporated into the LNG loop. Therefore, CCC ES™ can store and release most of its energy consumption in the form of stored refrigerant, or LNG. The energy density of LNG suffices to store several hours' worth of refrigeration in tanks that are smaller than commercially available storage tanks. Therefore, CCC ES™ has the capacity to store enough energy to supply refrigerant for the entire peak demand time of a typical power plant.

CCC ES™ operates with the carbon capture portion of the process matching boiler load, which is typically essentially constant, while the LNG generation portion follows power demand. Power demand on grids with intermittent supplies can change significantly within minutes. Transient analyses and experiments showed that heat exchangers may be able to keep up with such rapidly changing demands, but that they experience rapid internal temperature changes that may exceed thermal stress limits. SES-developed (patent-pending) dynamic heat exchangers remove or greatly reduce these thermal stresses. This project demonstrated that such heat exchangers can follow even step changes in flowrates without compromising heat exchanger efficiency or inducing thermal stresses.

Detailed analyses of energy-storing carbon capture demonstrate that, for example, an 800 MW power plant with this technology can manage  $\pm 400$  MW swings in energy demand on a grid that includes coal, natural gas, wind, and varying daily demands. The data included actual demand variations and corresponding costs of power production. The revenue generated by storing

energy during low-demand (low-cost) periods and releasing during high-demand (high-cost) periods represented a net revenue to the CCC ES<sup>TM</sup> system of slightly over \$20/MWh, which would cover 80–90% of the total cost of carbon capture. This large economic benefit can only be realized for a load-following power station, so it is not included in the economic analyses of this report. However, the CCC ES<sup>TM</sup> process allows the power plant to follow load while the boiler remains at a constant firing rate, so nearly every power plant should be able to benefit from this technology.

### 3.8 Discussion

The CCC process is a retrofit, post-combustion technology that desublimates CO<sub>2</sub> in the flue gas and produces a separate liquid CO<sub>2</sub> product. Figure 27 illustrates the major process steps. The process (1) dries and cools flue gas, (2) further cools it in a heat recovery heat exchanger to nominally –107 °C, (3) condenses contaminants (e.g., mercury, SO<sub>2</sub>, NO<sub>2</sub>, Hg, and HCl) at various stages during cooling, (4) separates the solid CO<sub>2</sub> that forms during cooling from the remaining gas, (5) pressurizes the solid CO<sub>2</sub> to 70–80 bar, (6) reheats the CO<sub>2</sub> and the remaining flue gas to near ambient conditions (15–20 °C) by cooling the incoming gases, and (7) compresses the pressurized and now melted CO<sub>2</sub> stream to final delivery pressure (nominally 150 bar). There is a small external refrigeration loop in the process that transfers the enthalpy of pure CO<sub>2</sub> melting to cooler temperatures to avoid a heat exchanger temperature crossover.

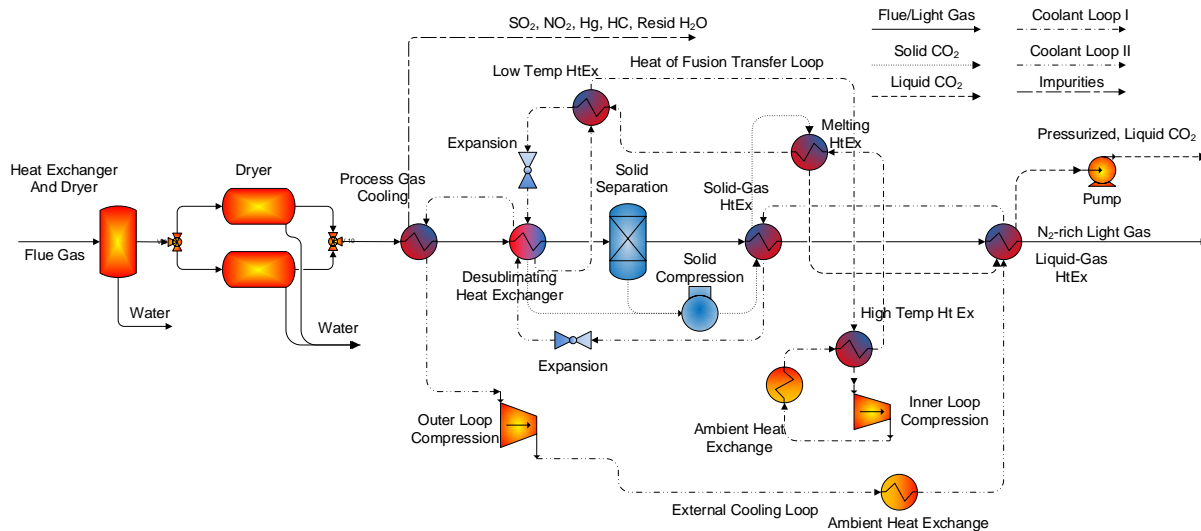


Figure 27. CCC CFG<sup>TM</sup> version of the CCC process.

SES's CCC ES<sup>TM</sup> process separates CO<sub>2</sub> from flue gases and other CO<sub>2</sub>-laden streams and pressurizes the resulting liquid in preparation for transport and storage. Some of its distinguishing characteristics compared to the leading alternatives (i.e., advanced amine systems) include:

1. Consumes about half of the energy;
2. Costs less than half;
3. Stores energy in a highly efficient, grid-scale, rapidly responding process;
4. Retrofits to existing coal, natural gas, biomass, cement kiln, and other systems;

## Non-Confidential Report

5. Captures most pollutants (CO<sub>2</sub>, SO<sub>x</sub>, NO<sub>x</sub>, Hg, PM<sub>xx</sub>, VOCs, etc.) in a single, multipollutant, platform;
6. Recovers flue gas moisture, reducing water demand;
7. Capable of very high capture rates at modest costs.

The energy and cost advantages are the most important on this list and combine to make CCC a very promising alternative to other processes. The energy and costs associated with this technology and all other carbon capture technologies exceed those of technologies used for mitigating other pollutants. A modern coal-fired power plant, for example, consumes 11–14% of the power plant output to capture and store CO<sub>2</sub> using this technology. By comparison, less than 5% of a non-capture plant provides the energy for all of the parasitic losses. The capture plant increases electrical power generation costs by about 2.5 ¢/kWh, possibly much less if the energy storage option is used. For comparison, the US national average residential electricity price is about 13¢/kWh. CO<sub>2</sub> abatement requires more energy and more money than all traditional pollutant reductions combined. However, the CCC process costs less than other widely analyzed options and is in any case well within the regional variation of power costs in the US.

This project focuses on the energy-storing version of this process (i.e., CCC ES<sup>TM</sup>). During off-peak hours, the energy storing version of the process generates more refrigerant than is needed for the process and stores the excess in an insulated vessel as a liquid at the low-temperature, low-pressure point in the cycle. Such vessels and processes are common commercially. During peak demand, the stored refrigerant could be used in place of continuously generating refrigerant in a steady-state system. This would eliminate nearly all of the energy demand required by CCC for as long as the stored refrigerant lasts.

CCC ES<sup>TM</sup> makes the technology as strategically important for renewable fuels as it is for fossil fuels. The energy storage version generates excess refrigerant at night or at other times when there is excess and inexpensive power available on the grid. During peak demand, the stored refrigerant drives the capture process, decreasing the normal energy demand to near zero and increasing power plant output by the amount by which the parasitic load decreases. On utility-scale power plants, this energy storage scheme can absorb intermittent power from large wind or solar sources and deliver during peak demand times, typically the next afternoon. This makes renewables much more effective than they otherwise can be and decreases the need to build additional power plants to compensate for carbon capture. This is the primary subject of this investigation and fits into the other process features as described in this section.

The retrofit importance of carbon capture systems is difficult to overstate. The great majority of the current growth in CO<sub>2</sub> emissions and the majority of total CO<sub>2</sub> emissions come from developing economies completing new power plants with very high opportunity costs. If carbon capture technologies cannot retrofit these relatively new power systems at reasonable costs, the prospects for carbon capture in such economies are very low. Global climate change mitigation cannot be successful without the active participation from these developing economies. Independent of the importance of retrofitting new plants in developing countries, future CO<sub>2</sub> emissions from the US and other mature economies are also projected to overwhelmingly come from currently existing plants.

## Non-Confidential Report

The multipollutant capture facet of CCC makes it ideally suited for current and essentially nearly all future environmental regulations. CCC removes every gas less volatile than CO, which includes nearly all current and foreseeable pollutants, except CO. In addition, the recovery of flue gas moisture to decrease water demand from power plants addresses some of the most critical power plant siting and operation issues.

Finally, managing global temperature increases to less than 2 °C requires capturing more CO<sub>2</sub> than the sum of all CO<sub>2</sub> currently emitted from all electrical power sources. This means that significant amounts of CO<sub>2</sub> from residential and commercial and mobile sources also must be captured. The costs associated with capturing CO<sub>2</sub> from intermittent, dispersed, small, and mobile sources will greatly exceed those from stationary, continuous large sources, such as power generation. Therefore, capture systems operating on large, stationary sources must remove as much CO<sub>2</sub> as possible (99%+) for successful climate management to succeed.

CCC addresses all of these issues. SES has demonstrated CCC up to skid scale, that is, with flowrates that produce up to 1 tonne of CO<sub>2</sub> per day processed through modular systems housed in a series of shipping containers. These demonstrations include flue gases containing CO<sub>2</sub> from subbituminous coal, bituminous coal, biomass, natural gas, and municipal waste and at locations that include utility power plants, heating plants, cement kilns, and pilot-scale combustion facilities.

### 3.9 Important Lessons Learned

All of the project milestones were completed successfully. However, capturing 99% of the CO<sub>2</sub> was difficult using LNG as a refrigerant (Milestone 22). The reason for this was that there were some natural gas liquids (propane, ethane, and/or butane) in the stream. This caused the LNG to boil at a warmer temperature when attempting to cool the cold liquid that would later come into contact with the flue gas in order to desublimates the CO<sub>2</sub>.

This was an important discovery that directly relates to full-scale plant operations, but is unlikely to be a major issue for scale up. There are 4 options for handling this issue:

1. The process will have to be operated at a lower capture rate, such as 95%, until the composition of the natural gas returns to normal.
2. The operating pressure will have to be low, perhaps lower than ambient
3. The plant will have to be located in a place where the concentration of natural gas liquids in the local pipeline is low or
4. The natural gas liquids will have to be removed.

Under Option 1, the current regulatory climate will have to be evaluated to see if this is feasible, but there is no commercially available carbon capture process that can effectively operate at above 90%. Under Option 2, changing the operating pressure of the energy storage system would not be difficult and will represent a functionality that the plant will have for pipeline composition changes. Lowering the pressure in the system below ambient will require specialized engineering

## Non-Confidential Report

and would probably make one of the other options more attractive. Under Option 3, a location where the natural gas liquid concentrations are low would be used. A site selection process would be necessary for any large-scale process such as CCC ES™. Finally, under Option 4, the natural gas liquids would be removed by either the producer or at the CCC ES™ site. Natural gas liquids are more valuable than methane and will be able to be sold at a higher price, so there is likely to be an incentive to remove them prior to using the natural gas for energy storage. Tackling this issue will have to be studied in the future, but many of these solutions would be feasible and therefor represents a relatively low risk for CCC ES™ implementation.

## 4. Greenhouse Gas and Non-GHG Impacts

### 4.1 Qualitative Impacts

During this project under CCEMC and other sponsorship, CCC ES™ has been demonstrated at small scale on fuels that include biomass, subbituminous coal, bituminous coal, natural gas, and municipal waste and on slip streams from utility power stations, cement kilns, heating plants, and pilot-scale combustors. Theoretical analyses of the transient behavior of CCC were undertaken and show that, with the use of the transient heat exchanger, the CCC ES™ process could allow a coal-fired power plant to operate continually at peak efficiency. This will allow the plant to produce more power while burning less coal and hence producing fewer greenhouse gases. Further, the boiler within a coal-fired power plant will last longer and will require less maintenance. At the same time, grid operators will be able to take full advantage of intermittent renewable resources. Figure 28 shows how the CCC ES™ process fits into the overall energy grid. The CCC process would ramp up and down as power is produced by intermittent sources or as the demand changes. The coal-fired power plant runs at a steady load, and power generation on this grid only produces clean exhaust gases. If the coal-fired power plant is situated in a good location, biomass can be mixed with the coal and the power produced can have a negative carbon footprint. The CCC ES™ process enables all of these benefits.

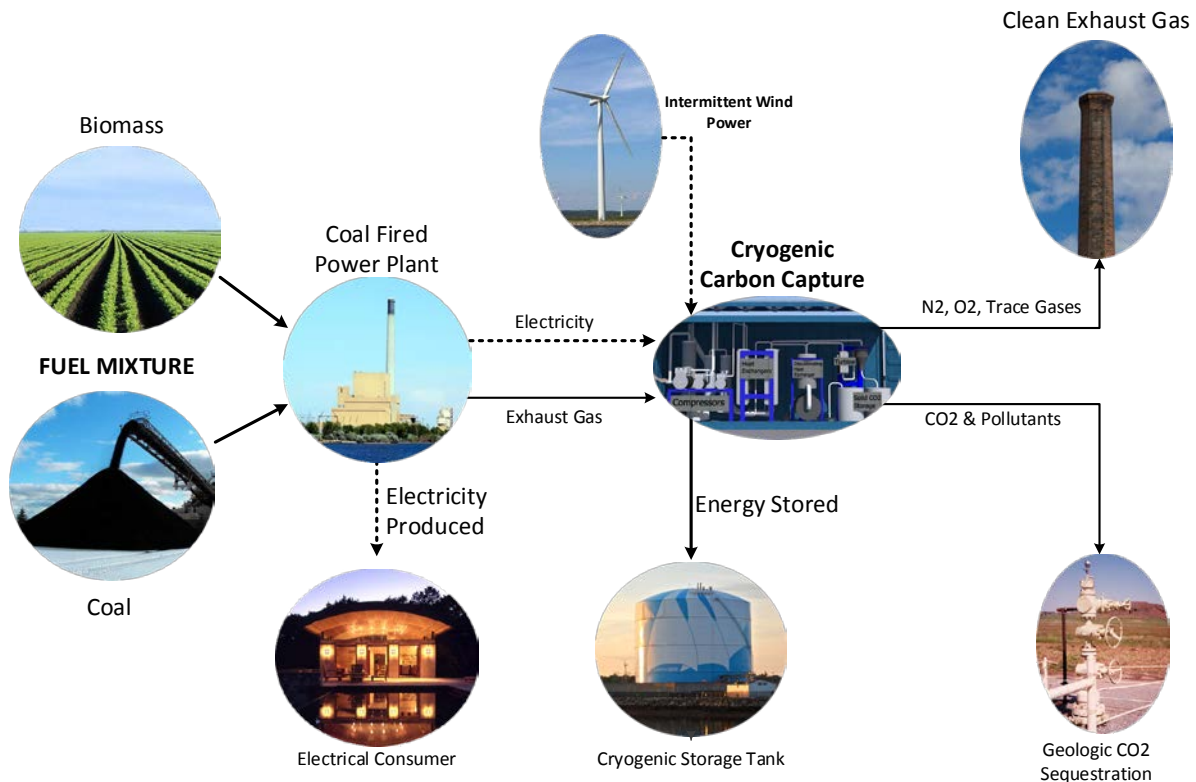


Figure 28. CCC ES™ integration into the grid resulting in a negative carbon footprint for electrical power production.

## 4.2 Qualitative Discussion

The immediate benefit of the completed project is a mobile skid unit capable of capturing 1 tonne CO<sub>2</sub>/day while simulating the energy storage capability of the CCC technology. The unit has operated on multiple gas streams, both simulated and industrial, and demonstrated a consistent ability to capture greater than 90% of the incoming CO<sub>2</sub> gas. Because of the lack of infrastructure for CO<sub>2</sub> sequestration, all tests until now have resulted in the venting of all captured CO<sub>2</sub> after characterization. This mobile test unit will remain operational and continue to be utilized for optimization of CCC parameters as well as further field testing.

## 4.3 Expected Annual GHG Benefits

The next logical step in the scaling up of the CCC process is a pilot-scale project. Preliminary design of this unit is complete and it has been designed as a 100 tonne CO<sub>2</sub>/day processing unit. Once project funding is secured, it is anticipated that the first two years of the project will be design and construction of the unit, and the first operational year would be Year 3 of the project. For the first year of operation, the capacity factor is assumed to be 50%, ramping up to 75% in the second year of operation. Thereafter, a commercial-scale installation will occur. It is anticipated that the first commercial-scale projects would come on smaller plants, somewhere between 10 and 15 times greater than the pilot plant discussed above. Larger commercial-scale installations, such as the 550 MW plant that is the basis for the numbers stated above, would probably occur near the end of the 10-year time period. The number of commercial-scale CCC installations depends heavily upon currently unpredictable market forces. However, each installation will be capable of greater than 90% of CO<sub>2</sub> capture at each facility where it is installed. Environment Canada's GHG Facility Data Search [29] places Alberta's current CO<sub>2</sub> emissions at 125,232,373 tonne/yr. Long-term, it can be assumed that all major GHG emission point sources (defined as installations that vent greater than 1,000,000 tonnes/yr) can be retrofitted with CCC technology. This includes coal-fired power plants, natural gas power and cogeneration plants, and refineries. Wide-scale CCC implementation on these plants would result in a capture of 85,000,000 tonne/yr of Alberta's CO<sub>2</sub> emissions, including 23,800,000 tonne/yr of emissions from oil sands processing.

Utilizing the parasitic load as described in the preceding sections, and using the US DOE NETL report also cited above [3], the net reduction of emissions for a 550 MW coal-fired power plant with CCC is 88.5%. A 550 MW plant without carbon capture emits 441.9 tonne/hr of carbon dioxide. The CCC system has been simulated to capture 90% of the emissions—including extra emissions due to the parasitic load of the CCC installation. This results in an emission of 50.9 tonne/hr from the stack. The net reduction is therefore 391.0 tonne/hr, which corresponds to the 88.5% number quoted above. This is nominally the same with and without the energy storing technology since both have a very similar net parasitic load and are able to maintain 90% capture at all times. We have also included a "Long-Term Potential" row in Table 17. Global CO<sub>2</sub> emissions for 2013 were approximately 36 gigatonnes for fossil fuel burning and cement production alone. If CCC were to gain widespread implementation, a conservative estimate is that at least a third of this emitted carbon would be able to be captured by the CCC process, putting our long-term potential at 12 gigatonnes of CO<sub>2</sub> annually.

## Non-Confidential Report

Table 17 shows the GHG reduction potential of CCC ES™. Even excluding all the benefits of energy storage and multipollutant capture, the CCC process has the potential to have a major impact on global warming. The table also includes the number of CCC installations of different size. We believe that CCC is within five years of commercialization

Table 17. Worldwide CCC ES™ CO<sub>2</sub> capture potential by year.

| Year                | CO <sub>2</sub> Captured | Skid-Scale Installations | Pilot Installations      | Small Commercial Installations | Large Commercial Installations |
|---------------------|--------------------------|--------------------------|--------------------------|--------------------------------|--------------------------------|
|                     | tonne/yr                 |                          | 100 tonne/day capability | 50–75 MW coal plant equivalent | 550 MW coal plant equivalent   |
| 1                   | 15                       | 2                        |                          |                                |                                |
| 2                   | 20                       | 2                        |                          |                                |                                |
| 3                   | 18,300                   | 2                        | 1                        |                                |                                |
| 4                   | 27,500                   |                          | 1                        |                                |                                |
| 5                   | 30,000                   |                          | 1                        |                                |                                |
| 6                   | 325,000                  |                          | 1                        | 1                              |                                |
| 7                   | 600,000                  |                          |                          | 2                              |                                |
| 8                   | 1,000,000                |                          |                          | 3                              |                                |
| 9                   | 1,500,000                |                          |                          | 4                              |                                |
| 10                  | 5,500,000                |                          |                          | 4                              | 1                              |
| Long-Term Potential | 12,000,000,000           |                          |                          |                                |                                |

### 4.4 Non-GHG Benefits

This project primarily dealt with getting energy storage caught up with the development of CCC. Some of the same equipment was used to complete pollutant capture testing. Adding energy storage to CCC and then considering several other ancillary benefits (including pollutant capture) makes CCC one of the most attractive technologies in the energy industry.

#### 4.4.1 Multipollutant capture

While CCC would never be implemented unless you were already committed to carbon capture, the low temperatures associated with this process also capture most other pollutants at little to no additional cost.

#### *Mercury Capture Offset*

The EPA has recently instituted the Mercury and Air Toxics Standards (MATS), which are regulations designed to limit mercury and other hazardous emissions. This new standard would restrict new coal-fired power plants from being built without additional controls, and will also impact older power plants built without controls. State-of-the-art for mercury controls generally involves an activated carbon bed, which has the disadvantage of requiring a fairly large pressure drop across the bed.

## Non-Confidential Report

The cost for mercury removal and the offset described above was based on a report done by the EPA in 2003 [30]. The minimum removal cost for mercury is 0.03 \$/MWh, which can be the case when both an FGD and baghouse are in place, although there are reasonable estimates for an offset being up to 3.1 \$/MWh in a greenfield plant. The minimal cost is based on the following: (a) 0.07 mg/kg Hg produced from subbituminous coal, (b) plant capacity factor of 65%, (c) powdered activated carbon at \$1000/ton of carbon, and (d) capital recovery factor of 0.133

The CCC process offsets the costs of this mercury removal by condensing and desublimating nearly all of the mercury in the stream. During the process, the flue gas stream is brought to low enough temperatures such that 99.9+% mercury in the stream will be captured. At these temperatures, the process is not only condensing mercury that originated from the coal, but also 99+% of atmospheric mercury. SES demonstrated these Hg capture efficiencies during a skid-scale field test campaign in 2015.

### *SO<sub>x</sub> Capture Offset and FGD Replacement*

Flue gas desulphurization (FGD) units are based on a solids or solutions used to scrub the flue gas and remove SO<sub>2</sub> and SO<sub>3</sub> as an acid gas. This process and its costs are widely implemented and well known. The 2013 NETL report indicates that the cost for an FGD at this scale is 3.90 \$/MWh [3].

SO<sub>2</sub> and SO<sub>3</sub> desublimates at CCC process temperatures. They accumulate as solids, and exit the system with the CO<sub>2</sub> or, if sufficiently concentrated in the flue gas, a large fraction desublimates before CO<sub>2</sub> starts to desublimates. Laboratory-, bench-, and skid-scale versions of CCC all demonstrate effective SO<sub>2</sub> removal. SO<sub>x</sub> removal requires minimal changes to the current CCC system and, with some development, could replace FGD units at plants.

### *NO<sub>x</sub> Capture Offset*

The CCC process also captures high levels of NO<sub>2</sub> from the process stream, and recent experiments show that CCC also captures NO (Table 18). NO capture likely involves its conversion to NO<sub>2</sub> at CCC operating temperatures and pressures. These efficient capture rates, with minimal additional costs to the process, mean that nearly the entire cost of additional equipment (e.g., selective catalytic reduction (SCR) process) could be offset.

Table 18. NO concentration into and out of the skid-scale CCC system (FTIR measurements).

|                   |     | <b>1/6/2015</b> | <b>1/8/2015</b> |
|-------------------|-----|-----------------|-----------------|
| <b>NO In</b>      | ppm | 57.825          | 23.941          |
| <b>NO Out</b>     | ppm | 0.311           | 1.834           |
| <b>NO Capture</b> | %   | 99.5            | 92.3            |

The model used to estimate the SCR cost offset came from a report prepared by Sargent & Lundy [31] evaluating the EPA's cost estimates for SCRs in use at coal-fired power plants of various sizes. For a coal-fired power plant in the 550 MW range, the SCR costs are about 5.5 \$/MWh.

## Non-Confidential Report

## 5. Overall Conclusions

The objective of this project was to explore the energy storage capability of CCC. This project

1. shows that NG can be used as effectively as other refrigerants in the CCC process;
2. determines that stored LNG refrigerant represents a significant portion of the CCC energy demand;
3. calculates that the LNG energy density suffices to be able to store energy at grid scale;
4. develops heat exchanger technologies that allow LNG flow transients to follow energy storage and recovery transients without damage;
5. simulates grid-level incorporation of energy storage into a realistic system;
6. demonstrates as many of these processes as possible at small scale.

The following paragraphs summarize the conclusions related to each of these points in turn.

This project demonstrates experimentally and theoretically that natural gas provides essentially identical (very slightly better) refrigeration performance as alternative refrigerants and refrigerant blends. Because the critical point of LNG (as low as  $-83\text{ }^{\circ}\text{C}$ ) is well below ambient temperature, it is not possible to compress and then condense LNG near room temperature, as is commonly done with traditional refrigerants. However, LNG can still be generated efficiently, albeit in a slightly more complex circuit compared to traditional refrigerant. The project also demonstrated that some NG supplies may require process set point modification or removal of natural gas liquids since there are variations in the amounts of heavy hydrocarbons among NG supplies.

Refrigeration in general represents about 80% of the total energy demand for CCC, depending on amount of  $\text{CO}_2$  in the flue gas, over half of which can be incorporated into the LNG loop. Therefore, CCC ES<sup>TM</sup> can store and release most of its energy consumption in the form of stored refrigerant, or LNG.

The energy density of LNG suffices to store several hours' worth of refrigeration in tanks that are smaller than commercially available storage tanks. Therefore, CCC ES<sup>TM</sup> has the capacity to store enough energy to supply refrigerant for the entire peak demand time of a typical power plant.

CCC ES<sup>TM</sup> operates with the carbon capture portion of the process matching boiler load, which is typically essentially constant, while the LNG generation portion follows power demand. Power demand on grids with intermittent supplies can change significantly within minutes. Transient analyses and experiments showed that heat exchangers may be able to keep up with such rapidly changing demands, but that they experience rapid internal temperature changes that may exceed thermal stress limits. SES-developed (patent-pending) dynamic heat exchangers remove or greatly reduce these thermal stresses. This project demonstrated that such heat exchangers can follow even step changes in flowrates without compromising heat exchanger efficiency or inducing thermal stresses.

## Non-Confidential Report

Detailed analyses of energy-storing carbon capture demonstrate that, for example, an 800 MW power plant with this technology can manage  $\pm 400$  MW swings in energy demand on a grid that includes coal, natural gas, wind, and varying daily demands. The data included actual demand variations and corresponding costs of power production. The revenue generated by storing energy during low-demand, low-cost periods and releasing during high-demand, high-cost periods represented a net revenue to the CCC ES<sup>TM</sup> system of slightly over \$20/MWh, which would cover 80–90% of the total cost of carbon capture. This large economic benefit can only be realized for a load-following power station, so it is not included in the economic analyses of this report. However, the CCC ES<sup>TM</sup> process allows the power plant to follow load while the boiler remains at a constant firing rate, so nearly every power plant should be able to benefit from this technology.

While not strictly part of the CCEMC project, SES has already demonstrated at small scale (up to one tonne of CO<sub>2</sub> per day) the essential components of CCC ES<sup>TM</sup>, including using LNG as a refrigerant, energy storage, and energy recovery.

## 6. Scientific Achievements

### 6.1 Journal Articles

Fazlollahi, Farhad; Bown, Alex; Ebrahimzadeh, Edris; Baxter, Larry L. “Design and analysis of the natural gas liquefaction optimization process-CCC ES™ (energy storage of Cryogenic Carbon Capture™).” *Energy*, 2015, *in press*.

Jensen, Mark J.; Russell, Christopher S.; Bergeson, David; Hoeger, Christopher D.; Frankman, David J.; Bence, Christopher S.; Baxter, Larry L. “Prediction and validation of external cooling loop Cryogenic Carbon Capture™ (CCC-ECL) for full-scale coal-fired power plant retrofit.” *International Journal of Greenhouse Gas Control*, 2015 (42), 200–212.

Safdarnejad, Seyed Mostafa; Hedengren, John D.; Lewis, Nicholas R.; Haseltine, Eric L. “Initialization strategies for optimization of dynamic systems.” *Computers & Chemical Engineering*, 2015 (78), 39–50.

Safdarnejad, Seyed Mostafa; Hedengren, John D.; Baxter, Larry L. “Plant-level dynamic optimization of Cryogenic Carbon Capture™ with conventional and renewable power sources.” *Applied Energy*, 2015 (149), 354–366.

Edris Ebrahimzadeh, Paul Wilding, David Frankman, Farhad Fazlollahi, Larry Baxter “Theoretical and Experimental Analysis of Dynamic Heat Exchanger: Non-retrofit Configuration”, *Applied Thermal Engineering*, (Revision Submitted).

Edris Ebrahimzadeh, Paul Wilding, David Frankman, Farhad Fazlollahi, Larry Baxter “Theoretical and Experimental Analysis of Dynamic Heat Exchanger: Retrofit Configuration”, *Energy* (Revision Requested).

### 6.2 Conference Presentations

Fazlollahi, Farhad; Bown, Alex; Baxter, Larry L. “Transient natural gas liquefaction process comparison–dynamic heat exchanger under transient changes in flow.” *AIChE Annual Meeting*, Salt Lake City, UT, Nov 2015.

Safdarnejad, Seyed Mostafa; Hedengren, John D.; Baxter, Larry L. “Reduction in cycling of the boilers by using large-scale energy storage of Cryogenic Carbon Capture™.” *AIChE Annual Meeting*, Salt Lake City, UT, Nov 2015.

Safdarnejad, Seyed Mostafa; Kennington, Lindsey; Baxter, Larry L.; Hedengren, John D. “Investigating the impact of Cryogenic Carbon Capture™ on the performance of power plants.” *American Control Conference (ACC)*, Chicago, IL, Jul 2015.

Safdarnejad, Seyed Mostafa; Hedengren, John D.; Baxter, Larry L. “Effect of Cryogenic Carbon Capture™ (CCC) on smart power grids.” *AIChE Spring Meeting*, Austin, TX, Apr 2015.

Fazlollahi, Farhad; Baxter, Larry L. “Comparison of two difference liquefaction models for Cryogenic Carbon Capture™ Process.” *AIChE Annual Meeting*, Atlanta, GA, Nov 2014.

## Non-Confidential Report

Fazlollahi, Farhad; Baxter, Larry L. “Liquefaction process, energy storage of Cryogenic Carbon Capture™.” *AIChE Annual Meeting*, Atlanta, GA, Nov 2014.

Safdarnejad, Seyed Mostafa; Hall, Trent; Hedengren, John D.; Baxter, Larry L. “Dynamic optimization of Cryogenic Carbon Capture™ with large-scale adoption of renewable power.” *AIChE Annual Meeting*, Atlanta, GA, Nov 2014.

### 6.3 Student Theses

Jensen, M. J.; *Energy Processes Enabled by Cryogenic Carbon Capture*. PhD Dissertation, Brigham Young University: Provo, 2014.

## 7. Next Steps

The modeling and testing performed under this CCEMC project resulted in the first significant analysis and demonstration of the CCC ES™ process. The next steps in the commercialization plan of this important technology include a market analysis that will include a detailed model of the value of the technology in different markets, the most applicable markets for the technology, and the markets where the technology could be adopted first. The next steps in the technology development plan are to increase the scale and duration of CCC ES™ testing to the same level as the CCC skid demonstrations, demonstrate the CCC ES™ technology in a field test, and integrate CCC ES™ into the next scale up of the Cryogenic Carbon Capture™ technology. Specifically, SES will be seeking funding to integrate the CCC ES™ process into a field demonstration of the carbon capture technology in one of several potential applicable markets. One very important potential market is the Canadian industrial sector. There are many emissions sources specifically related to the Alberta oil sands for which this technology is well-suited.

To fully realize its potential, the CCC ES™ process needs to be installed at a full-scale commercial plant where it can have significant positive effects on the plant and the surrounding grid. The first demonstration of this scale will cost hundreds of millions of dollars and will be a major engineering project. To accomplish this, SES will need to partner with a commercial engineering firm that has the reach and capability to scale the technology and take it to a global market. SES will do this by engaging in a long-term contractual or equity agreement with one of these potential partners. SES will engage with at least one such partner in the next stage of development to initiate important technical and business collaboration.

SES has secured letters of support from host-sites for the next scale of development in Europe and the United States and is currently pursuing relationships with similar entities in Canada. In addition to these host sites, SES has a bid from a global engineering contractor to build the pilot facility and is pursuing more permanent relationships with other engineering firms. SES is already working on scaling the CCC ES™ technology to skid scale under separate funding and is actively seeking funding for a pilot demonstration of the technology. Within the next two years, SES anticipates forming a formal relationship with a commercialization partner and securing funding for a pilot demonstration of the technology.

## 8. Communications Plan

As noted earlier in this report, the work related to this project has already resulted in the publication of several peer-reviewed articles. SES anticipates that more technical papers will be prepared that are related to the CCC ES™ process. Additionally, SES frequently presents results from its projects—including the CCEMC project—at conferences where interested parties gather. Private meetings with vendors, adopters, investors, and partners are also expected to continue where SES will provide verbal reports and presentations regarding the development of its processes, including the CCC ES™ process. In all cases, some of what SES has performed under CCEMC funding will be considered confidential and will only be shared under appropriate confidentiality agreements with groups that SES deems important to the development of the technology.

## 9. Abstract and Keywords

### 9.1 Abstract

The Cryogenic Carbon Capture™ (CCC) process is a retrofit, post-combustion technology that desublimates CO<sub>2</sub> in the flue gas and produces a separate liquid CO<sub>2</sub> product. This project focuses on the energy-storing version of this process, which is designated CCC ES™. During off-peak hours, the energy-storing version of the process would generate more refrigerant than is needed for the process, which would be stored in an insulated vessel as a liquid at the low-temperature, low-pressure point in the cycle. Such vessels and processes are common commercially. During peak demand, the stored refrigerant could be used in place of continuously generating refrigerant in a steady-state system. This eliminates nearly all of the energy demand required by CCC for as long as the stored refrigerant lasts.

The objective of this project was to explore the energy storage capability of CCC. This project

1. shows that NG can be used as effectively as other refrigerants in the CCC process;
2. determines that stored LNG refrigerant represents a significant portion of the CCC energy demand;
3. calculates that the LNG energy density suffices to be able to store energy at grid scale;
4. develops heat exchanger technologies that allow LNG flow transients to follow energy storage and recovery transients without damage;
5. simulates grid-level incorporation of energy storage into a realistic system;
6. demonstrates as many of these processes as possible at small scale.

CCC ES™ operates with the carbon capture portion of the process matching boiler load, which is typically essentially constant, while the LNG generation portion follows power demand. Power demand on grids with intermittent supplies can change significantly within minutes. Transient analyses and experiments showed that heat exchangers may be able to keep up with such rapidly changing demands, but that the lifetime of the heat exchangers is significantly reduced by such thermal stresses. SES-developed (patent-pending) dynamic heat exchangers remove or greatly reduce these thermal stresses. This project demonstrated that such heat exchangers can follow even step changes in flowrates without compromising heat exchanger efficiency or inducing thermal stresses.

Detailed analyses of CCC ES™ demonstrate that, for example, an 800 MW power plant with this technology can manage  $\pm 400$  MW swings in energy demand on a grid that includes coal, natural gas, wind, and varying daily demands. The data included actual demand variations and corresponding costs of power production. The revenue generated by storing energy during low-demand, low-cost periods and releasing during high-demand, high-cost periods represents a net revenue to the CCC ES™ system that covers 80–90% of the total cost of carbon capture. The CCC ES™ process allows the power plant to follow load while the boiler remains at a constant firing rate, so nearly every power plant should be able to benefit from this technology.

## Non-Confidential Report

### 9.2 Keywords

Cryogenic Carbon Capture™, CCC ES™, energy storage, carbon capture and storage, CCS

## 10. References

1. Akhil, A.A.; Huff, G.; Currier, A.B.; Kaun, B.C.; Rastler, D.M.; Chen, S.B.; Cotter, A.L.; Bradshaw, D.T.; Gauntlett, W.D. *DOE/EPRI 2013 Electricity Storage Handbook in Collaboration with NRECA*. Sandia National Laboratories: Albuquerque, New Mexico. SAND2013-5131. Jul 2013.
2. NETL/DOE. *Cost and performance baseline for fossil energy plants volume 1: Bituminous coal and natural gas to electricity*. DOE/NETL 202010/1397 Revision 2a, Sep 2013.
3. Jensen, M. J.; *Energy Processes Enabled by Cryogenic Carbon Capture*. PhD Dissertation, Brigham Young University: Provo, 2014.
4. Gopan, A.; Kumfer, B. M.; Phillips, J.; Thimsen, D.; Smith, R.; Axelbaum, R. L.; Process design and performance analysis of a Staged, Pressurized Oxy-Combustion (SPOC) power plant for carbon capture. *Applied Energy* 2014, 125, (0), 179–188.
5. Matuszewski, M. N.; Woods, M. B. A. H.; Brasington, R. D. *Advancing Oxycombustion Technology for Bituminous Coal Power Plants: An R&D Guide*; NETL: 2012.
6. Zaman, M. H. L., Jay, Carbon capture from stationary power generation sources: A review of the current status of the technologies. *Korean Journal of Chemical Engineering* 2013, 30, (8), 1497–1526.
7. Skorek-Osikowska, A.; Janusz-Szymańska, K.; Kotowicz, J., Modeling and analysis of selected carbon dioxide capture methods in IGCC systems. *Energy* 2012, 45, (1), 92–100.
8. Sanchez Fernandez, E.; Goetheer, E. L. V.; Manzolini, G.; Macchi, E.; Rezvani, S.; Vlugt, T. J. H., Thermodynamic assessment of amine based CO<sub>2</sub> capture technologies in power plants based on European Benchmarking Task Force methodology. *Fuel* 2014, 129, (0), 318–329.
9. Porcheron, F.; Gibert, A.; Jacquin, M.; Mougine, P.; Faraj, A.; Goulon, A.; Bouillon, P.-A.; Delfort, B.; Le Penne, D.; Raynal, L., High throughput screening of amine thermodynamic properties applied to post-combustion CO<sub>2</sub> capture process evaluation. *Energy Procedia* 2011, 4, 15–22.
10. Morton, F.; Laird, R.; Northington, J., The National Carbon Capture Center: Cost-effective test bed for carbon capture R&D. *Energy Procedia* 2013, 37, 525–539.
11. Le Moullec, Y.; Kanniche, M., Screening of flowsheet modifications for an efficient monoethanolamine (MEA) based post-combustion CO<sub>2</sub> capture. *International Journal of Greenhouse Gas Control* 2011, 5, (4), 727–740.
12. Duan, L.; Zhao, M.; Yang, Y., Integration and optimization study on the coal-fired power plant with CO<sub>2</sub> capture using MEA. *Energy* 2012, 45, (1), 107–116.
13. Cohen, S. M.; Rochelle, G. T.; Webber, M. E., Optimizing post-combustion CO<sub>2</sub> capture in response to volatile electricity prices. *International Journal of Greenhouse Gas Control* 2012, 8, (0), 180–195.
14. Amrollahi, Z.; Ystad, P. A. M.; Ertesvåg, I. S.; Bolland, O., Optimized process configurations of post-combustion CO<sub>2</sub> capture for natural-gas-fired power plant – Power plant efficiency analysis. *International Journal of Greenhouse Gas Control* 2012, 8, 1–11.

## Non-Confidential Report

15. Boot-Handford, M. E.; Abanades, J. C.; Anthony, E. J.; Blunt, M. J.; Brandani, S.; Mac Dowell, N.; Fernandez, J. R.; Ferrari, M.-C.; Gross, R.; Hallett, J. P.; Haszeldine, R. S.; Heptonstall, P.; Lyngfelt, A.; Makuch, Z.; Mangano, E.; Porter, R. T. J.; Pourkashanian, M.; Rochelle, G. T.; Shah, N.; Yao, J. G.; Fennell, P. S., Carbon capture and storage update. *Energy & Environmental Science* 2014, 7, (1), 130–189.
16. Ishibashi, M.; Ota, H.; Akutsu, N.; Umeda, S.; Tajika, M.; Izumi, J.; Yasutake, A.; Kabata, T.; Kageyama, Y., Technology for Removing Carbon Dioxide from Power Plant Flue Gas by the Physical Adsorption Method. *Energy Conversion and Management* 1996, 37, 929–933.
17. Scholes, C. A.; Ho, M. T.; Aguiar, A. A.; Wiley, D. E.; Stevens, G. W.; Kentish, S. E., Membrane gas separation processes for CO<sub>2</sub> capture from cement kiln flue gas. *International Journal of Greenhouse Gas Control* 2014, 24, 78–86.
18. Gazzani, M.; Turi, D. M.; Ghoniem, A. F.; Macchi, E.; Manzolini, G., Techno-economic assessment of two novel feeding systems for a dry-feed gasifier in an IGCC plant with Pd-membranes for CO<sub>2</sub> capture. *International Journal of Greenhouse Gas Control* 2014, 25, 62–78.
19. Pan, X.; Clodic, D.; Toubassy, J., CO<sub>2</sub> capture by antisublimation process and its technical economic analysis. *Greenhouse Gases: Science and Technology* 2013, 3, (1), 8–20.
20. Schach, M.-O.; Oyarzún, B.; Schramm, H.; Schneider, R.; Repke, J.-U., Feasibility study of CO<sub>2</sub> capture by anti-sublimation. *Energy Procedia* 2011, 4, (0), 1403–1410.
21. Lee, A.; Gonzalez, M.; Eakin, B. “The viscosity of natural gases.” SPE Paper 1340, *Journal of Petroleum Technology* 1966 (18), 997–1000.
22. Davisson, E.G. *A computer program for flow calculations*. Tech Report ORNL-TM-1093, OAK Ridge National Laboratory, U.S. Atomic Energy Commission, USA. 1965.
23. Turton, R.; Bailie, R.C.; Whiting, W.B.; Shaeiwitz, J.A. *Analysis, Synthesis and Design of Chemical Processes*. 3<sup>rd</sup> Ed. Prentice Hall: Upper Saddle River, New Jersey. 2009.
24. Pauschert, D. *Study of Equipment Prices in the Power Sector*. Energy Sector Management Assistance Program (ESMAP), International Bank for Reconstruction and Development: Washington D.C., 2009.
25. Zhao, M.; Minett, A.I.; Harris, A.T. “A review of techno-economic models for the retrofitting of conventional pulverized-coal power plants for post-combustion capture (PCC) of CO<sub>2</sub>”. *Energy & Environmental Science* 2013 (6), 25–40.
26. Dave, N.; Do, T.; Palfreyman, D.; Feron, P.H.M.; Xu, S.; Gao, S.; Liu, L. “Post-combustion capture of CO<sub>2</sub> from coal-fired power plants in China and Australia: An experience based comparison.” *Energy Procedia* 2011 (4).
27. Protection of the Environment. *Code of Federal Regulations*, Part 63, Title 40, 1995.
28. Environment Canada. *Results of GHG Facility Data Search*. <http://www.ec.gc.ca/ges-ghg/donnees-data/index.cfm?do=results&lang=en&year=2013> Accessed 09/28/2015.
29. Staudt, J.; Jozewicz, W. *Performance and cost of mercury and multipollutant emission control technology applications on electric utility boilers*. EPA20600/R2003/110, Oct 2003.

Non-Confidential Report

30. Sargent & Lundy, LLC. *IPM Model – Updates to Cost and Performance for APC Technologies: SCR Cost Development Methodology*. Project 12847-002. Systems Research and Application Corporation: Chicago, Illinois. 2013.